5.2 SWIFT HEAVY IONS IN MATERIALS SCIENCE

D.K. Avasthi and D. Kanjilal

There were more than eighty five experiments performed in the last one year as compared to fifty one experiments in the preceding year. The experiments were on polymers, metal-semiconductor interfaces, semiconductors, oxide materials, magnetic materials etc. The problems were mainly related to electronic sputtering, ion beam mixing, nanostructuring of the materials, surface modifications, ion beam induced crystallization.

Large area position sensitive detector was effectively utilized for the electronic sputtering measurements in LiF and graphite. The electronic sputtering clearly showed the dependence on the film thickness and on the substrate, which were qualitatively explained by thermal spike model.

The hypothesis that the ion beam mixing is due to the inter diffusion at the interface during transient temperature spike was confirmed by detailed experiments and elaborate calculations taking into account the contribution due to the nuclear energy loss in evaluating the temperature spike duration. The ion beam mixing in Au/Ge (1 nm thin layers) was shown in nanoscale. It may be noted that the materials tend to become sensitive to S_e in nano dimensions. Other than this, Zr and Co silicide were formed by ion beam mixing as expected from thermal spike speculations depending on the sensitivity to S_e.

A clear TEM investigation revealed the role of 70 MeV Si ion irradiation at 150 °C in crystallizing the amorphous silicon nitride formed by irradiation of Si by low energy N ions. SHI induced surface modifications in HOPG and GaAs have been studied.

Swift heavy ion (SHI) induced conducting channels were demonstrated in fullerene using conducting atomic force microscopy. Different phases in irradiated fullerene film were investigated by XPS. Nanopatterns in SHI irradiated metglass were observed. Creation of Ge nanoclusters was attempted in different ways using SHI. Aligned C clusters were formed by SHI irradiation of Si based polymers.

SiC was successfully formed by implantation of Si by C and subsequent annealing at 1000 °C. SHI induced modifications in various semiconductors such as GaN, ZnSe, GaAs, ZnO were investigated to look into the narrowing of band gap due to defects generated by ion beam.

SHI induced modifications were studied in different polymers, PET, polycarbonate, rubber lattices and their blends, Li based gel polymer electrolytes, polypyrrole conducting polymer, nanocomposite membranes.

SHI irradiation effects have been studied in manganites, ferrite nanoparticles, spinel ferrites.

There were experiments on single event upset by Indian Space Research Organization in collaboration with Bangalore University to simulate the effect of cosmic radiation on radiation sensitive electronic components.

5.2.1 Electronic Sputtering of LiF Thin Film

M. Kumar[1], S.A. Khan[2], F. Singh[2], A. Tripathi[2], D.K. Avasthi[2] and A.C. Pandey[1]

[1]Department of Physics, University of Allahabad, Allahabad 211 002
[2]Nuclear Science Centre, Post Box -10502, New Delhi 110 067

The electronic sputtering of LiF films due to 120 MeV Ag^{9+} irradiation has been studied. The sputtering yield of these films of different thicknesses (80, 160 and 265 nm) deposited on Si, glass and quartz substrates is determined by elastic recoil detection analysis technique. New LAPSDT was used to detect the recoils during the irradiation.

The stoichiometry of the films was determined from the data and it is observed that the Li and F are nearly equally present in the film before and after sputtering as shown in fig. 1. The sputtering yield estimated from the data is plotted in fig. 2 for different film thickness. The results show that the sputtering yield is of the order of 10^3 atoms/ion. The electronic sputtering is found to decreases with increase in the film thickness. According to thermal spike model, the temperature liberated in thinner film is higher and give rise to higher sputtering [1,2].

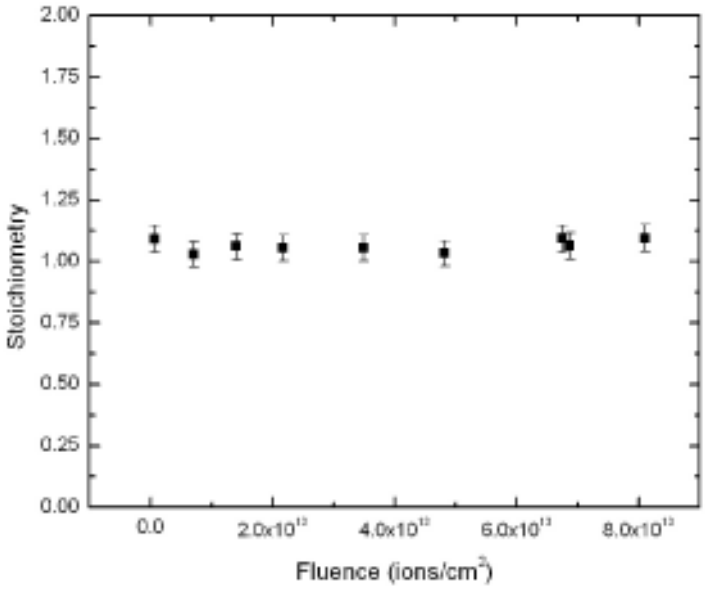

Fig. 1

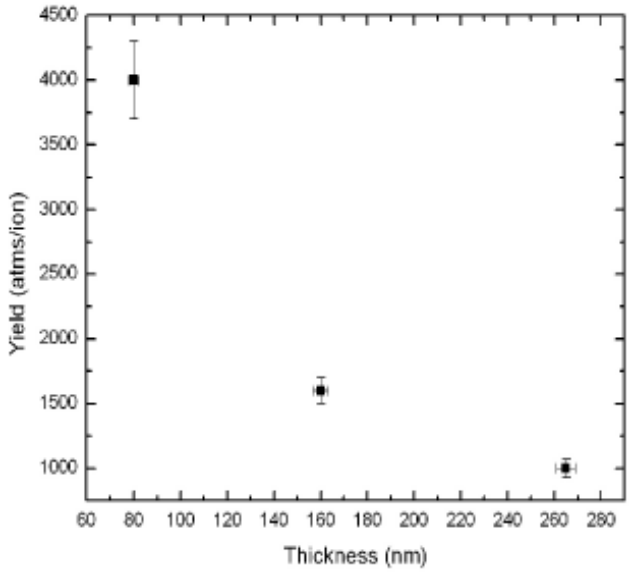

Fig. 2

The estimated electronic sputtering yield in case of the film deposited on Si is less than for the other substrates, whereas film on glass and quartz substrates shows same amount of sputtering. The higher sputtering in case of insulator substrate can also be explained by thermal spike model. As the range of ion is more than the film thickness, a thermal spike will be developed in the substrate also. This temperature spike will increase the temperature generated in the film due to ion interaction resulting in higher sputtering. The temperature in Si substrate will smear out more efficiently due to its higher conductivity as compared to glass/quartz. In case of film deposited on Si or glass, the thermal spike develop in the film will be same but the additional heat emerging from substrate will be less in case of Si. Thus the sputtering is lower in case of the film deposited on Si substrate than that is for glass/quartz.

REFERENCES

[1] A. Gupta and D.K. Avasthi, Phys. Rev. B 64 (2001) 155407.

[2] S. Ghosh,D.K. Avasthi, A. Tripathi, S.K. Srivastava, S.V.S. Nageswara Rao, T. Som, V.K. Mittal, F. Gruner, W. Assman, Nucl. Instru. And Meth., B190 (2002) 169.

5.2.2 Electronic Sputtering from HOPG: A Study of Angular Dependence

A. Tripathi[1,2], S.A. Khan[1], M. Kumar[2], V. Baranwal[2], R. Krishna[2] , S. Kumar[3], A.C. Pandey[2] and D.K. Avasthi[1]

[1]Nuclear Science Centre, New Delhi 110067
[2]University of Allahabad, Allahabad 211002
[3]RBS college, Agra 282002

Recent molecular dynamic (MD) simulations by Bringa et al have shown that at high energy densities, the sputtering process is described by a combination of melted track and pressure pulse [1]. Jakas et al [2] have showed that the high pressure built up within the thermal spike causes a rapid expansion which plays an important role in sputtering process. It has been emphasized by Tombrello et al [3] that the careful study of sputtering from surface is expected to throw light on the mechanism as the same process leads to track formation in bulk and sputtering from surface. At higher energies the electronic energy loss induced sputtering gives much higher yields than predicted by Sigmund's theory [4]. Johnson et al. explained that at high S_e sputtering yield is found to scale as Se^n and described its angular distribution [5].

In the present experiment the HOPG sample was irradiated with a 120 MeV Au^+ beam from the 15 MV Pelletron at the Nuclear Science Centre, New Delhi. Sputtered carbon atoms were collected on 10mm x 5mm Si catcher kept at a distance of 5 cm from the samples. The catchers were mounted at angles of 10^0 to 90^0 from the beam direction, on the secondary electron suppressor in such a way that all the catchers were equidistant in the horizontal plane. The sample was irradiated for a fluence of $2.7x10^{12}$ ions/cm^2 to collect sufficient carbon on small catchers for ERD analysis. Each catcher subtends an angle of 6^0, with an error of $\pm 3^0$ in the angular measurement, and an equal contribution is expected from the error due to beam spot size (2mm x 5mm).

The carbon collected on the catcher is analysed using the ERDA technique using 120 MeV Au beam. The sample was kept at an angle of 30^0 to the beam direction and the recoils were detected at an angle of 45^0. The recoils were detected using a large area gaseous ΔE-E detector. Isobutane gas at 40 torr pressure was used in the detector. The absolute quantity of collected carbon was obtained from total counts for each catcher.

HOPG with normal incidence

The total carbon collected for the ten catchers is shown in Figure 1. As is clear from the figure, the measured quantity of the sputtered carbon for the 20^0 catcher is approximately $8.4x10^{16}$ atoms/cm^2 . There is a decrease in the carbon content for the the next two catchers of 30^0 and 40^0 catchers though a peak appears for the 50^0 catcher which shows a carbon content of $11.4x10^{16}$ atoms/cm^2. The catchers at 60^0 onwards show a continuous decrease in the carbon content. For the total incident beam fluence of $2.7x10^{12}$ ions/cm^2, the average sputter rate of $7.2x10^6$ atoms/ion is obtained.

HOPG with 70° incidence

The total carbon collected for the catchers is shown in Figure 2. The curve shows that the measured quantity of the sputtered carbon for the 20^0 catcher is approximately $4.8x10^{16}$ atoms/cm^2 . The carbon content for the the next two catchers of 30^0 to 55^0 catchers shows a carbon content of between 1-2 $x10^{16}$ atoms/cm^2. The catchers from 60^0

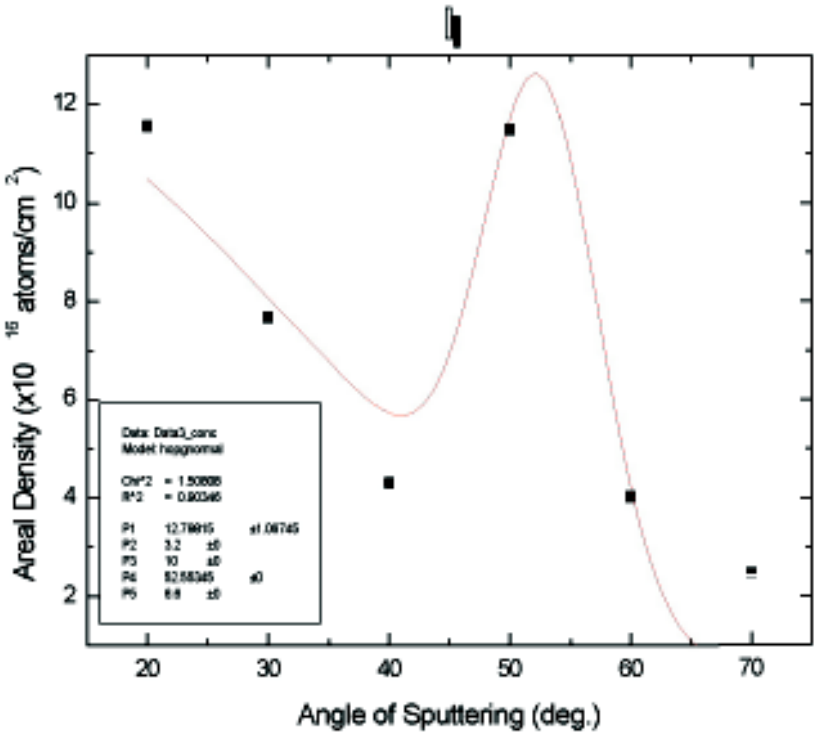

Fig. 1 : The angular distribution of sputtering yield from HOPG sample for normal incidence

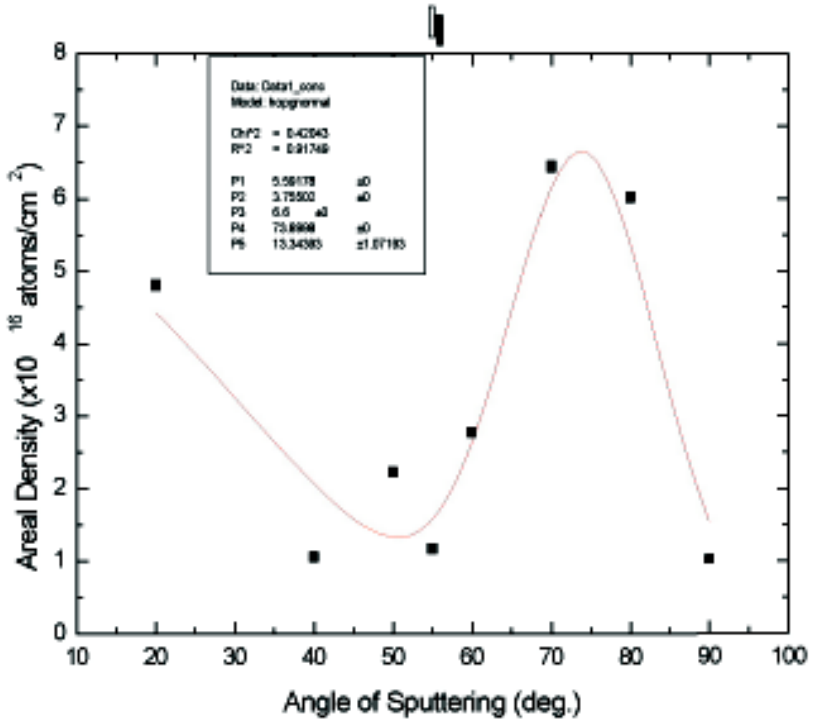

Fig. 2 : The angular distribution of sputtering yield from HOPG sample for 70° tilt Angular Distribution.

onwards show a continuous increase in the carbon content with maximum content of $6.0x10^{16}$ atoms/cm^2, for catcher at 80^0 after which it goes down to $1.1x10^{16}$ atoms/cm^2 for 90^0 catcher. The total sputtering yield is calculated as in the last case and for the total incident beam fluence of $2.17x10^{12}$ ions/cm^2, the average sputter rate of $3.3x10^6$ atoms/ ion is obtained.

The observations show a similar trend with an overall decay with an overcosine distribution. The main difference lies in the exponent which is found to be have a large value of 3.2. This large exponent signifies a distribution which is more confined towards the 0^0 direction. In the present case the linear energy transfer is larger, resulting in much larger energy deposition per unit path length. This is expected to cause initial gas phase inducing higher pressure along the track core responsible for rapid upward expansion which releases by emission of jet of atoms.

As the sample is tilted by 20^0 the peaks as found for the normal incidence are expected to shift to 55^0 as predicted by sum of impulses model, whereas the peak for the axis should shift to 72^0. This observed peak at 73.9^0 is very close to third expected value and is within 3^0 error expected in angle measurements. Hence this peak is interpreted as a combined effect of peak predicted at 45^0 by sum of impulses model and a crystal axis lying at 72^0.

REFERENCES

[1] E.M. Bringa et al, Phys Rev Lett, 88, 165501 (2002).
[2] Jakas et al, Phys Rev B65, 165425, (2002).
[3] Tombrello et al, NIMB 2,555 (1984).
[4] J. Chaumont, H. Bernas, A. Kusnetsov, C. Clerc, L. Damoulin, Nucl. Instru, Meth. B129, 436, (1997).
[5] R.E. Johnson et al. Phys. Rev. B 40 (1989) 49.

5.2.3 Test of the Hypothesis of Transient Molten State Diffusion for Swift Heavy Ion induced Mixing

S.K. Srivastava[1,5], D.K. Avasthi[1], W. Assmann[2], Z.G. Wang[3], H. Kucal[4], E. Jacquet[4], H.D. Carstanjen[5], and M. Toulemonde[4]

[1]Nuclear Science Centre, New Delhi 110067
[2]Sektion Physik, Universität München, D-85748 Garching, Germany
[3]CIRIL, Laboratoire mixte CEA-CNRS, BP 5133, 14040 Caen Cédex, France
[4]CIRIL, BP 5133, F-14070 Caen Cédex 5, France
[5]Max-Planck-Institut für Metallforschung, Heisenbergstr.-3, 70569 Stuttgart, Germany

The recently proposed hypothesis that swift heavy ion induced mixing is a consequence of a diffusion in the transient molten state as predicted by the thermal spike model (TSM) is tested by studying 230 MeV Au ion induced mixing at a metal/ semiconductor (59 nm Fe/Si) interface. On-line elastic recoil detection analysis (ERDA) of the sample was performed using 230 MeV Au ions at an incidence angle of 10°. The electronic energy loss S_e in Fe (45.80 keV/nm) is above the S_{eth} (~30 keV/nm) for latent track formation in Fe.[1] According to a recent report,[2] Si also undergoes melting close to an interface upon irradiation. For an additional experimental check of the applicability of the TSM, a high-resolution Rutherford backscattering spectrometry study of 100 MeV Ag irradiation on the same system is made which shows no mixing as expected for the S_e (28.2 keV/nm) less than S_{eth} . From the ERDA spectra for four fluences ($n\Phi$; n = 1, 2, 3, 4, $\Phi = 8.75\times10^{13}$ ions/cm^2) as shown in Fig. 1, a monotonic increase in the amount of intermixing with increasing fluence is evident. The Fe and Si recoil spectra are fitted using SIMNRA code. The resulting concentration-versus-depth profiles (inset of Fig. 1) are 'Matano' analyzed[3] in order to derive the concentration dependent interdiffusivities for four different ion fluences. The effect of the oblique incidence angle ($\alpha = 10^o$) manifests itself into diffusivity calculation as an additional factor of $(\sin\alpha)$[3,4]. The required size r (~ 4 nm) and duration τ_s (~1.2 ps) of the transient melt phase have been calculated theoretically from the thermal spike model which includes the melting by nuclear energy loss S^n. For a given fluence Φ, the time of diffusion τ is taken (for the case of ERDA) as $\tau = [(\pi r^2\Phi\text{-}1)\ \tau_s]$. The intrinsic diffusivities D_I of Fe in Si and D_{II} of Si in Fe are taken as the values of interdiffusion coefficients in the limits of infinite dilution. The diffusivities so obtained are then compared with the existing literature values.

The concentration dependent interdiffusion coefficients thus calculated for the four analyzed fluences are plotted in Fig. 2. The two diffusivities are $(1.1\pm0.4)\times10^{-9}$ and $(5.1\pm2.0)\times10^{-10}$ m^2/s, respectively. These values are close to (only about an order of

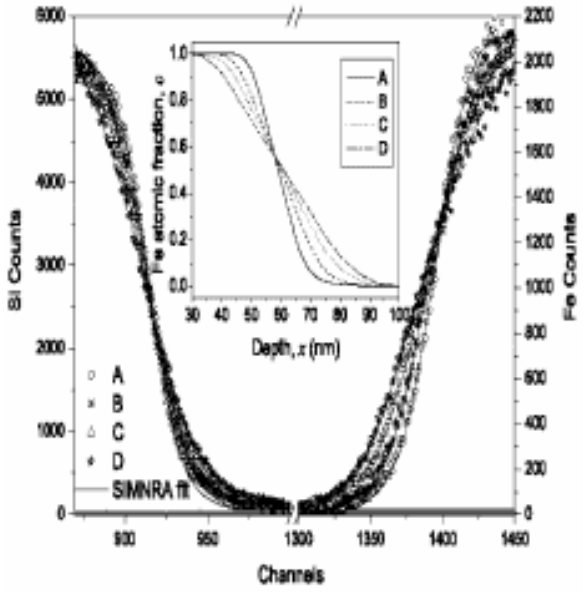

Fig. 1

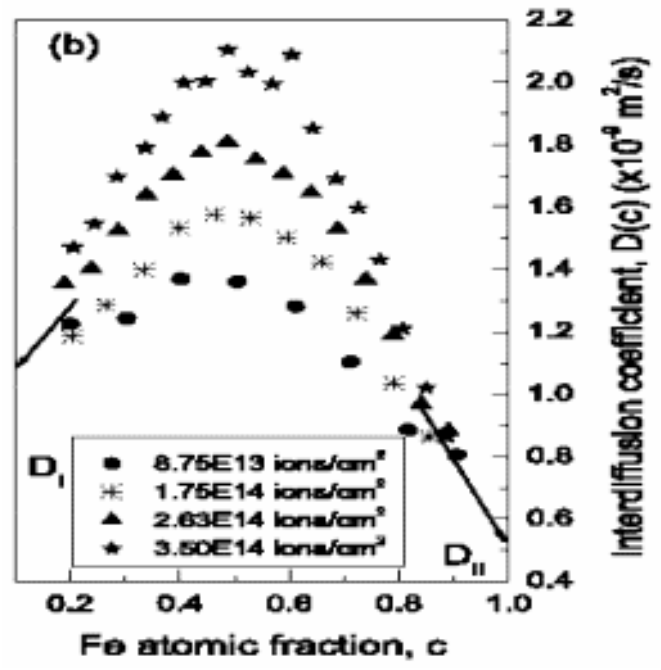

Fig. 2

magnitude less than) the literature values of diffusivities in liquid metals and liquid Si. The observed difference is due to the viscous drag of the melts along the track wall. The corresponding solid state diffusivities even at melting temperatures are 3.0×10^{-11} and 1.0×10^{-11} m^2/s, respectively[4] respectively - about two orders of magnitude less than the observed diffusivities. Therefore, the possibility of a solid state diffusion is ruled out. The hypothesis that the SHI mixing is a consequence of a transient molten state diffusion is, thus, verified [5].

REFERENCES

[1] Z.G. Wang, C. Dufour, E. Paumier, and M. Toulemonde, J. Phys.: Condens. Matter 6, 6733 (1994).

[2] Z.G. Wang, C. Dufour, S. Euphrasie, and M. Toulemonde, Nucl. Instr. Meth. Phys. Res. B 209, 194 (2003).

[3] F.Guillemot, I. Thibon, J.Debuigue, and D. Ansel, Defect and Diffusion Forum 194, 247 (2001).

[4] R.J. Borg and D.Y.F. Lai, J. Appl. Phys. 41, 5193 (1970).

[5] S.K Srivastava at al, Phys. Rev.B (In Press)

5.2.4 Zirconium silicide formation study using high-energy swift heavy ion

Veenu Sisodia[1], W.Bolse[2], D. Kabiraj[3] and I.P. Jain[1]

[1]Centre for Non-Conventional energy resources, Univ. of Rajasthan, Jaipur-302004
[2]Institut fur strahlenphysik, Allmandring 3, Stuttgart 70569, Germany
[3]Nuclear science center, New Delhi-110 067

Low specific contact resistivities are essential to realize ultra-large scale integrated circuits (ULSI) [1]. Zr is considered to be one of the candidate materials for contact with a low contact resistivity and high reliability for ULSI's. Zr system is highly sensitive to electronic excitation [2]. Si followed with Zr was evaporated on to Si substrate by means of electron beam evaporation method in the target preparation lab at Nuclear Science Centre, New Delhi, India. The base pressure in the deposition chamber was pressure of $4x10^{-8}$ Torr. Two sets of specimen were prepared with different Zr thickness. Zr film thickness in first set was ~ 25 nm with a top layer of 30 nm of Si and ~ 115 nm in the other set over Si ~ 150 nm with a top Au layer to avoid oxidation. In order to study mixing effects systematically in the samples, three sets of fluences were taken. Samples were irradiated using 350 MeV Au ions of 0.46 $X10^{14}$, 1.85 X 10^{14} and 4.62 X 10^{14} ions/ cm^2 using the accelerator at HMI Berlin, Germany. The sample temperature was held constant at LN_2 temperature. Irradiated and pristine samples were studied by RBS at the van de graff accelerator of the University of Stuttgart, using 2 MeV He^+ ions.

RBS spectra of Zr and Si thin films on Si [100] of first set for highest fluence are shown in Fig.1 and confirmed the presence of a layer of ~ 25 nm of Zr with a top layer of 30 nm of Si. RBS also confirmed the absence of oxygen at the interface. The RBS simulation using the RUMP shows the mixing of the order of roughly 50 Å for Zr/Si specimen for highest fluence. This simulation also confirms that the defects are created at the high electronic energy loss value of Au ions; 34.28 keV/nm in Zr and 19.76 KeV/nm in Si.

Diffraction spectra of the as-deposited specimen give the Bragg peaks corresponding to Zr. This system after irradiation at sufficient fluences shows crystalline peaks of Zr as well as Bragg peaks corresponding to different planes of ZrSi having d values as, d= 2.03955, 1.43276 and 1.73936 for the Au ion irradiated samples. These diffractograms and X-ray analysis clearly indicates the formation of mixed phase at the interface.

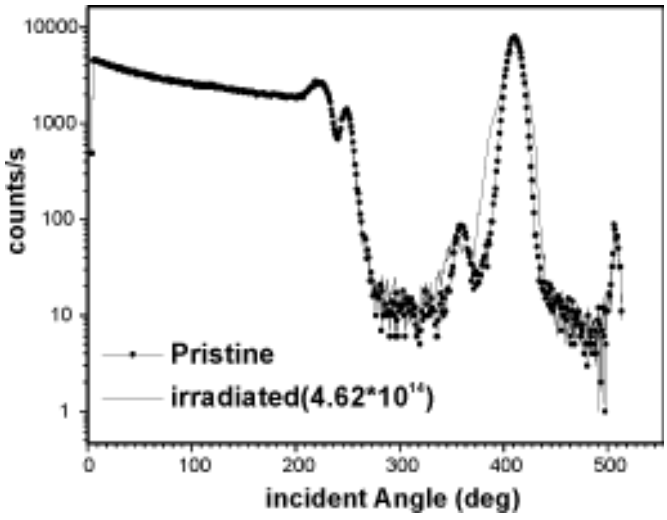

Fig. 1

REFERENCES

[1] S.Q.Wang, J.W.Mayer, J.Appl.phys 64(9), Nov(1988), 4711-4716
[2] Z.G.Wang, Ch.Dufour, E.Paumier, M.Toulemonde, Journal of Physics: Condensed Matter (6) (1994), 6733

5.2.5 Ion Beam Irradiation of Fe/Si Bilayers.

S. Senthilarasu[1], R. Sathyamoorthy[1] and D.K. Avasthi[2]

[1]R&D Dept. of Physics, Kongunadu Arts and Sc. College, Coimbatore-29, Tamil Nadu
[2]Nuclear Science Centre, P.O.Box. 10502, New Delhi 67

β-$FeSi_2$ is a novel direct band gap semiconductor and opens new fields of wide applications, e.g., for high efficiency solar cells, photodetectors, and thermoelectric devices [1,2]. Fe/Si bilayer was prepared by electron beam evaporation on (100) and (111) oriented single crystal silicon substrates. The iron coating was done under a vacuum of ~10^{-8} Torr using cryo pump and turbo based UHV evaporator. The ion irradiation was carried out at Nuclear Science Center, New Delhi using a 15UD Pelletron accelerator. The multilayer was irradiated at room temperature by 100MeV Au and Ag ions with varying fluencies of $1x10^{12}$ ions/cm^2 $2x10^{12}$ ions/cm^2, $1x10^{13}$ ions/cm^2 and $2x10^{13}$ ions/cm^2. The vacuum inside the irradiation chamber was of the order of $1x10^{-6}$ Torr. The projected range of 100MeV ions in the multilayer as calculated using TRIM95 code is about 8.93 ìm, which is greater than the total thickness of the multilayer. Thus, the bombarding ions pass through the entire film and deposit in the Si substrates. The electronic energy loss (Se) is of ~3.91keV/nm against the elastic nuclear energy loss (Sn) of 0.022 keV/nm. These multilayers in the as deposited state and after irradiation treatments were characterized by High-resolution X-ray diffraction (HRXRD) using CuK_α radiation. Vander Pauw technique was used to measure the conductivity. The conductivity measurements were made on irradiated and unirradiated samples to identify the conduction mechanism in these films.

The fig.1 shows the X-ray diffraction patterns of 100MeV Ag ion beam irradiated Fe/Si thin films at Si (100) substrate with different fluencies. The diffraction peaks at 2θ = 44.83º, 65.28º corresponding to the (421), (424) planes, allows the positive identification of the β-$FeSi_2$ phase in the films and confirms the orthorhombic β-$FeSi_2$ phase (JCPDS X-ray powder file data file 20-0532). The lattice mismatch between β-$FeSi_2$ and Si varies from about 1.2 to 5.5% depending on the type of Si substrate and epitaxial relationship [3]. The polycrystalline single phase β-$FeSi_2$ is formed during ion irradiation with swift heavy ions and nearly identical spectra were obtained for the films prepared in two different substrates Si (100) and Si (111).

As can be seen from the XRD patterns, the sample irradiated with the both ion beams shows formation of β-$FeSi_2$. The results clearly leads us to understand that the

peak intensity increase with the increase in ion fluence for the films formed on Si (100) where as the peak intensity decrease with increase in ion fluence for the film formed on Si (111). More over the Ag ion irradiation with ion fluence of $1x10^{13}$ ions/cm^2 on Si (111) induces the formation of β-$FeSi_2$ along (100) and (312) orientations with very weak intensity. The Au ion beam irradiation on Si (100) substrates the β-$FeSi_2$ phase grew along (222) orientation and it is absent in the Si (111) substrates. The crystallite size increases with increase in ion fluence whereas the dislocation density decreases with increase in ion fluence.

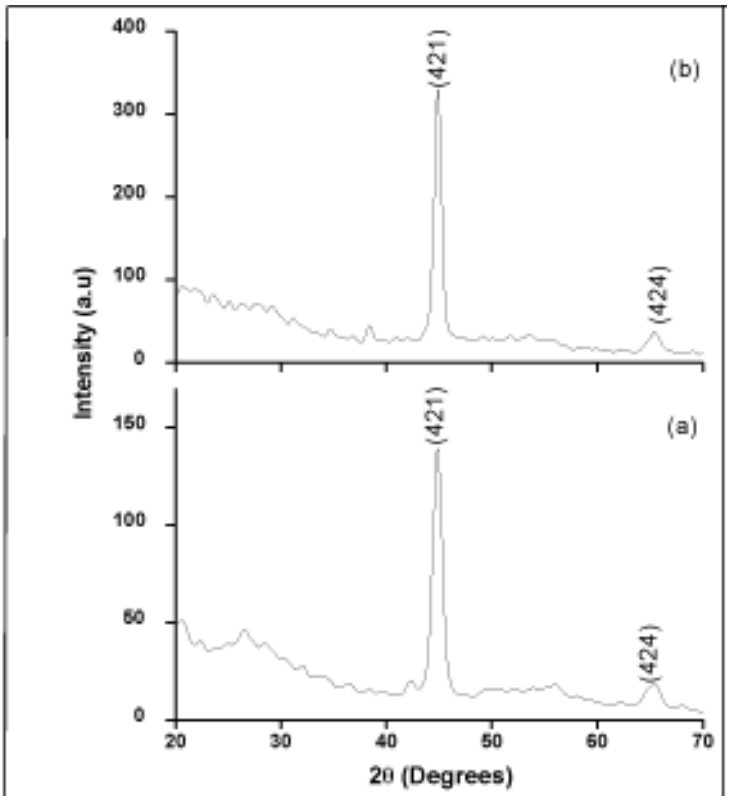

Fig. 1 : X-ray diffraction spectrum of β-$FeSi_2$ thin films on Si (100) irradiated with 100MeV of Ag ions (a) fluence at $1x10^{12}$ ions/cm^2 (b) fluence at $1x10^{13}$ ions/cm^2

Conductivity measurements were made on irradiated and unirradiated samples. It was observed that the conductivity increases with increasing temperature as expected for a semiconductor.

References

[1] P.Han and T.Yoshida J.App. Phys 92 4772 (2002)

[2] S.Fang, K.Adomi, S.Iyer, H.Morkoc, H.Zabel, C.Choi and N.Otsuka, J. App. Phys. 68 (1990)R30.

[3] J.Derrien, J.Chevrier, V.Le Thanh, J.E.Mahan, Appl. Surf. Sci. 56(1993) 382.

5.2.6 Study of Ag^{12+} ion irradiated Al-Sb and In-Sb bilayer thin films

Y.K. Vijay[1], M. Singh[1], N.K. Acharya[1], R.K. Mangal[1], Balram Tripathi[1], D.K. Avasthi[2], B.R. Shekhar[3]

[1]Department of Physics, University of Rajasthan Jaipur-302004
[2]Nuclear Science Centre, New Delhi-110 067
[3]Institute of Physics, Sachivalaya Marg, Bhubaneswar-751005

In present work, Al-Sb and In-Sb bilayer thin films were deposited using thermal evaporation (resistive heating) at the pressure 10^{-5} torr varying thickness of Sb and keeping constant thickness of Al & In. These films were irradiated by heavy Ag^{12+} ion beam having energy 160 MeV of fluence 10^{13} ions/ cm^2 at General Purpose and Scattering Chamber Nuclear Science Centre, New Delhi.

The optical absorption spectra of as deposited and ion irradiated films have been recorded at room temperature. The optical band gap of ion irradiated films give better (approachable) results compare to as deposited films. The RBS was performed using pelletron facility of Institute of Physics, Bhubaneswar using α-particles having energy 3 MeV. Above both techniques were confirmed mixing of bilayer thin film structure. The Figure 1(b) shows the variation of band gap with variable thickness that confirms the phase transformation with variable thickness. The optical photograph of untreated and ion irradiated films in Fig.2 (a&b) shows the cluster formation for Al-Sb bilayer structure after irradiation.

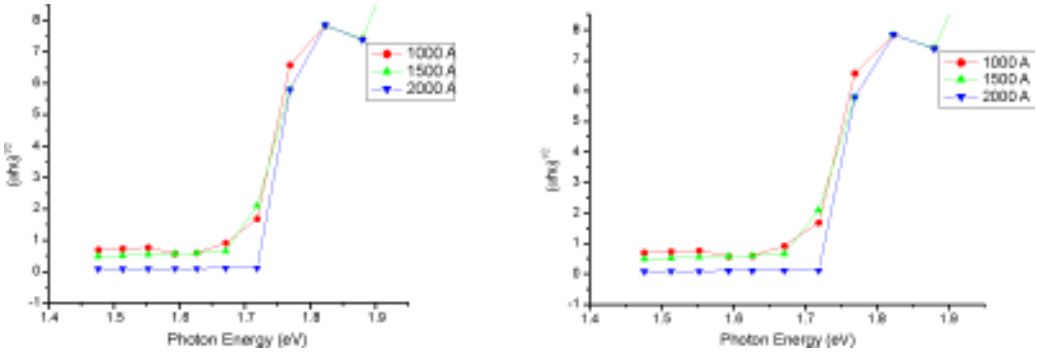

Fig. 1 : Graph showing (a) Wavelength v/s Absorption (b) Photon Energy v/s $(\alpha h\upsilon)^{1/2}$ of ion irradiated Al-Sb bilayer thin films having different thickness of antimony

Table 1: Variation of optical band gap with thickness of antimony

S.No.	Thickness of Al/In-Sb (Å)	Ion irradiated Al-Sb films (eV)	Ion irradiated In-Sb films (eV)
1.	3000-1000	1.70	0.168
2.	3000-1500	1.69	0.168
3.	3000-2000	1.71	0.168

(a) (b)

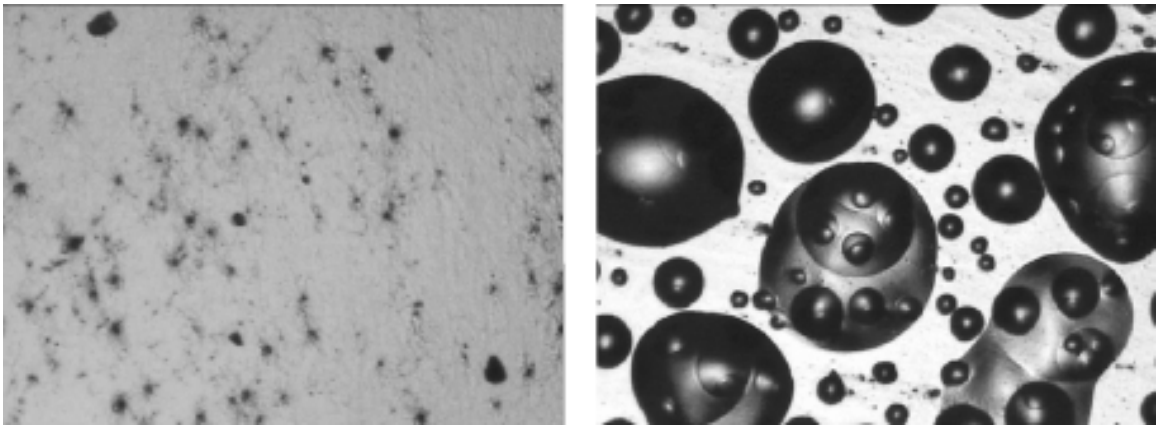

Fig. 2: Photographs of Al-Sb bilayer (a) untreated thin film (b) Ion irradiated thin film

5.2.7 Study of Au ion beam induced mixing at Co/Si interface

I.P. Jain[1], Garima Agarwal[1], Shivani Agarwal[1], Veenu Sisodia[1], Pratibha Sharma[1], A.K. Tyagi[2], D. Kabiraj[3], R.N. Dutt[3]

[1]Centre for Non-Conventional energy Resources, Univ. of Rajasthan, Jaipur 302004
[2]Indira Gandhi Centre for Atomic Research, Kalpakkam
[3]Nuclear Science Centre, Aruna Asaf Ali Marg, New Delhi-110067

For the present study the irradiation effect on the electrical properties of the Co/Si interface has been undertaken. Co thin metal film of thickness 30nm deposited on clean Si (100) substrate by electron beam evaporation at vacuum of 4 x 10^{-8} Torr at NSC, New Delhi. The Co/Si samples were irradiated by 120 MeV Au ions using 15 UD Pelletron Accelerator at NSC New Delhi having 10^{-6} Torr vacuum in the material science chamber at different fluences from 10^{12} to 10^{14} ions/cm^2 at RT. SIMS investigation revealed that the interface width incurred from 16nm to 39nm at a fluence of 10^{14} ion/cm^2

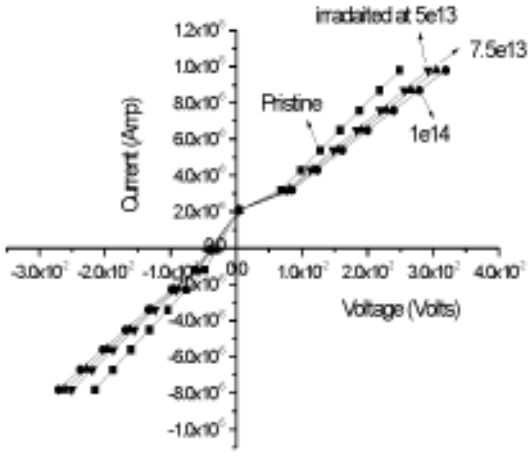

Fig. 1 : Online I-V characteristics

Online I-V measurements on Co/Si interface having top and the back contacts were carried out at RT during irradiation in the irradiation chamber, by stopping the beam every time during measurement as shown in fig 4.

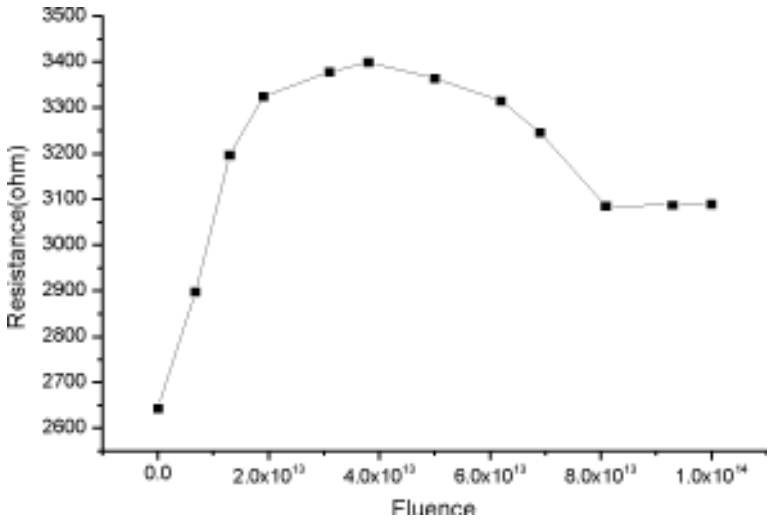

Fig. 2 : Fluence Vs resistance

All measurements show the linear behaviour confirming the ohmic contact at the metal/Si interface. The effective resistances of the samples have been estimated from the linear portion of the I-V curves. The room temperature resistance values for the pristine sample is 2.6 kΩ and for the samples irradiated at fluences $7.5x10^{13}$, $1x10^{14}$ ions / cm^2, the values are 3.2 kΩ and 3.1kΩ respectively. However for the sample irradiated at the dose $5x10^{13}$ ions / cm^2, the resistance value was found to be 3.4 kΩ which is very much higher as compared to the resistance values obtained for higher dose samples. This higher value of resistance for low dose sample is due to generation of radiation induced defect states energy levels within the energy gap and compensate the free carriers in the substrate. The comparatively lower resistance values measured for samples irradiated at higher doses of $7.5x10^{13}$ and $1x10^{14}$ ions/cm^2 indicate conduction via the defect states. Thus the electrical conduction in these samples is defect dominated. Fig. 2 shows the room temperature variation of the effective resistance calculated from the Online I-V curves, with fluence. It has been seen that at the beginning of the ion irradiation on Co/Si interface, the resistance value increases and then as the irradiation increases it goes on decreasing and after a certain higher dose of $8x10^{13}$ ions/cm^2, the resistance values continuously become constant upto the highest dose of $1x10^{14}$ ions/cm^2.

REFERENCES

[1] M. Milosavljevic, G.Shao, N. Bibic et al, Nucl. Instr. Meth Phys. Res. 188 (2002) 166.
[2] M. Masoud D.E. Arafah and K.H. Beeker, Nucl. Instr. Meth Phys. Res. 198 (2002) 64.
[3] S. Dhar, P.Schaaf, K.P. Lieb et al, Nucl. Instr. Meth Phys. Res. 205 (2003) 741.

5.2.8 Synthesis of surface alloy by nanomixing

T. Som[1], B. Satpati[1], P.V. Satyam1[*], D. Kabiraj[2] and D. Kanjilal[2]

[1]Institute of Physics, Sachivalaya Marg, Bhubaneswar - 751 005
[2]Nuclear Science Centre, Aruna Asaf Ali Marg, New Delhi - 110 067

In this work, we demonstrate room temperature (RT) synthesis of Au-Ge alloy on a Si surface covered with a thin native oxide layer. It can be mentioned here that Au-Ge alloy has a low resistivity (~10^{-6} Ω-cm or less) and is used as ohmic contact on n-type GaAs [1]. Sequential deposition of 1 nm each Ge and Au layers were performed in UHV evaporator on an ultrasonically cleaned p-type Si (100) wafer. The samples were irradiated by 1.5 MeV Au^{+2} ions at RT with different fluences in the range of 1×10^{13} to 1×10^{15} ions cm^{-2}. We also used 800 keV Ar and Xe ions over a fluence range of $0.5\text{-}2\times10^{16}$ ions cm^{-2}. Ar and Xe irradiations were performed at NSC using the LEIBF, while the Au-ion irradiation was performed using the IOP Pelletron accelerator. A uniform irradiation was achieved for all the samples using a 1×1 cm^2 scanned beam. Irradiations were performed at a normal incidence and using a secondary electron suppressed geometry. During irradiation, a clean vacuum of 1×10^{-7} mbar (or even better) was maintained in the chamber. Samples were analyzed using a JEOL UHR2010 transmission electron microscope (TEM) under planar and cross-sectional geometries.

The microstructure of the pristine sample is studied by TEM, which reveals that particles are more or less circular in nature with an average particle size of ~5 nm. Rutherford backscattering spectrometric analysis is employed to determine the effective thickness of the Au and Ge island films, which are given by 2.1×10^{16} and 7.4×10^{15} at. cm^{-2}, respectively. A careful observation reveals the lattice fringes from some of the islands, whose d-spacings match well with only that of Au. However, we did not see any signature of crystallinity close to Ge, which indicates that either the growth of the Ge nanoislands was amorphous in nature or they became oxidized upon exposure to air. The presence of a thin (~2 nm) native oxide layer on Si substrate is also evident from the cross-sectional TEM (XTEM) study. The island thin film structures, upon RT irradiation by 1.5 MeV Au ions up to the fluence of 1×10^{13} ions cm^{-2} do not show any significant change as revealed by the TEM measurements. However, at this fluence Au islands start forming bigger islands through coalescence [2].

Fig. 1 presents the plan-view TEM micrograph of a specimen irradiated to a fluence of 1×10^{14} ions cm^{-2}. It is observed that worm-like bigger islands with a wide size distribution (6-30 nm parallel to the surface) are formed. High-resolution lattice imaging obtained from one such bigger island indicates to have a d-spacing (0.309±0.01 nm), which but matches quite well with the (225) plane of metastable γ-$Au_{0.6}Ge_{0.4}$ [3]. We have performed high-resolution lattice imaging from many big islands to observe the close proximity of their d-spacings to that of tetragonal $Au_{0.6}Ge_{0.4}$ alloy phase. Thus, irradiation of Au/Ge nanoislands thus, leads to the formation of nano-dimensional Au-Ge

alloy islands at the surface due to RT irradiation of 1.5 MeV Au^{2+} ions using a fluence of 1×10^{14} ions cm^{-2}. Islands of similar shapes (but much bigger in size: up to 50 nm) are formed corresponding to a higher fluence of 1×10^{15} ions cm^{-2} [3].

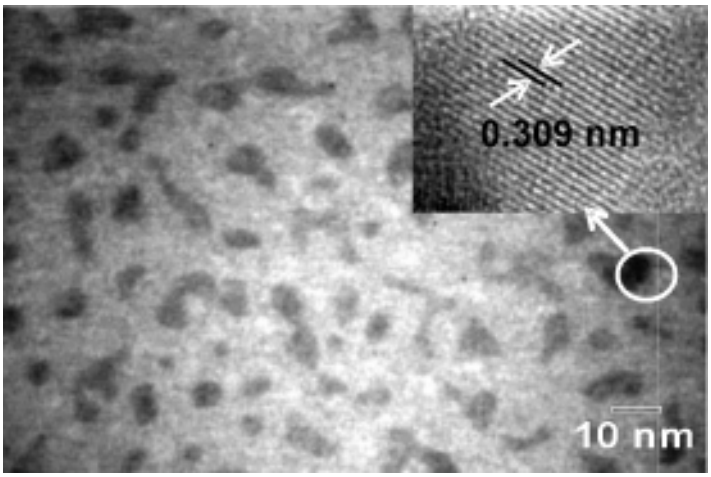

Fig. 1 : Plan-view TEM mcirograph of Au/Ge island thin films irradiated by 1.5 MeV Au^{2+} ions at RT with a fluence of 1×10^{14} ions cm^{-2}.

We have also irradiated the island thin films by 800 keV Ar and Xe ions in the fluence range of $0.5\text{-}2\times10^{16}$ ions cm^{-2}. The XTEM micrograph obtained from Au/Ge island thin film structure irradiated with Ar ions corresponding to a fluence of 1×10^{16} ions cm^{-2}, shows isolated island structures of nearly similar dimension (18±2 nm) to get formed parallel to the surface, where the presence of native oxide is also evident. High-resolution lattice imaging obtained from a bigger island shows a d-spacing of 0.306±0.01 nm that matches well with that of (225) reflection of $Au_{0.6}Ge_{0.4}$ alloy phase. On the other hand, 800 keV Xe ion-irradiated Au/Ge island thin film shows a nearly continuous layer formation of Au-Ge alloy corresponding to the similar ion fluence of 1×10^{16} ions cm^{-2}. Therefore, it is clear that Au-Ge alloy nanoislands of different size distribution can be formed by varying the ion mass, energy and/or fluence.

REFERENCES

[1] A..P. Pitrowska, A. Guivarch, and G. Pelous, Solid-State Electron. 26 (1983) 179.
[2] T. Som, B. Satpati, P.V. Satyam, and D. Kabiraj, J. Appl. Phys. 97 (2005) 014305.
[3] T.R.Anantharaman, H-L. Luo, and W.Klement, Jr., Trans.Am.Inst. Min. Eng. 283 (1965) 2014.

5.2.9 Ion Beam Modification and Analysis of Organometallics Dispersed Polymer Films

Anjum Qureshi[1], N.L.Singh[1*], A.K. Rakshit[2], F. Singh[3], D.K. Avasthi[3], V.Ganesan[4]

[1]Physics Department, M. S. University of Baroda, Vododara-390002

[2]Chemistry Department, M. S. University of Baroda, Vododara-390002
[3]Nuclear Science Centre, New Delhi-110067, India.
[4]UGC-DAE Consortium for Scientific Research, University Campus, Indore-452017

Thin films of Polymethyl methacrylate (PMMA) were synthesized. Ferric oxalate (fo) was dispersed in PMMA films at various concentrations (i. e. 5%, 10% & 15%). These films were irradiated with 80MeV O^{6+} ions at a fluence of 1×10^{11} ions/cm^2 at NSC, New Delhi. The radiation induced changes was studied by electrical conductivity, microhardness tester, and atomic force microscopy (AFM).

AC electrical measurement was performed for pristine and irradiated samples. Fig.1 shows the variation of conductivity with log of frequency for the irradiated samples at different fo concentrations.

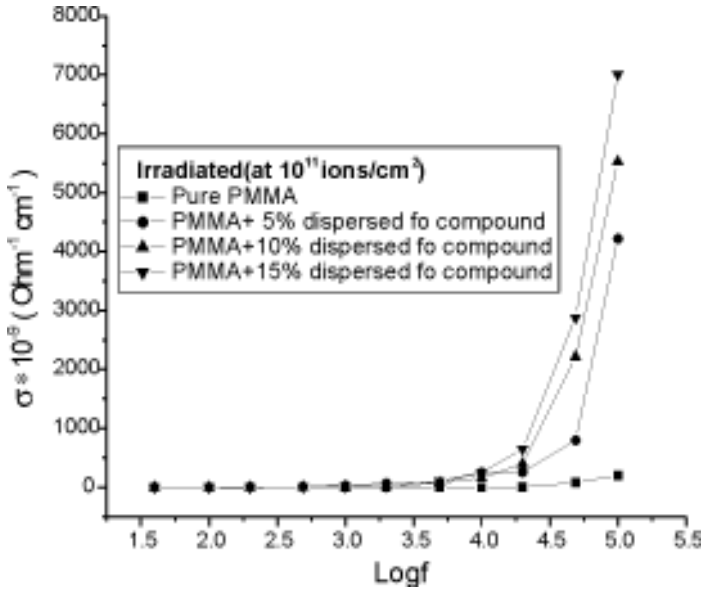

Fig. 1

It is observed from Fig.1 that after the irradiation the conductivity increases with the increasing concentration of dispersed organometallic compound. It is expected to promote the metal to polymer adhesion and convert the polymeric structure to a hydrogen depleted carbon network.

Fig. 2 Shows the plot of the Vickers' microhardness (Hv) versus applied load (P) for irradiated films of pure PMMA, and dispersed fo compound of 5%, 10% and 15% in PMMA films. It is found that hardness increases as fo concentration increases. It may be due to the improvement in bonding properties. The hardness also increases on irradiation of the samples. This may be attributed to hydrogen depleted carbon network which make polymer harder.

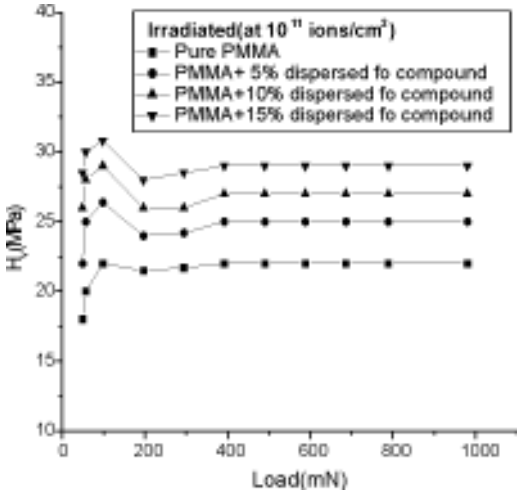

Fig. 2

The surface morphology of pristine and irradiated films of pure PMMA, and dispersed for compound of 15% in PMMA was measured by AFM on 2×2μm^{2}area and are shown in Fig 3.

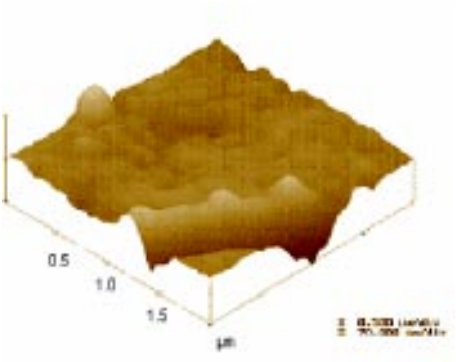

Fig. 3(a) : pure PMMA film (pristine)

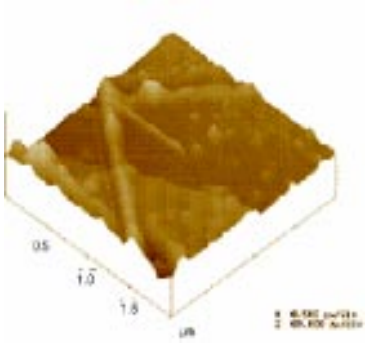

Fig. 3(b) : pure PMMA film (irradiated)

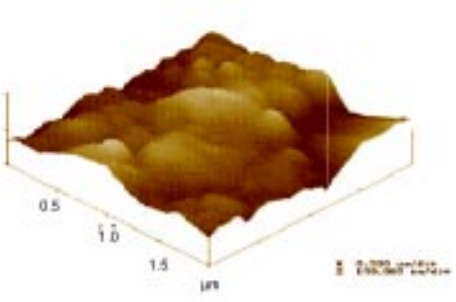

Fig. 3(c) : dispersed fo 15% in PMMA film film (pristine)

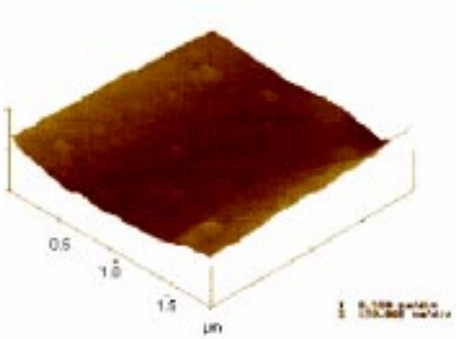

Fig 3(d) dispersed fo 15% in PMMA (Irradiated)

Each AFM image is analyzed in terms of surface average roughness (Ra). The roughness values are 13nm and 26nm for pristine and 6nm and 19.52nm for irradiated (at the fluences of 10^{11} ions/cm^2) samples respectively. The increase in roughness may be due to the increase of density and size of metal particles on the surfaces of the PMMA films. It is also observed that after irradiation the roughness of the surface decreases and the surface becomes significantly smoother. This relative smoothness is probably due to the sputtering effects.

REFERENCES

[1] P. S. Ho, R. Height, R. C B. D. Silverman and F. Faupel, in: Fundamentals of Adhesion, edited by L. H. Lee, (Plenum Press, New York, 1991) p. 383.

[2] V. Zaporojtchenko, T. Strunskus, K. Behnke, C. von Bechtolsheim, M. Keine and F. Faupel, J. Adhesion Sci. Technol., 14 (2000), p. 467.

5.2.10 Swift heavy ion induced conducting tracks formation in C_{60}

A. Tripathi[1], D. Kabiraj[1], A. Kumar[1], S.A. Khan[1], V. Baranwal[2] and D.K. Avasthi[1]

[1]Nuclear Science Centre, New Delhi, 110 067
[2]Department of Physics, Allahabad University, Allahabad, 211 002

The swift heavy ion (SHI) irradiation induced surface modifications of C_{60} (fullerene) has been widely studied using surface/ near surface study tools such as scanning tunneling microscope (STM) and atomic force microscope (AFM). SHI induced surface modifications of C_{60} which have shown dimerisation, polymerization and damage of C_{60} film have been studied by different groups [1-3] . Though the increase in conductivity of irradiated C_{60} samples was observed earlier in bulk, no such measurement at microscopic level was available. In this work we report observation of conducting ion tracks in C_{60} films.

Fullerene thin films were deposited on Si(100) substrate in a vacuum of $1x10^{-6}$ torr by resistive heating of commercially available 99.9% pure C_{60} in a Ta boat. The thickness of the film as measured by quartz crystal thickness monitor was 150 nm. A layer of Au was first deposited on the Si substrate and it was used for making the contact (Figure 1) so to be able to measure the conductivity across the C_{60} layer. The samples were irradiated with 120 MeV Au ion beam (S_e=18.2 keV/nm, S_n=215 eV/nm) from NSC Pelletron with fluences of $2x10^{10}$, $6x10^{10}$, $2x10^{11}$ and $5x10^{11}$ ions/cm^2. Samples irradiated with higher flunce are not discussed here so as to emphasize single ion induced effects. The properties of these channels were studied by means of conducting atomic force microscopy (C-AFM) using a diamond coated silicon nitride (DDESP) tip. The topographic and conductivity features are studied with Nanoscope IIIa AFM at NSC, New Delhi.

Initial measurements were done for un-irradiated samples but no current was observed for the sample bias of up to 10V, thus showing the insulating nature of the

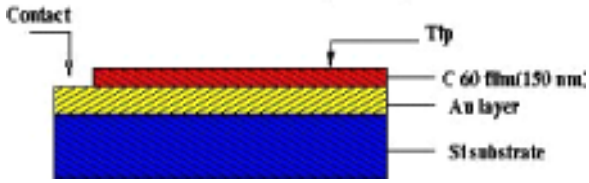

Fig. 1 : The arrangement for making the contact for measurement

fullerene film. However for the irradiated samples current of the order of 5 nA was observed for a bias of 500 mV. A typical current image of sample irradiated with 120 MeV Au ions with a fluence of $2x10^{10}$ ions/cm^2 is shown in figure 2.

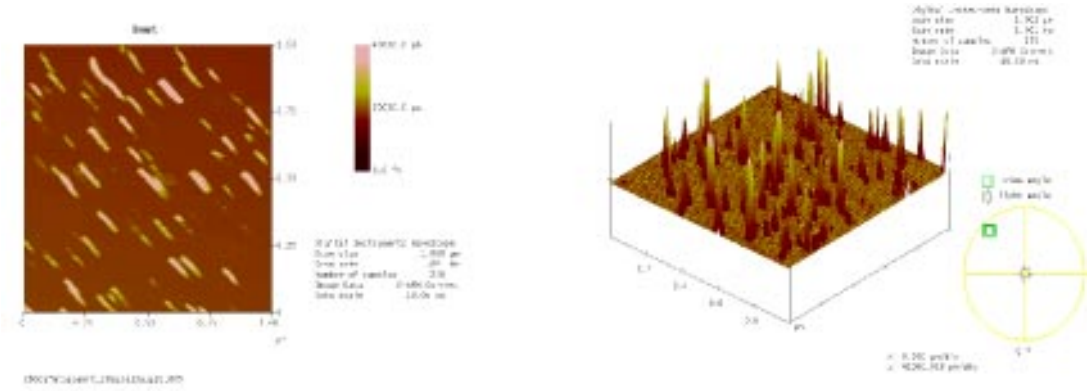

Fig. 2 : 2D and 3D 1μ x 1μ icurrent images of C_{60} film irradiated wth 120 MeV Au ions ($2x10^{10}$ ions/cm^2). The conducting impact sites are shown by high current bright zones.

The conducting impact sites are shown by high current bright zones. The image clearly shows high current zones separated by insulating zones. The increase in conductivity is attributed to electronic energy loss induced transformation from insulating C_{60} to conducting graphite like carbon. The number of these zones doesn't match with fluence showing a ratio of 0.4 impact sites per ion. The three dimensional image is also shown. As is clearly seen in figure, the image shows different heights for current peaks. This is attributed to very close/ overlapping ion impacts resulting in increased current at these spots. Such overlapping tracks also explain the factor of 0.4 between impact sites per ion.

The current image of sample irradiated with a fluence of $2x10^{11}$ ions/cm^2 is shown in figure 3. As is clearly seen many more impact zones are seen. As the fluence is further increased to $5x10^{11}$ ions/cm^2, the overall conductivity increases. The current image shows that the number of high current zones is much higher and average current increases to approximately 10 nA. The current image now loses a clear contrast as insulating zones showing zero conductivity have disappeared**.**

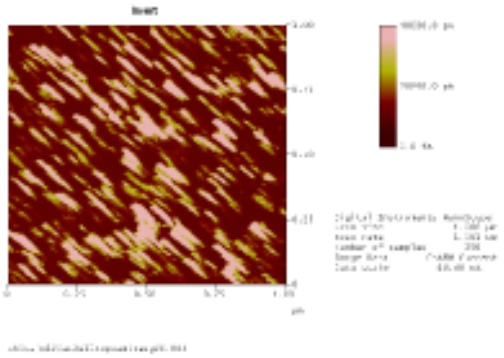

Fig. 3 : 1μ x 1μ Current image of a C_{60} film irradiated with 120 MeV Au ions ($2x10^{11}$ ions/cm^2). Many more impact zones are seen.

The I-V characteristic showing the current between the substrate and the AFM tip as a function of bias voltage is presented in figure 5 for ion impact zones. The measurements shown are plotted for 5 times averaged values. The increase in conductivity with increasing fluence, is due to the combination of single ion impacts as mentioned earlier.

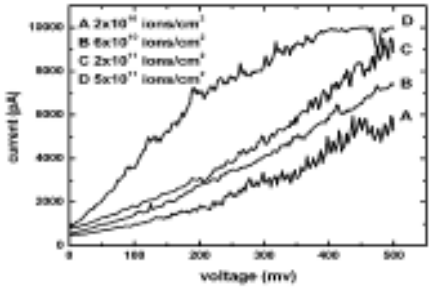

Fig. 4 : The current between the substrate and the AFM tip as a function of bias voltage

REFERENCES

[1] A. Itoh et al, , Nucl. Instru. And Meth. B129, (1997),363.
[2] N. Bajwa et al, J. Appl. Phys, 94, (2003), 326.
[3] S. Lotha, et al, Solid State Commun. 111, (1999),55.

5.2.11 SHI induced surface modification studies of HOPG using STM

A. Tripathi[1,2], S.A. Khan[1], M. Kumar[2], V. Baranwal[2], R. Krishna[2], A.C. Pandey[2] and D.K. Avasthi[1]

[1]Nuclear Science Centre, New Delhi 110067
[2]Department of Physics, University of Allahabad, Allahabad

The irradiation with swift heavy ions (SHI) has become one of the most important methods of surface modification of solids. The slowing down of energetic heavy ions creates a zone of intense electronic excitation along its path and the resulting surface modifications have been widely studied with scanning tunneling microscope (STM) [1] and other surface/ near surface study tools such as atomic force microscope (AFM) and transmission electron microscope (TEM). The defect structures created by low energy impacts were studied earlier, though the work with SHI with ion velocities comparable to electron Bohr velocity (2.2×10^6 m/s), started more recently. The large energy (few keV/ nm) deposited by SHI around their path in a small cylindrical zone of the order of few nanometres affects the lattice drastically. This results in dramatic modifications in bulk and on surface including breaking of atomic bonds [2], formation of latent tracks [3] and ejection of atoms and molecules [4,5].

The surface modifications induced by swift heavy ions (SHI) in various carbon allotropes, such as highly oriented pyrolytic graphite (HOPG), diamond-like carbon (DLC) and amorphous carbon (a-C), etc. have previously been studied using different surface characterization tools such as STM and AFM [6-8]. In our earlier study, HOPG samples irradiated with 200 MeV Au beam were studied with STM [8]. In the present work, we have studied 150 MeV Au ions induced surface modifications by STM.

The HOPG samples used in the study were irradiated with 150 MeV Au ions (S_e=19.6 keV/nm and S_n=180 eV/nm). A fresh surface is prepared by cleaving the samples before irradiation. The topographic features of the HOPG samples are studied with Digital Multimode SPM with Nanoscope IIIa controller at NSC. HOPG being a semi-metal with a conducting surface, the samples are studied in STM mode. Pt/Ir tip is used for scanning the samples. For the measurement the bias current is kept at 500 mV whereas a preamplifier gain of 1×10^8V/A is selected. To obtain the images with atomic resolution a 400-nm scanner is used.

The STM study of an unirradiated HOPG sample shows atomically resolved images of carbon atoms. The topographic image shows three to hexagonal moire pattern with an inter-atomic distance of ~2.5 Å as expected (Figure 1). The samples irradiated with 150 MeV Au ions at a low fluence (1×10^{11} ions/cm^2) show the formation of hillocks with a mean diameter of about 6.2 nm. A typical image is shown in Figure 2. With increasing fluence (1×10^{12} ions/cm^2 and 1×10^{13} ions/cm^2) the hillock diameter decreases to 2.2 nm and 1.5 nm respectively as shown. Sputtering from surface leading to formation of small craters is also seen. No hillocks were observed for the sample irradiated with fluence of 2×10^{13} ions/cm^2 , though the formation of small craters at some places is observed. It should be noted that the hillocks which are nearer to the surface will show a larger dimension as compared to those which are deeper away from the surface due to finite tip dimensions and hence we have assumed the dimension of the hillocks where lateral and vertical dimensions are comparable.

The formation of hillocks in the present case has been attributed to nuclear

energy loss induced collision cascades which take place near the surface and are responsible for displaced atoms forming clusters. As the fluence is further increased, electronic energy loss induced sputtering effects remove the surface layers and subsequent reduction in the hillock diameter is seen. Even though continuous tracks are not expected at these energies, the amorphization of the material in discontinuous isolated tracks will result in higher electronic sputtering from these zones. At even higher fluences, the amorphised hillock formation zones, which have a higher sputtering rate contribute in formation of craters.

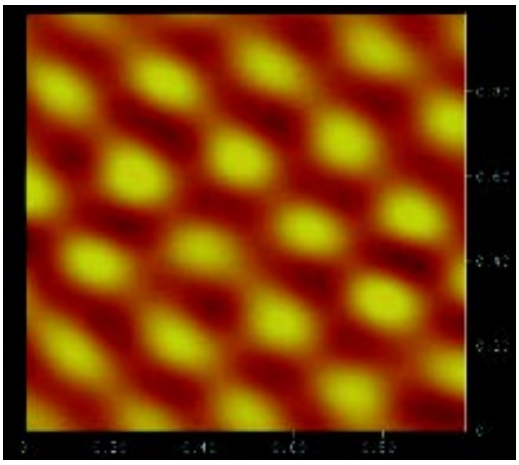

Figure 1

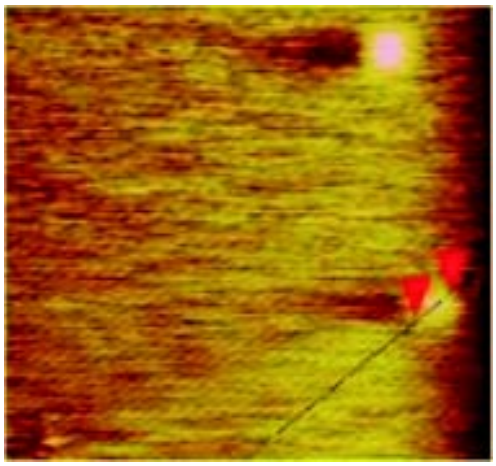

Figure 2

REFERENCES

[1] G. Binnig, H. Rohrer, Ch. Gerber and E. Weibel, Phys. Rev. Lett., 49,57 (1982).

[2] H. Dammak, A. Dunlop, D. Lesuer, A. Brunnelle, S. Della-Negra, Y.L. Beyec, Phys. Rev. Lett., 74, 1135, (1995).

[3] S. Ghosh, A. Tripathi, T. Som, S.K. Shrivastava, V. Ganeshan, D.K. Avasthi, Rad. Eff. and Defects, 154, 151, (2001).

[4] C. Trautmann, M. Toulemonde, K. Schwartz and A. Muller, Nucl. Instru and Meth, B164/ 165,365(2000).

[5] E.M. Bringa and R.E. Johnson, Phys. Rev. Lett 88,165501(2002).

[6] J. Liu. M.D. Hou, C.L. Liu, Z.G. Wang, Y.F. Jin, P.J. Zhai, S.L. Feng and Y. Zhang, Nucl. Instr. and Meth B146(1998)356.

[7] J. Liu, R. Neumann, C. Trautmann, and C. Muller, Phys. Rev. B64(2001)184115.

[8] A. Tripathi, J.P. Singh, R. Ahuja, R.N. Dutt, D. Kanjilal, Ayan Guha, Amlan Biswas, A.K. Roychaudhari, Rev. Sci. Instr. 72(2001)3884.

5.2.12 XPS study of swift heavy ion irradiated Fullerene (C_{60}) films

Amit Kumar[1], F. Singh[1], Govind[2], S. M. Shivaprasad[2], J. C. Pivin[3], D. K. Avasthi[1]

[1]Nuclear Science Centre, New Delhi 110067
[2]Surface Physics and nanostructures, NPL, New Delhi 110060
[3]CSNSM, 91405 Orsay Campus, France

Structure modification of fullerene thin films induced by swift heavy ion irradiation have been investigated. Thin films of fullerene deposited by thermal evaporation on Si substrate. These films have been irradiated with 200 MeV Au^{+15} ions at fluences from 3×10^{10} to 1×10^{13} ions/cm^2. The changes in the C 1s core level peak and its shake-up satellite of pristine and irradiated fullerene have been studied by X-ray photoelectron spectroscopy (XPS). It is observed that the binding energy of C 1s core level peak for the irradiated C_{60} film is lower than pristine film and the FWHM also shows broadening in the ion irradiated C_{60} films as shown in figure 1a. The lineshift and FWHM broadening of C 1s core level peak is due to formation of sp3 hybridization form by addition of two fullerene molecule [1,2]. Figure 1b shows the enlarged region to see the change in the shake-up satellite. It is found that the intensity of the C 1s shake-up satellite peak decreases with increasing ion fluence, manifesting the decrease of the number of conjugated pi-electron on C_{60} molecules upon ion irradiation [2]. This is interpreted as a consequence of polymerization of the C_{60} molecule by the bonds forming cycloadditional bonds.

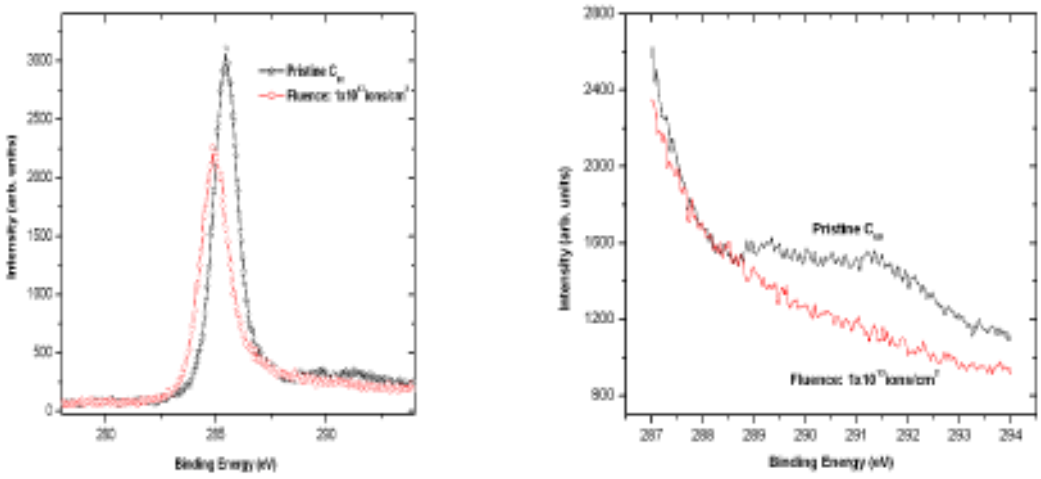

Figure 1. a) XPS spectra of C 1s core peak, b) XPS spectra of the C 1s shake-up satellite, of the fullerene film before irradiation and after 200 MeV Au ion irradiation.

REFERENCES

[1] D. M. Poirer et al., Surf. Sci. Spectra 2,239 (1994).
[2] Jun Onoe et al., Phy. Rev. B, 55, 10051 (1997).

5.2.13 Irradiation Effects of 190 MeV Ag Ion on the Properties of $Ni_{0.65}$ $Zn_{0.375}$ $In_{0.10}$ $Ti_{0.025}$ $Fe_{1.85}$ O_4 Ferrite Nanoparticles

B. Parvatheeswara Rao[1], P.S.V. Subba Rao[1], A. Mahesh Kumar[1], K.H.Rao[1], V.V. Siva Kumar[2], K. Asokan[2], Ravi Kumar[2] and O.F. Caltun[3]

[1]Department of Physics, Andhra University, Visakhapatnam 530 003, India
[2]Nuclear Science Centre, New Delhi110 067
[3]Department of Electricity and Electronics, A.Z. Cuza University, Iasi, Romania

The aim of this study is to carry out structural, magnetic and resonance parameters of ball milled Ni-Zn-In-Ti ferrite nanoparticles both before and after 190 MeV Ag ion irradiations and understand the modifications in the light of the ion induced disorder.

Sintered pellets of the ferrite system, $Ni_{0.65}\ Zn_{0.375}\ In_{0.10}\ Ti_{0.025}\ Fe_{1.85}\ O_{4,}$ have been ground to make nano scale particles using a ball mill for 5 hours with a ball-to-powder ratio of 10:1. One part of the resulting powder was kept as pristine and another part was irradiated with 190 MeV Ag ion with different fluences in the range from 5×10^{11} to 1×10^{13} ions/cm^2 using the 15 UD Pelletron Accelerator system at NSC. The samples were then characterised by X-ray diffraction technique to establish cubic spinel structure. Typical XRD patterns of unirradiated and irradiated samples with a fluence of 1×10^{13} ions/cm^2 are shown in figure 1 and 2. Both the samples showed all major peaks related to a cubic spinel structure reported for ferrites, but smaller intensities and slightly larger peak broadening were observed for irradiated sample. The lattice constants of pristine and irradiated samples are found to be 0.8402nm and 0.8395nm respectively. Particle sizes for these samples are estimated using Scherrer equation while taking into account of instrumental broadening and they are found to be 6.8 and 5.2 nm respectively for pristine and irradiated samples.

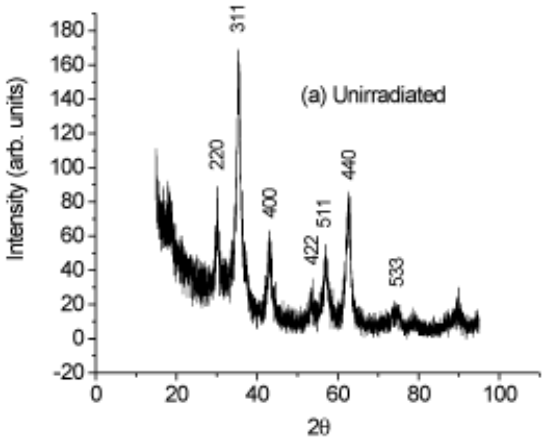

Fig. 1 : XRD pattern of unirradiated ball milled $Ni_{0.65}\ Zn_{0.375}\ In_{0.25}\ Ti_{0.025}\ Fe_{1.70}\ O_4$ particles

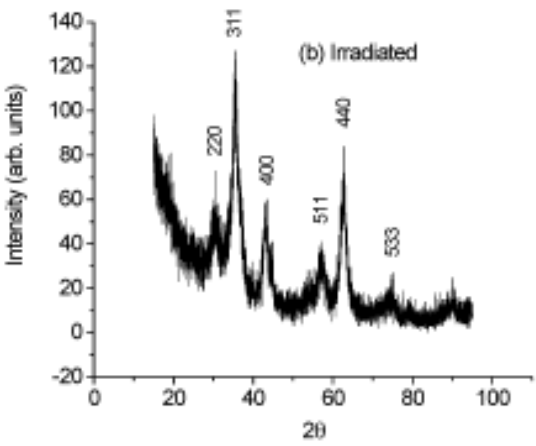

Fig. 1 : XRD pattern of irradiated ball milled $Ni_{0.65}\ Zn_{0.375}\ In_{0.25}\ Ti_{0.025}\ Fe_{1.70}\ O_4$ particles with a fluence of 1×10^{13} ions/cm^2

Though the irradiations have made marked impact from XRD study, further studies of magnetisation, FMR and SEM are underway for both pristine and irradiated samples with a view to estimate the impact of irradiations more clearly.

5.2.14 Swift Heavy Ion Induced Modifications in Coprecipitated Mn-Zn Nanoferrites

B. Parvatheeswara Rao[1], K.H.Rao[1], P.S.V. Subba Rao[1], A. Mahesh Kumar[1], S. Srinivasa Rao[2], Y.L.N. Murthy[2], K. Asokan[3], Ravi Kumar[3] and O.F. Caltun[4]

[1]Department of Physics, Andhra University, Visakhapatnam 530 003, India
[2]Department of Chemistry, Andhra University, Visakhapatnam 530 003, India
[3]Nuclear Science Centre, New Delhi110 067
[4]Department of Electricity and Electronics, A.Z. Cuza University, Iasi, Romania

Synthesis of nanoparticles is of great interest in recent times for studying and tailoring of desired magnetic properties. Soft magnetic materials of the kind of Mn-Zn ferrites find large number of applications as they combine useful electromagnetic parameters. In order to study the effect of heavy ion irradiations, the sample of $Mn_{0.75}$ $Zn_{0.18}$ Fe_{67} O_7. was irradiated with 190 MeV Ag ion with a fluence of 5×10^{12} ions/cm^2 using the 15 UD Pelletron Accelerator system at NSC. The samples were then characterized by X-ray diffraction and vibrating sample magnetometer techniques.

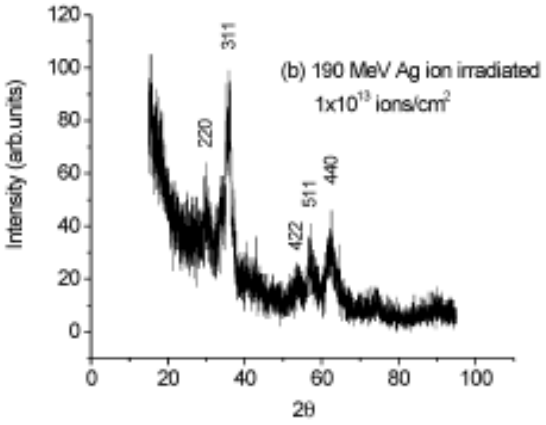

Fig. 1 : X-ray diffraction pattern of irradiated $Mn_{0.75}$ $Zn_{0.18}$ $Fe_{2.07}$ O_4 particles

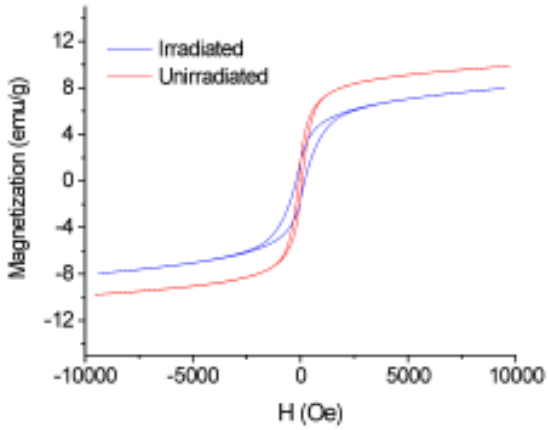

Fig. 2 : Hysteresis loops of unirradiated and irradiated $Mn_{0.75}$ $Zn_{0.18}$ $Fe_{2.07}$ O_4 particles

Though the XRD patterns of the materials exhibit spinel structure, it appears that there is only a low degree of crystallinity present as evident from the pattern of irradiated sample shown in figure.

The particle sizes of the pristine and irradiated samples have been estimated using the high intensity XRD peak and the Scherrer equation [1] while taking into account the instrumental broadening [2], and the values are observed to be 3.9 and 2.4 nm respectively for unirradiated and irradiated samples. The irradiation of high energy as a result of inelastic collisions in their trajectory with the host atoms and molecules brings about a reduction in the particle size as well as slightly amorphizing the column as evidenced from the figure.

Hysteresis loops of the sample for unirradiated and irradiated states are shown in fig.2. The samples are not saturated even at 10 kOe and exhibited small hysteresis loss which is even still smaller for the irradiated sample. The irradiated sample showed lower

magnetisation and larger hysteresis loss compared to the unirradiated sample. The coercivities are observed to be large in both the cases. The small particles of a few nanometer size lying in mono domain state of these samples with large coercivities and vanishing nature of hysteresis are typical of superparamagnetic character [3]. Further results are underway to complement the observations made in this study.

REFERENCES

[1] B.D.Cullity, Elements of X-ray diffraction, Adison –Wesley Publ. Co., London (1967).
[2] X. Zeng et al, Mater. Chem. Phys. 77, 209 (2002)
[3] K. Mandal, S. Chakravorty, S. Pan Mandal, P.Agudo, M. Pal and D. Chakravorty, J. Appl. Phys. 92, 501 (2002)

5.2.15 Nanopatterning in metglas thin films by Swift Heavy Ion irradiation

[1]Hysen Thomas, [2]Raju V.Ramanujan, [3]D.K.Avasthi, [4]P.A.Joy, [1]M.R.Anantharaman

[1]Department of Physics, Cochin University of Sc. and Technology, Cochin 682022
[2]School of Materials Engineering, Nanyang Technical University, Singapore 639798
[3]Nuclear Science Centre, New Delhi 110 067
[4]National Chemical Laboratory, Pune 411 008

Thin films of METGLAS^{TM} ($Fe_{40}Ni_{38}B_{18}Mo_4$) magnetic amorphous alloys are important because of their potential applications in devices like sensors, GMR films etc [1-3]. This report presents an investigation carried out using the 15 UD Pelletron accelerator at Nuclear science centre, New Delhi.

Thin films of amorphous alloys having the initial composition $Fe_{40}Ni_{38}B_{18}Mo_4$ were grown on ultrasonically cleaned glass substrates by two different techniques. Metglas ribbons having the composition $Fe_{40}Ni_{38}B_{18}Mo_4$ were vacuum evaporated under high vacuum of $1x10^{-6}$ using Molybdenum boat. In a similar manner these ribbons were also subjected to electron beam evaporation and thin films having thickness lying in the range of 30-100nm were prepared. These thin film samples were also annealed at different temperatures ranging from 100-500^{0}C under high vacuum conditions. Bombardment of SHI on these films can induce latent tracks, facilitate amorphization and nanocrystallization. These pristine samples were then evaluated for their structural and magnetic properties by VSM. A representative hysteresis loop of the as prepared thin film is shown in figure 1. These samples were then subjected to 120 MeV Au^{+9} beam with fluences ranging from $1x10^{11}$ to $3x10^{13}$.

The initial AFM studies carried out on this thin film samples indicate that the as prepared samples are crystalline. However it must be mentioned here that the phases present in the ribbon as well as the as grown films differ considerably from that of the reported phases for bulk ribbons [4]. It can be seen that the nonmagnetic phase present in the sample is simple cubic $(FeNiMo)_{23}B_6$ [5]. The results of AFM and MFM studies

carried out on the SHI irradiated samples are very interesting. Representative AFM and MFM of selected samples are depicted Fig 2a, 2b & 2c. It can be seen that regular patterning is visible at a fluence of $1x10^{11}$. This is found to be reproduced in the MFM patterns too.

Further, the periodicity of the patterning [6] is found to be decreasing at higher fluences. At the same time indications of the formation of latent tracks can be observed at higher fluences, which is evident from the AFM images. This indicates that the irradiation of SHI on these films is not only useful for studying the fundamental aspects but also for creating patterns. VSM studies on irradiated samples also indicate that they are magnetic in nature with low coercivity. Laser damage studies are also conducted on these samples to study the damage threshold and it was found that the samples are relatively stable and have a good damage threshold.

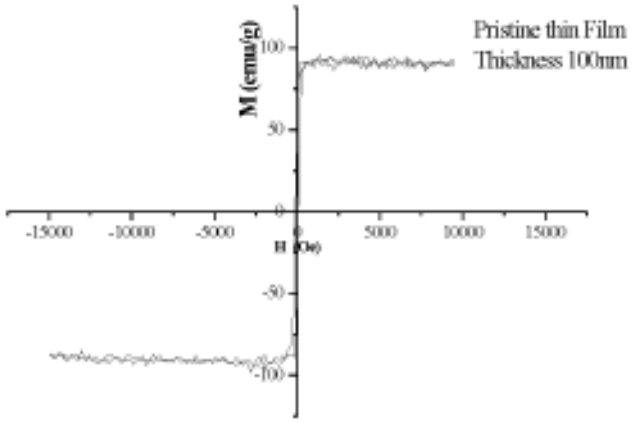

Fig. 1 : VSM of Pristine Thin Film (EBE).Thickness 100nm

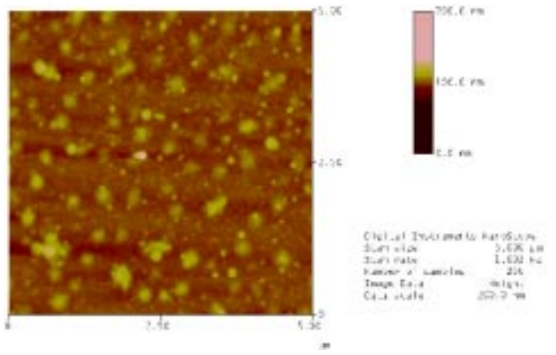

Fig. 2a : AFM Image of Pristine Thin Film

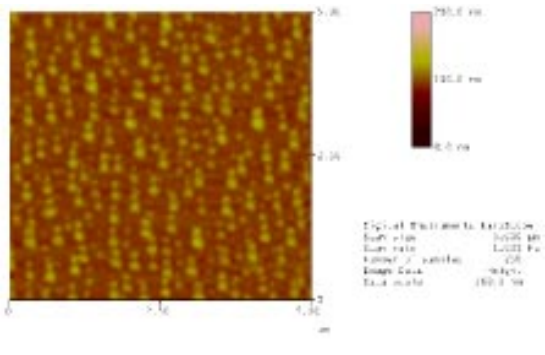

Fig. 2b : AFM Image of Thin Film Irradiated at Fluence $1x10^{11}$

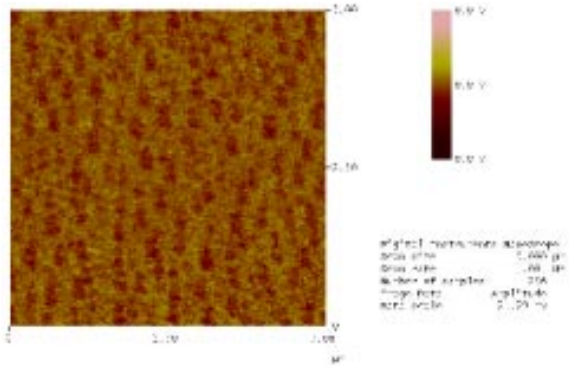

Fig. 2c : AFM Image of Thin Film Irradiated at Fluence 1x10^{11}

REFERENCES

[1] Hernando, 2003. Europhy. 34
[2] Available online at www.metglas.com (Product catalogue for Metglas 2826 MB)
[3] G Herzer, IEEE Trans. Magn., 26 (1990),1397
[4] F. Amalou and M A M Gijs, Appl. Phys. Lett. 81, 9 (2002), 1654
[5] S W Du and R V Ramanujan, Mater. Sci. Engg. A375-377 (2004) 1040
[6] M Kopcewicz and A Dunlop, J. Phys. Cond. Mater, 13 (2001) 6067

5.2.16 Ion Beam Synthesis of SiC nano-phase

Y.S. Katharria, F. Singh, P. Kumar, D. Kanjilal

Nuclear Science Centre, New Delhi-67

N-type silicon (Si) samples having (100) and (111) orientations were implanted with 150 keV carbon (C^+) ions at room temperature with doses varying from 4x10^{17} ions-cm^{-2} to 8x10^{17} ions-cm^{-2} in different samples of both the orientations. Post implantation annealing at 1000°C done in argon ambiance. Detailed Fourier transform infrared spectroscopy analysis and x-ray diffraction studies confirms the formation of cubic phase (β-SiC). The grain size of the SiC precipitates is estimated to be a few nanometer (~9nm) using x-ray diffraction technique. The area under the FTIR peak characteristic of SiC is plotted with dose in figure 1.The area under peak (a measure of amount of SiC precipitates) increases monotonically with dose fluence and almost saturates for a fluemce of 8×10^{17} ions-cm^{-2} (figure 2). This behavior of area under peak can be explained using ion beam induced crystallization (IBIC) and amorphization (IBIA).

The area divided by FWHM (a measure of SiC precipitates size) may be taken as a measure of the amount of the SiC precipitates with long range order is plotted with dose is shown in figure 2. The area/FWHM increases with increasing dose up to a dose of 6×10^{17} ions-cm^{-2} and then decreases slightly for the dose of 8×10^{17} ions-cm^{-2}. This indicates an increasing amount of long range SiC precipitates and can be due to IBIC. The

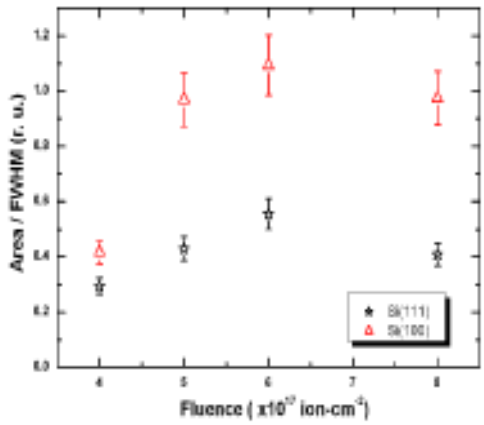

Fig. 1 : Dependence of amount of SiC precipitate characterized by area under peak in FTIR spectra on implanted C^+ dose for Si (100) and Si (111) samples.

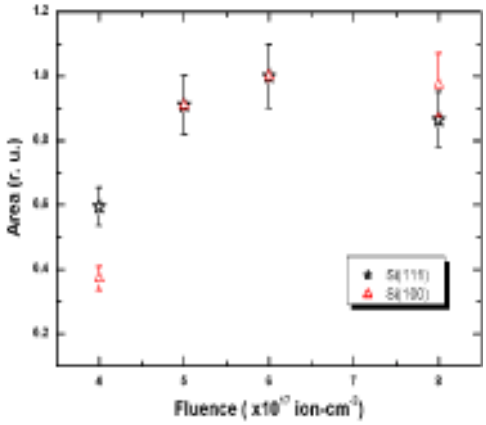

Fig. 2 : Dose Dependence of periodic order of SiC precipitates characterized by area of FTIR absorption band divided by FWHM of that band

decrease in area /FWHM can be attributed to IBIA which is dominant over IBIC for the doses above a critical level. The area/FWHM was found to be more for Si (100) samples then for Si (111) samples indicating a longer range order of SiC crystallites in Si (100) substrates than in Si (111) substrates. This is also obvious from XRD size calculations and the ratio of integrated intensities of SiC (111) peaks for the two substrates.

REFERENCES

[1] H. Morkoc, S. Strite, G. B. Gao, M. E. Lin, B. Sverdlov, and M. Burns, J. Appl. Phys. 76 (1994) 1336.

[2] W.G. Spitzer, D. Kleinman, and C. J. Frosch, Phys. Rev., 113 (1959) 133 .

[3] C. Serre, L. Calvo-Barrio, A. Perez-Rodriguez, A. Romano-Rodriguez, J.R. Morante, Y. Pacaud, R. Kögler, V. Heera, and W. Skorupa, J. Appl. Phys. 79, (1996) 6907.

[4] L. Wang, Y.E. Zhao, Dihu Chen, and S.P. Wong, Nucl. Instr. and Meth. B 22 (2005) 282.

5.2.17 Online ERDA and AFM Studies on 100 MeV Ag^{7+} Ions Irradiated Nanocrystalline Ferrite Thin Films

Sanjukta Ghosh[1, 2], Chanchal Ghosh[1], and Saif Ahmed Khan[3]

[1] Department of Physics, University of Calcutta, 92 A.P.C. Road, Kolkata 700009
[2] Institute of Physics, Sachivalaya Marg, Bhubaneswar 751 005
[3] Nuclear Science Centre, New Delhi 110 067

Earlier we have reported [1-2] the effect of swift heavy ion irradiation at two different experimental conditions namely $S_e > S_{eth}$ and $S_e < S_{eth}$. At present we report the observed effects at $S_e \sim S_{eth}$ condition. From damage morphology that this condition leads to extended defects with some point defects in it. From the AFM measurements,

shown in fig. 1 we notice some interesting changes in the surfaces of the films after irradiation. Existence of some deep valleys and ditches indicate that lateral momentum induced mass transfer takes place to some extent. We have studied online ERDA to observe whether preferential sputtering and oxygen loss take place in our systems. The results obtained do not indicate no such drastic changes in oxygen concentration.

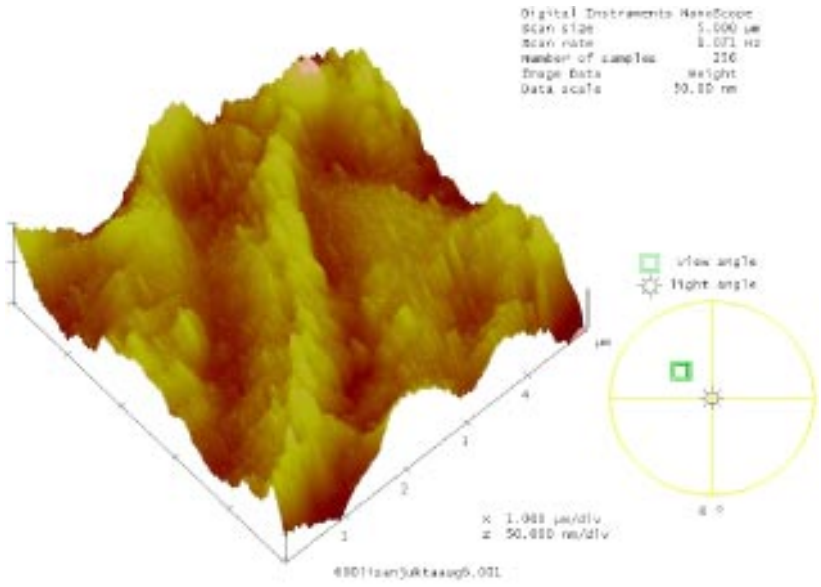

Fig. 1 AFM image of 600ºC annealed Li ferrite thin films irradiated with 100 MeV Ag ions

REFERENCES

[1] Sanjukta Ghosh et al. NIM B 212 (2003) 510
[2] Sanjukta Ghosh et al. NIM B 225 (2004) 310

5.2.18 80 MeV Gold Ion Irradiation Effects in ZnSe, GaN Thin Films and $CuInTe_2$

S. Soundeswaran[1], E. Varadarajan[1], O. Senthil Kumar[1], P. Prabukanthan[1], D. Kabiraj[2], D.K. Avasthi[2], and R. Dhanasekaran[1]

[1]Crystal Growth Centre, Anna University, Chennai - 600 025
[2]Nuclear Science Center, New Delhi - 110067

ZnSe, GaN and $CuInTe_2$ compound semiconductors are important for the fabrication of many optoelectronic devices. Compounds like CdS and GaN are having wide bandgap in the visible region. ZnSe thin films were prepared using novel photochemical deposition method (PCD), GaN by Vapour Phase Epitaxial method (VPE) and $CuInTe_2$ by Chemical Vapour Transport method (CVT). Irradiation of these materials

by high-energy ions may create some complex defects and in some cases and result in formation of the luminescent centers. Au ion irradiation of ZnSe, GaN and $CuInTe_2$ was performed with energy of 80 MeV at a fluence of 1 $x10^{11}$, 5 $x10^{11}$, 1 $x10^{12}$ and 5 $x10^{12}$ ions/cm^2 using tandem Pelletron accelerator.

80 MeV Au ion irradiation was carried out on samples at room temperature at fluences ranging from $1x10^{11}$ to $1x10^{13}$ cm^{-2}. The ion beam was scanned on the samples to ensure uniform irradiation. Ex-situ characterization have been carried out for, pristine and irradiated samples. Raman analysis has been performed on the as-grown and irradiated PCD-ZnSe samples (Fig. 1). The Raman peak position does not change much and it remains constant. The FWHM does not increase considerably at a low fluence ($1x10^{11}$ and $5x10^{11}$ ions/cm^2) but increased continuously at higher fluences ($1x10^{12}$ and $5x10^{12}$ ions/ cm^2). The decrease in peak height at higher fluences is expected due to the irradiation-induced defects.

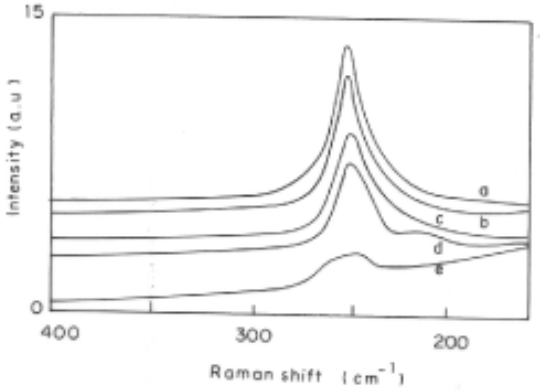

Fig. 1 : The room temperature Raman spectra of as-grown and Au ion irradiated ZnSe thin films a) Pristine b) $1x10^{11}$ ions/cm^2, c) $5x10^{11}$ ions/cm^2, d) $1x10^{12}$ ions/cm^2 and e) $5x10^{12}$ ions/cm^2

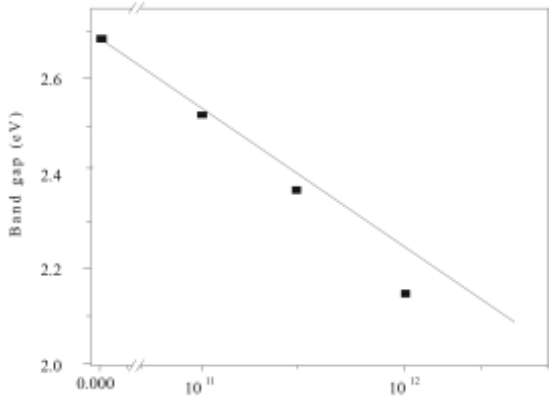

Fig. 2 : Band gap variation (eV) of Au ion irradiated ZnSe thin film as a function of ion fluences

The bandgap value of the ZnSe samples decreases from 2.67 eV to 2.1 eV (Fig.2). Optical absorption spectra were recorded for as-grown and irradiated $CuInTe_2$ single crystals (Fig.3). The bandgap value of the $CuInTe_2$ samples decreases from 1.04 eV to 0.9 eV. Thus, the high-energy ion irradiation can be considered as an effective process for optical isolation of semiconducting thin films [1,2]. The surface analysis of as-grown and Au^+ irradiated GaN layer have been carried out using Atomic Force Microscopy (AFM). The surface roughness (R_{ms}) value of the as-grown GaN layer is observed as 21.1 nm.

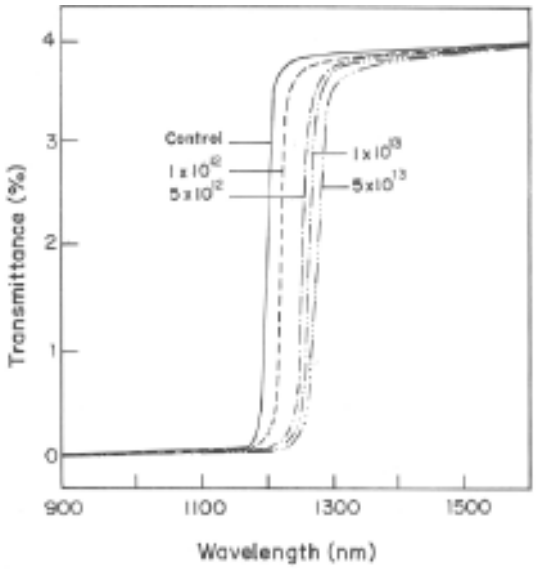

Fig 3. UV-visible spectra of as-grown and for Au ion irradiated GaN samples

REFERENCES

[1] K.L. Narayanan, K.P. Vijayakumar, K.G.M. Nair, R. Kesavamoorthy, Nucl. Instr. and Meth. in Phys. Res. B 160 (2000) 471

[2] S.Soundeswaran, O. Senthil Kumar, P.Ramasamy, D. Kabiraj, D.K.Avasthi and R.Dhanasekaran Physica B, 355(2004)222

5.2.19 Generation of Ge nanostructures by swift heavy ion irradiation

S. Rath[1], D.K. Avasthi[2], D. Kabiraj[2], Manoj Kumar[3], V.V. Sivakumar[2], H.S. Mavi[3], A.K. Shukla[3] and K.P. Jain[2]

[1]Dept. of Physics and Astrophysics, University of Delhi, Delhi-110007
[2]Nuclear Science Centre, New Delhi-110067
[3]Dept. of Physics, Indian Institute of Technology, Hauz Khas, New Delhi

Samples fabricated by the following techniques were irradiated with heavy ions to generate Ge nanostructures: (i) Ge/SiO_2 multilayer consisting of alternate layers of SiO_2 (10 nm) and Ge (2 nm) deposited on Si substrate by e-beam evaporation. Five such layers amounting to a total thickness of 60 nm were deposited; (ii) Ge oxide on Si substrate by e-beam evaporation and (iii) co-sputtering of Ge and SiO_2 on a Si substrate by rf sputtering using a rf power of 100 W. Ion irradiation was done with 150 MeV Ag ions at various fluences. The range of these ions is 14 μm in Ge and 17.5 μm in SiO_2. The samples were characterized by x-ray diffraction and FT-IR spectroscopy.

X-ray diffraction was measured with a Philips x-ray diffractometer with the CuKα radiation. X-ray diffraction of the as-dep Ge/SiO_2 multilayers shows three diffraction

peaks corresponding to reflections from Ge(111), (220), and (311) planes. The changes in the FWHM and peak position of the (111) peak on irradiation exhibit changes indicating formation of nanocrystals. The nanocrystal sizes, as calculated from Scherrer's formula, decreases from 34 nm for the as-deposited sample to 20.6 nm for samples irradiated with a fluence of $3x.10^{13}$ ions/cm^2. The GeO_x film clearly shows emergence of the Ge(111) reflection peak at 24° n irradiation. (Fig. 1)

The oxide formation on ion-irradiation was monitored through FT-IR spectroscopy. A bare Si substrate was used as reference and all spectra were subtracted from the reference Si spectrum. Peaks at 470, 820 and 1090 cm^{-1} correspond to rocking, bending and asymmetric stretching modes of SiO_2. Bending and stretching vibrations of Ge-O-Ge occur at around 580 and 870 cm^{-1} respectively.

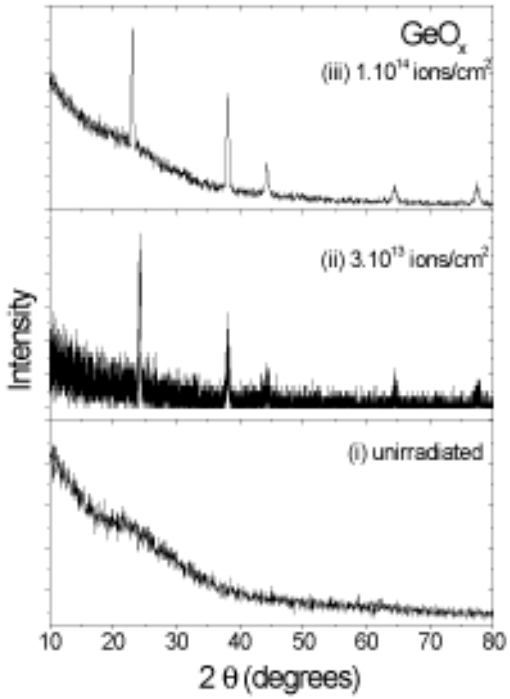

Fig. 1 : X-ray diffraction spectra of (i) as-dep and (ii) &(iii) irradiated GeO_x gives a comparison of the as-deposited and films irradiated with a fluence of $3x.10^{13}$ and $1x.10^{14}$ ions/cm^2.

However, the ion–irradiated co-sputtered Ge-SiO_2 shows no evidence of Ge peaks. In the Ge/SiO_2 ML, peaks at 580 and 870 cm^{-1} are clearly observed for irradiation at $3x.10^{13}$ ions/cm^2, suggesting that irradiation has led to oxidation of Ge. The peaks at around 700 and 800 cm^{-1} shift to lower frequencies with increasing dose. The Ge-SiO_2 co-sputtered sample shows emergence of Ge-O-Ge bending and stretching vibrations in the ion-irradiated samples.

Preliminary experiments did not show photoluminescence emission from any of the samples. More detailed characterisation through Raman and photoluminescence

spectroscopy is ongoing. Further work will be aimed at achieving a uniform size distribution through a combination of thermal annealing and ion-irradiation.

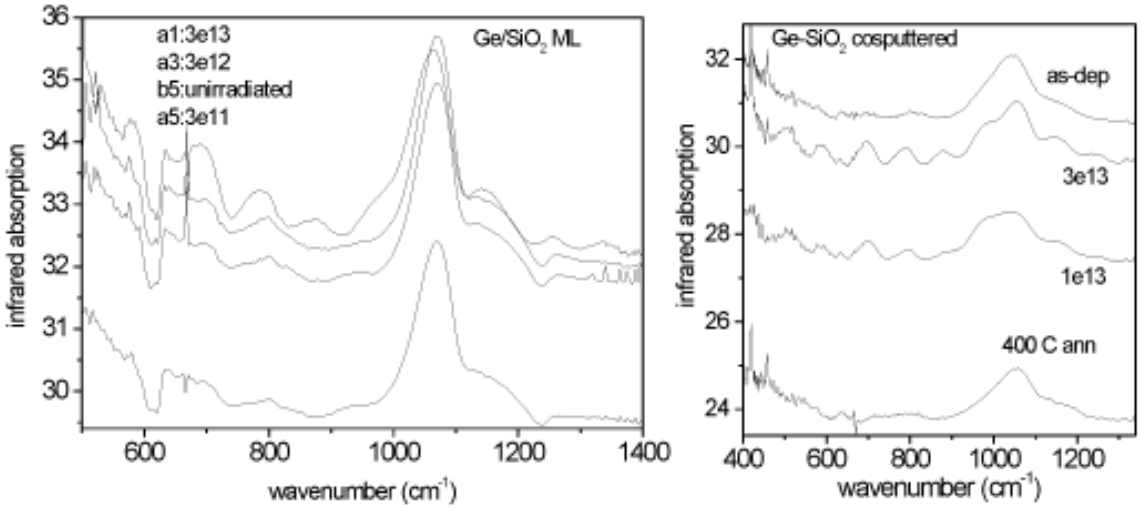

Fig. 2 : FT-IR spectra of Ge/SiO_2 multilayer and co-sputtered $Ge\text{-}SiO_2$.

5.2.20 Effect of Swift Heavy Ions of Silver and Oxygen on GaN

V. Suresh Kumar[1], P. Puviarasu[1], K. Prabha[1], K. Thangaraju[1], R. Thangavel[1], V. Baranwal[2], F. Singh[2], T. Mohanty[2], D. Kanjilal[2], K. Asokan[2] and J. Kumar[1]

[1]Crystal Growth Centre, Anna University, Chennai 600 025
[2]Nuclear Science Centre, New Delhi 110 067

Swift heavy ion (SHI) beams play a vital role in the field of modifications of the properties of films, foils and surface of bulk solids. Study of radiation-induced defects in semiconductors is important for their role in device fabrication [1].

The samples used in this study are of 3μm thick n–GaN epilayers grown by Metal Organic Chemical Vapour Deposition (MOCVD) technique on sapphire substrates at the growth temperature of 1035 ºC [2]. These GaN samples were irradiated with 100 MeV Ag and O ions of fluence 1×10^{13} ions.cm^{-2} at room temperature using 15 UD Pelletron accelerator of Nuclear Science Centre, New Delhi under a vacuum in the range of ~ 3×10^{-7} torr.

The surface of *as-grown* pattern does not show any special feature. The surface roughness value of the *as-grown* GaN layers is ~3.9 nm. This sharpness of the surface pattern of *as-grown* GaN layer gets blurred after Ag ion irradiation due to the ion beam induced damages in the surface. The roughness value of Ag ion irradiated sample increases

considerably to ~ 39.5 nm. It is clear that Ag ion irradiation creates hillocks in the GaN surface. From the AFM image of 100 MeV O ion irradiated GaN with the fluence of 1×10^{13} ions.cm^{-2}. It is observed that the surface is smoothened and the roughness value is 1.5 nm which is smaller than *as-grown* GaN. This indicates that GaN surface gets ordered arrangement and surface gets smoothened after O ion irradiation.

Fig.1 shows the PL spectra of *as-grown*, Ag , and O ions of 100 MeV irradiated GaN recorded in room temperature. The pristine GaN exhibits a near band-edge exciton luminescence peak at 3.4 eV and the emission of yellow line at 2.2eV and blue band at 2.55 eV. The peak with very high intensity of green line has been observed in case of *as-grown* GaN layers. As evident from these spectra, there is a low intensity emission peak at the wavelength of 363 nm and this is due to band – to – band transition of GaN. The calculated band – gap energy is 3.4 eV which is consistent with the reports available in the literature [3]. From 100 MeV Ag ion irradiated GaN sample, there is a decrease of emission intensity. The blue and yellow emissions also decrease after irradiation. The high energy radiation induced defects are responsible for the observed change in PL spectra.

After 100 MeV O ion irradiation, there is a shift in the blue, green and yellow bands. This may be due to the fact that the ion induced lattice damage may create defect energy levels below the conduction band and hence the band gap may decrease. Irradiation of the semiconductors with an ion-beam introduces electrically active defects, which change the property of the material at the surface or deep into the surface depending upon the energy and the species of ion.

High energy Ag and O ion irradiations were carried out on MOCVD *as-grown* GaN and their surface morphology were investigated using AFM and optical properties

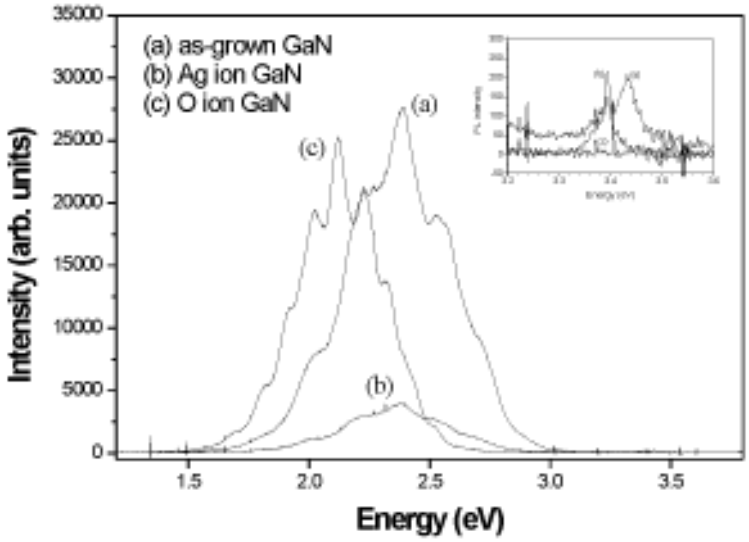

Fig. 1 : PL spectra of *as- grown* and SHI irradiated GaN epilayers. Inset shows the close view at band edge.

by PL. These studies indicate that there is considerable change in the roughness value of the surface of GaN after 100 MeV Ag and O ion irradiations. It is observed that the roughness of the surface reduces after O ion irradation and this increases after Ag ion irradiation. The PL spectra reveal that there is a significant change in luminesence characteristics after 100 MeV Ag and O ion irradiations. Oxygen ion irradiation gives the red shift.

Acknowledgments

The authors would like to thank Dr. M. Senthil Kumar, and Dr. Fareed for providing the GaN samples and Mr. A. Tripathi, NSC for support in AFM measurements.

REFERENCES

[1] S. J. Pearton, J. C. Zolper, R. J. Shul, F. Ren, J. App. Phy. 86 1998), 1.
[2] M. Senthil Kumar, G. sonia, D.Kanjilal, R.Dhanasekaran and J.Kumar, Nucl. Instr. and Meth. in Phys. Res. B207 (2003) 308.
[3] J. Zhang, X. Peng, X. Wang, Y. Wang, L. Zhang, Chem. Phys. Lett. 345 (2001) 372.

5.2.21 Ion beam induced surface modification of GaAs

V. Baranwal[1], R. Krishna[1], Y.S. Katharia[2], A. Tripathi[2], A.C. Pandey[1], D. Kanjilal[2]

[1] University of Allahabad, Allahabad-211002
[2] Nuclear Science Centre, New Delhi-110067

In this work we have used nitrogen beam at multiple energies for implantation into Zn doped GaAs using Electron Cyclotron Resonance ion source at Nuclear Science Centre, New Delhi. Three different energies of 290 keV, 130 keV, 50 keV Nitrogen ions with varying fluences of $5x10^{16}$ ions/cm^2, $1x10^{17}$ ions/cm^2, $5x10^{17}$ ions/cm^2 are used for implantation into GaAs. Multiple energies are used in an attempt to create a uniform depth distribution of nitrogen in the implanted region[1]. Annealing of one sample implanted with dose of $5x10^{16}$ ion/cm^2 is done in vacuum in the tubular furnace at the temperature of 850^0C for 30 minutes using a GaAs wafer as a cap on the implanted sample.

The surface morphological features of the surface of GaAs samples is investigated using Nanoscope-IIIa at Nuclear Science Centre in the tapping mode using Si_3N_4 cantilevered tip. Implantation induced modification of the surface studied with Atomic Force Microscope (AFM).

AFM results shows that high dose ion bombardment results in anomalous swelling of the implanted region [2]. Ion implantation has caused pronounced material swelling with a height of 1?m for a dose of $5x10^{17}$ions/cm^2. A rapid height increase is due to the buried and surface amorphous layer expansion and finally overlapping, which results in a

thick continuous layer of amorphous material. Figure 1 shows the AFM images of virgin GaAs [1(a)], and of GaAs implanted with $5x10^{16}$ ions/cm^2 [1(b)], $1x10^{17}$ ions/cm^2 [1(c)], $5x10^{17}$ions/cm^2 [1(d)]. It is clearly seen from figure 1 that high dose ion bombardment dramatically changes the surface morphology of GaAs.

Implantation with dose of $5x10^{16}$ ions/cm^2 reduced the surface roughness. However when the implantation dose increases to $5x10^{17}$ ions/cm^2 the morphology and the roughness of the surface changes drastically. The trend of the surface roughness is given in table 1. It was found that the roughness of the sample implanted at a dose of $5x10^{16}$ ions/cm^2 was reduced from 2.7 nm to 2.4nm after annealing at 800^0C or 30 minutes.

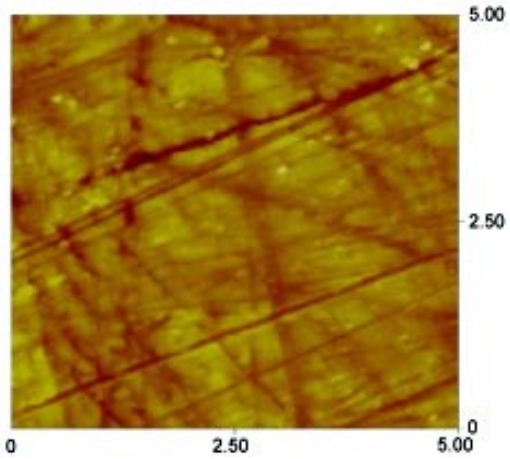

Fig. 1(a) Pristine sample.

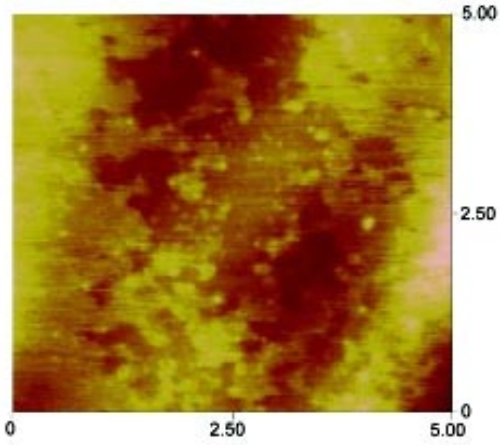

Fig. 1(b) Implanted with dose of $5x10^{16}$ ions/cm2

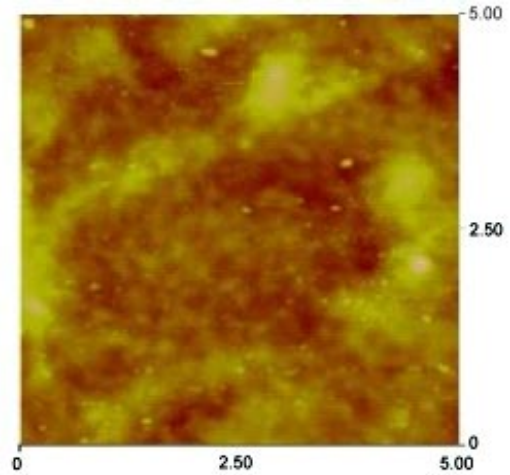

Fig. 1(c) Implanted with dose of $1x10^{17}$ ions/cm^2

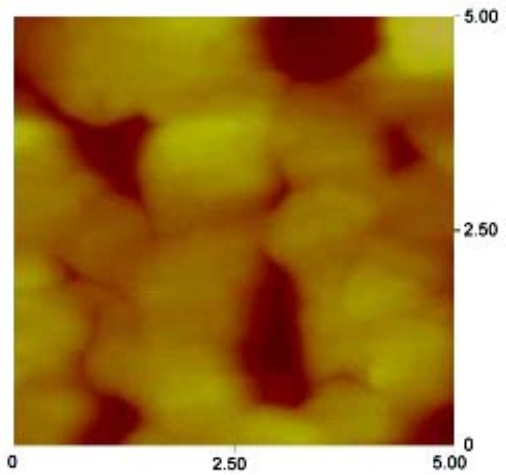

Fig. 1(d) Implanted with dose of $5x10^{17}$ ions/cm^2

Table 1:

Fluence	Roughness (nm)
Pristine	4.32
$5x10^{16}$ ions/cm	2.70
$1x10^{17}$ ions/cm	5.0
$5x10^{17}$ ions/cm	142.82

REFERENCES

[1] W. Shan et al. Appl. Phys. Lett. 75(1999), 1410
[2] S. O. Kucheyev et al. Appl. Phys. Lett. 77(2000),1455.

5.2.22 SHI Induced Modification of ZnO thin film

D.C. Agarwal[1], A. Kumar[2], D. Kabiraj[2], F. Singh[2], S.A. Khan[2], J.C. Pivin[3], R.S. Chauhan[1], D.K. Avasthi[2]

[1]Department of Physics, R. B. S. College, Agra, 282 002
[2]Nuclear Science Centre, New Delhi, 110 067
[3]CSNSM, IN2P3-CNRS, Batiment 108, F-91405, Orsay Campus, France

Thermally evaporated ZnO thin films have been irradiated with 100 MeVAu^{+8} ions at different fluence from 5 x 10^{11} ions/cm^2 to 5 x 10^{13} ions/cm^2. There are only few reports on swift heavy ion induced modification (SHI) of optical properties of ZnO [1]. The very high value of energy transferred induces an unusual density of defects in the material. Analysis of the change in optical properties of the ZnO thin film under the defect production has continuing interest.

Figure (1) shows the absorption spectra of Pristine and irradiated samples. It shows that there is no significant change in the band edge. This implies that the basic lattice of ZnO is not modified. Figure (2) shows the XRD spectra of pristine and irradiated ZnO films. XRD spectra shows (002) peak at 34.45^o with another peak (103) at 62.88^0. It reveals that the grain size and texturing of the film increases at low fluence whereas as we go to higher fluence the grain size decreases. FTIR spectra shows the peak at 409 cm^{-1} [2-3] related to the ZnO absorption band in all films. The films are also characterized by Photoluminescence (PL). The films are displaying the defects related emission in the PL spectra. After irradiation, there is blue shift in PL due to the defect created by ion beam.

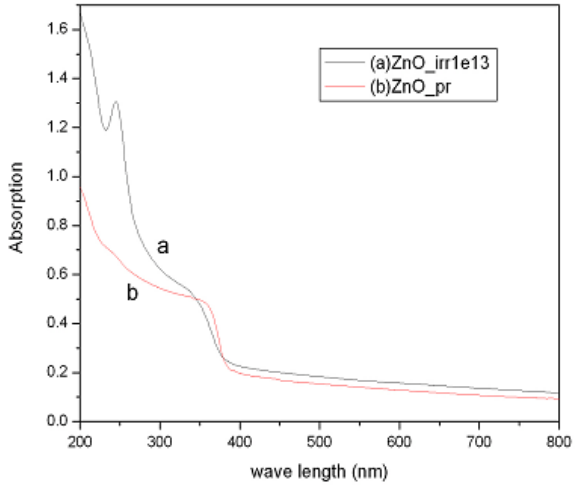

Fig. 1 : Absorption spectra of pristine irradiated ZnO thin film

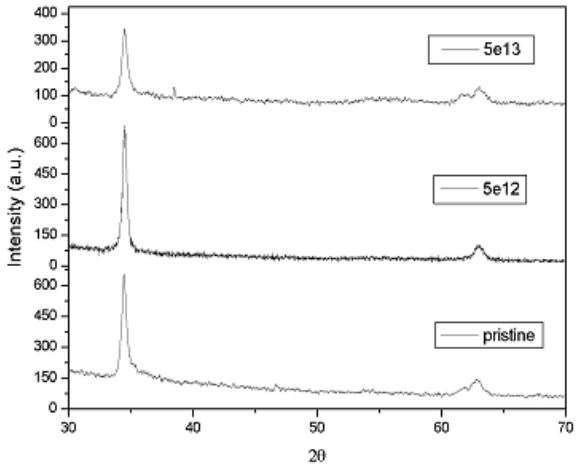

Fig. 2 : XRD spectra of pristine and irradiated thin film

REFERENCES

[1] P. M. Rathees Kumar et. al., *J Appl. Phys.* 97(2005)13509.
[2] Andres-Verges, A. Mifsud, C. J. Serna, *J. Chem. Soc., Faraday Trans.* 86 (1990) 959
[3] S. Hayashi, et. al. *Surface Sci.,* 86(1979)665.

5.2.23 MeV heavy ion beam induced epitaxial crystallization of buried Si_3N_4 layer

T. Som[1], B. Satpati[1], O.P. Sinha[1], N.C. Mishra[2], D.K. Avasthi[3], and D. Kanjilal[3]

[1]Institute of Physics, Sachivalaya Marg, Bhubaneswar 751 005
[2] Physics Department, Utkal University, Bhubaneswar 751 004
[3]Nuclear Science Centre, New Delhi 110 067

We have studied swift heavy ion beam induced epitaxial crystallization (SHIBIEC) of a buried Si_3N_4 layer at temperatures as low as 150 - 200°C, where the projectile ions lose their energy mainly by inelastic collision processes. 70 MeV Si^{5+} ions and 100 MeV Ag^{8+} were used (up to a fluence of 1×10^{14} ions cm^{-2}) to induce recrystallization in the thin Si_3N_4 layer, which was produced by high current (30-40 μA cm^{-2}) N ion implantation at 300°C. Such high current density implants would lead to rise in the sample temperature due to heating effect of the ion beam itself (self-annealing) [1,2], which in turn would result in recrystallization of the top Si layer. It can be mentioned here that this is a typical silicon-on-insulator (SOI) structure consisting of an almost defect-free device-worthy Si layer at the top, a good dielectric layer in the form of a buried silicon nitride/oxide layer, and two high-quality abrupt interfaces of the buried insulating layer with the top as well as the substrate Si. We have demonstrated that SHIBIEC would be governed by the electronic energy loss (S_e) processes and the mechanism of epitaxial growth is different as compared to the one based on nuclear energy loss (S_n) processes. Systematic transmission electron microscopy (TEM) and selected area diffraction (SAD) patterns are used to examine the microstructure formed in the buried layer [3-5].

Ultrasonically cleaned Si(100) samples were implanted with 100 keV N^+ ions (at a grazing incidence of 7°) at 300°C up to a fluence of 8×10^{16} ions cm^{-2} under a clean vacuum of 4×10^{-7} mbar. 100 keV N ions have a projected range of 245 nm as calculated by SRIM-2003 code. Later on, the N-implanted samples were irradiated by 70 MeV Si^{5+} and 100 MeV Ag^{7+} ions in a clean vacuum of 9×10^{-7} mbar and using a constant fluence of 1×10^{14} ions cm^{-2} at different temperatures, viz. room temperature (RT), 150°, 200°, 250°, and 300°C. The S_e and S_n values of 70 MeV Si ions in Si are given by 2.81 and 0.002 keV nm^{-1}, respectively, while that in Si_3N_4 are given by 4.46 and 0.004 keV nm^{-1}, respectively. These are accurate within 5% in terms of the experimental values and lead to the (S_e/S_n) ratio of 1067 and 1115 for Si and Si_3N_4, respectively. Similarly, for 100 MeV Ag ions, the implanted species would penetrate deep (≈16 μm) into the Si substrate. The S_e and S_n values of Ag ions in Si are given by 10.51 and 0.06 keV nm^{-1}, respectively, while that in Si_3N_4 are given by 17.87 and 0.09 keV nm^{-1}, respectively. Thus, for both Si and Ag irradiation, the implanted species would penetrate deep (≈21 μm) into the Si substrate. Microstructure and crystalline quality of the as-implanted and Si-ion irradiated samples were studied by cross-sectional TEM (XTEM) and selected area diffraction (SAD) pattern measurements.

Fig. 1(a) shows a low magnification bright field XTEM image obtained from an as-implanted sample. The presence of a thin implanted layer is clear in the Si substrate. To check the crystallinity of each layer, SAD patterns were collected from three distinctly different regions (as marked on Fig. 1(a)) and are presented in Fig. 1(b). The SAD patterns clearly indicate that although the implanted layer is amorphous, the layer above it and the substrate Si are crystalline. To study the nature of the a/c interfaces, we present the high-resolution TEM (HRTEM) images in Fig. 1(c) corresponding to the two a/c interfaces as marked on Fig. 1(a). This shows that the interfaces are sharp although implantation induced roughness prevails.

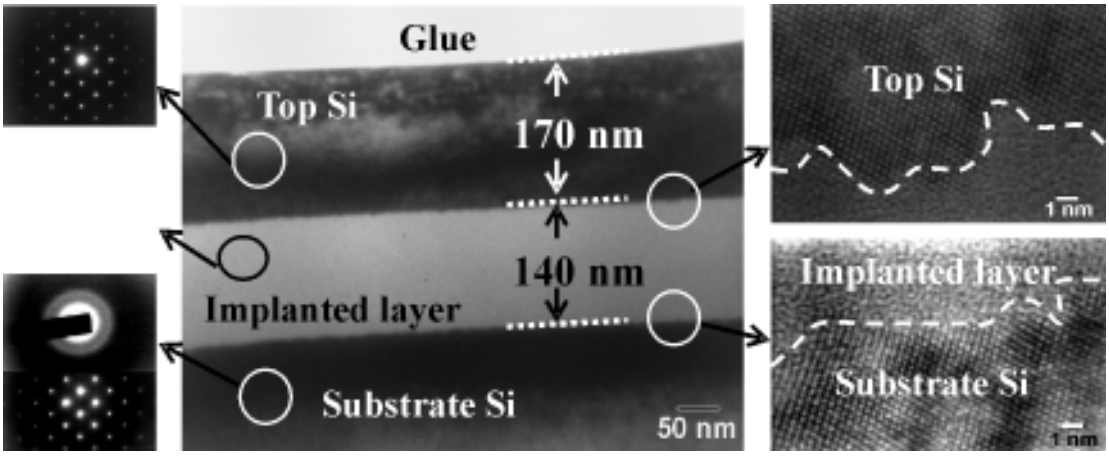

Fig. 1 : Bright field XTEM micrographs obtained from an as-implanted sample: (a) low magnification image showing three distinct regions, (b) SAD patterns obtained from the three marked regions, (c) HRTEM images obtained from the marked interfaces.

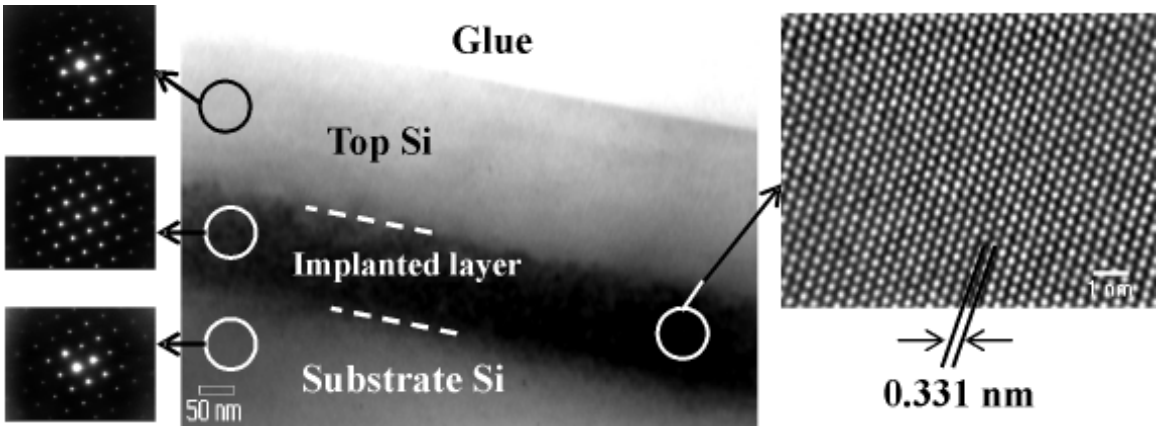

(b) (a) (c)

Fig. 2 : Bright field XTEM micrographs obtained from an as-implanted sample, which was subject to 70 MeV Si^{5+} irradiation to a fluence of 1×10^{14} ions cm^{-2} at 150°C: (a) low magnification image showing top Si, implanted layer, and the substrate Si, (b) SAD patterns obtained from the three marked regions, (c) HRTEM image obtained from the marked portion of the implanted layer.

Fig. 2(a) shows a low magnification TEM image obtained from an N implanted sample, which was irradiated to the fluence of 1×10^{14} ions cm^{-2} at 150°C. SAD patterns obtained from three different regions of the sample (as described above) are presented in Fig. 2(b). The SAD patterns clearly show that all the three layers are single crystalline in nature. The HRTEM image obtained from the intermediate layer is shown in Fig. 2(c)

and the corresponding *d*-spacing (0.331 ± 0.002 nm) matches very well with that of (200) reflection corresponding to the hexagonal α-Si_3N_4 phase. Therefore, it can be inferred that the formation of a buried amorphous Si_3N_4 layer takes place due to N implantation in Si at 300°C, which gets recrystallized due to 70 MeV Si-ion irradiation at 150°C. We have also studied the samples irradiated at even higher temperatures like 200, 250, and 300°C and high-resolution lattice imaging from all those samples indicates that the respective d-spacing obtained from the recrystallized layer has a good matching with that of α-Si_3N_4 [4]. However, the microstructure in the recrystallized layer arising due to SHI irradiation at different elevated temperatures shows the presence of dislocation. Similarly, we have obtained recrystallized Si_3N_4 layer due to irradiation by 100 MeV Ag ions at 200°C (micrograph not shown) [3].

REFERENCES

[1] G. Cembali, P.G. Merli, and F. Zignani, Appl. Phys. Lett. 38 (1981) 808.

[2] M. Berti, A.V. Drigo, G. Lulli, P.G. Merli, and M. Vittori Antisari, Phys. Status Solidi A 94 (1986) 85; M. Berti, A.V. Drigo, G. Lulli, P.G. Merli, and M. Vittori Antisari, Phys. Status Solidi A 97 (1986) 77.

[3] T. Som, B. Satpati, O.P. Sinha, and D. Kanjilal, J. Appl. Phys. (submitted).

[4] T. Som, B. Satpati, O.P. Sinha, N.C. Mishra, and D. Kanjilal, Nucl. Instr. Meth. Phys. Res. (submitted).

[5] T. Som, B. Satpati, O.P. Sinha, D.K. Avasthi, and D. Kanjilal, Nucl. Instr. Meth. Phys. Res. (to be submitted).

5.2.24 Effect of 50 MeV Li^{+3} Ion Irradiation on Polycrystalline MgB_2 Superconductor

A. Talapatra[1], S. K. Bandyopadhyay[1]*, Pintu Sen[1] and Ravi Kumar[2]

[1]Variable Energy Cyclotron Centre, 1/AF, Bidhan Nagar, Kolkata - 700 064
[2]Nuclear Science Centre, New Delhi - 110 067

The discovery of superconductivity in Magnesium Diboride, MgB_2 [1] has attracted a lot of interest because it is a simple binary intermetallic system with fairly high T_c. Its conductivity is also quite high. The flow of supercurrents in MgB_2 is not significantly hindered by grain boundaries [2] which are dominant in cuprates. The observation of significant B isotope effect on superconducting transition temperature T_c and heat capacity measurement indicate that MgB_2 is a phonon mediated s-wave superconductor [3-5]. Some particle irradiation studies have been pursued on this system [6-8]. The irradiation studies with heavy ions on thin films [7] and protons on bulk materials [6] of MgB_2 have not reflected any significant changes in T_c. It would be quite interesting to investigate this wide range of resistivity by generating disorder systematically by paricle irradiation as a function of dose. Li-ion was chosen with the motivation of thorough and fairly uniform radiation damage in bulk MgB_2.

MgB_2 pellets have been synthesized starting from Mg (> 97% pure) and B (99.9% pure) powder with 2 atomic percent Mg in excess to stoichiometry. The samples were characterized by X-ray Diffraction (XRD) pattern taken with Philips PW1710 diffractometer with Cu $K_?$ of wavelength 1.54 Å. Resistivities of the samples as a function of temperature were measured in a close cycle helium refrigerator (made of Cryoindustries of America) using four probe technique with HP 34220A Nanovoltmeter with resolution of 0.1 nanovolt and Keithley 224 programmable current source. 1mA current was employed. Tc of the unirradiated sample was 38.4K with a transition width (ΔT_c) of ~0.6K. Irradiation was carried out with 50 MeV Li-ions available at Nuclear Science Centre, New Delhi. Range of 50 MeV Li-ions in MgB_2 is 278 microns, significantly larger than the thickness of the samples employed (240 microns). The beam was Raster scanned over the sample to have uniform radiation throughout the surface of the sample. The irradiation was carried out at doses from $1x10^{14}$ to $2x10^{15}$ particles/cm^2. Irradiated samples were characterized with respect to crystal structure by XRD and Tc by resistive means.

XRD patterns of the samples-irradiated as well as unirradiated reflect that there has not been any significant development of other phase than MgB_2. Fig. 1 displays the resistivity plots of the irradiated and unirradiated samples. We do not notice any significant change in Tc due to irradiation though resistivity has increased quite fairly. The change

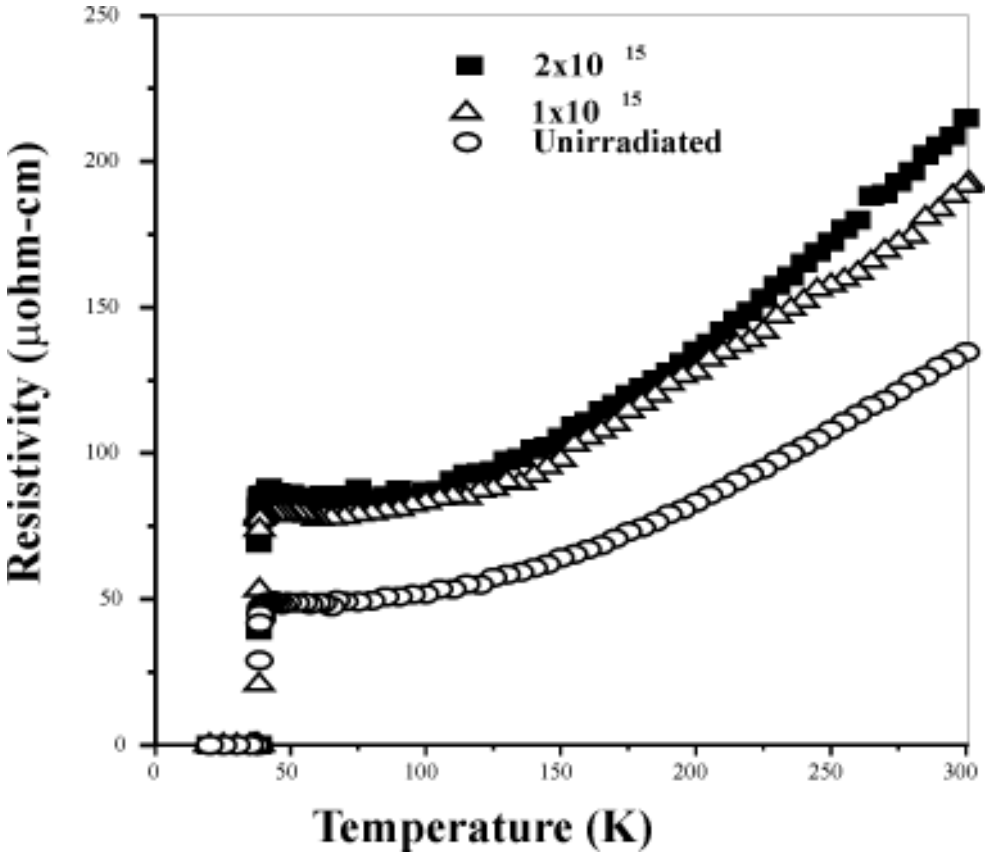

Fig. 1

is quite similar to our earlier irradiation studies with 160 MeV Ne ion [9]. The irradiation is thorough and quite uniform with particles penetrating throughout the samples, in contrast to Ne ion irradiation, where the range of the projectile was less than the thickness of the sample. Nuclear energy loss from SRIM calculations [10] reveal that the displacement per atom (d.p.a.)in MgB_2 for Li-ions is ~$1x10^{-19}$ per particle. Hence, for a dose of 10^{15} particles/cm^2, the d.p.a. is ~10^{-4} or, the defect concentration is ~100 ppm. Magnetoresistance measurements will be carried out to estimate pinning potentil and Jc.

REFERENCES

[1] J. Nagamatsu, N. Nakagawa, T. Muranaka, Y. Zenitani, and J. Akimitsu, Nature 410 (2001) 63.

[2] D.C. Larbalestier, L.D. Cooley, M.O. Rikel, A.A. Polyanskii, J. Jiang, S. Patnaik, X.Y. Cai, D.F. Feldmann, A. Gurevich, A.A. Squitieri, M.T. Naus, C.B. Eom, E.E. Hellstorm, R.J. Cava, K.A. Regan, N. Rogdo, M.A. Hayward, T. He, J.S. Slusky, P. Khalifah, K. Inumaru and M. Hass, Nature 410 (2001) 186.

[3] S.L. Bud'ko, G. Lapertot, C. Petrovic, C.E. Cunningham, N. Anderson and P.C. Cannfield, Phys. Rev. Lett. 86 (2001) 1877.

[4] R.K. Kremer, B.J. Gibson and A. Ahn, cond-mat/0102432.

[5] J. Akimitsu and T. Muranaka, Physica C 388-389 (2003) 98

[6] E. Mezzeti, D. Botta, R. Cherubini, A. Chiodoni, R. Gerbaldo, G. Ghigo, G. Giunchi, L. Gozzeline and B. Minetti, Physica C 372-376 (2002) 1277.

[7] A Gupta, H. Narayan, D. Astil, D. Kanjilal, C. Ferdeghini, M. Paranthaman and A.V. Narlikar, Supercond. Sci. Technol. 16 (2003) 951-955.

[8] G.K. Perkins, Y. Bugaslavsky, A.D. Caplin, J. Moore, T.J. Tate, R. Gwilliam, J. Jun, S.M. Kazakov, J. Karpiniski and L.F. Cohen, Supercond. Sci. Techhnol. 17 (2004) 232.

[9] A.Talapatra, S.K.Bandyopadhyay, Pintu Sen and P.Barat, Cond-Mat 0408175.

[10] J.F. Ziegler, www.SRIM.org.

5.2.25 Effect of heavy ion irradiation on anisotropy, irreversibility fields and critical current density in MgB_2 thin films

S. D. Kaushik[1], R. J. Choudhary[2], Ravikumar[2], S. Patnaik[1]

[1]School of Physical Sciences, Jawaharlal Nehru University, New Delhi 110067.
[2]Nuclear Science Center, New Delhi 110067.

The "serendipitous" superconductor MgB_2 (T_c = 39 K) [1], has attracted considerable attention in the recent past. While from the application point of view significant progress has been achieved in fabricating long length wires from this "off the shelf" material, from the theoretical angle, the fundamental superconducting parameters under the influence of two-band superconductivity are under scrutiny. The questions that we have set up for our research proposal are the following.

It is well known that the current carrying capacity of a superconductor is directly related to the vortex pinning mechanism, and addition of point and columnar defects through high-energy ion irradiation leads to improved superconducting properties. In MgB_2 however, because of intermetallic nature of the compound, no clear evidence of

post irradiation improvement has been reported. Our objective is to study the pinning properties of MgB_2 post irradiation with a variety of ions at different energies and compare the results with high T_c superconductor. Because of multi-gap superconductivity in MgB_2, the temperature dependence of anisotropy derived from penetration depth is predicted to be opposite to that derived from the upper critical field [2]. Using a tunnel diode oscillator circuit, we plan to study this issue in irradiated and unirradiated samples.

The relationship between H* (irreversibility field) and the upper critical field H_{c2} is open to interpretation in MgB_2. We plan to study the effect of thermal activation of vortices in MgB_2 near H* in pristine and irradiated samples of MgB_2.

a. A set of samples was irradiated at NSC, Suitable fluence and ions were chosen after elaborate literature survey. The thin films have been experimentally studied post irradiation using four probe resistivity technique and some of the samples have also been studied using a VSM at BARC.

b. A set up for direct measurement of penetration depth based on tunnel diode oscillator circuit has been designed and fabricated at NSC. Presently we are undertaking calibration of this set up.

Our preliminary results have indicated significant enhancement in superconducting properties in MgB_2 after 100 MeV Si^{+8} irradiation while no such enhancement was seen in Au irradiated films [2]. Figure 1 shows zero-field resistivity vs. temperature for all the three thin film samples of fluence $5x10^{12}$ ions/cm^2. While the onset T_c of unirradiated sample was 38.4 K, the Au irradiated sample showed maximum damage and the T_c was found to be 36.8 K. The Si irradiated sample is in- between, with T_c onset of 37.4 K. In the inset of the figure we show the resistivity up to room temperature.

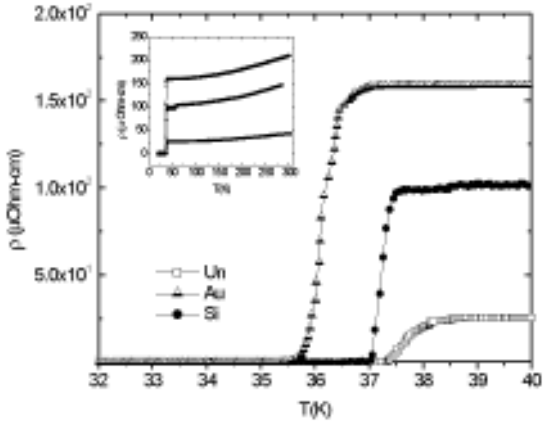

Fig. 1 : The resistivity of the unirradiated (open), Au irradiated (half filled) and Si irradiated (closed) samples is plotted against temperature. The inset shows the data up to room temperature.

The absolute value of resistivity as well as the residual resistivity ratio (RRR) showed that the damage with Si is intermediate between the unirradiated and Au irradiated sample. We also note that the transitions are sharper after irradiation. Plotted in Figure 2 is the normalized resistance versus temperature for the three samples in the presence of external magnetic field applied perpendicular to the ab plane. Clearly the best results are achieved with Si irradiation. At 1.25T the irreversibility temperature is 34.8 K for Si irradiated where as it is around 33.2 K and 33.6 K for the Au irradiated and unirradiated samples respectively.

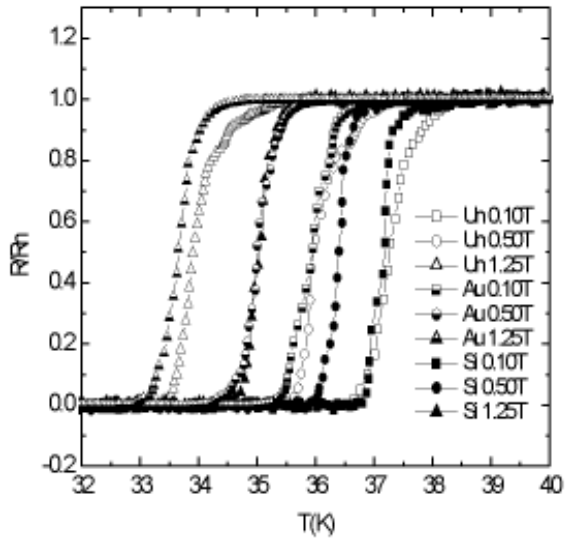

Fig. 2 : Normalized resistance for the samples Vs. temperature with external field applied perpendicular to the ab plane of the samples. The best improvement in the irreversibility field is achieved with the Si irradiated sample.

Our results clearly establish that low energy light ion irradiation yields far superior improvement as compared to heavy ion irradiation that sometimes actually lead to degradation of the superconducting property of MgB_2. We believe that the ratio of S_n to S_e is more suited for light ions for defect formation onto MgB_2. A detailed study using AFM to study the underlying defect structure is under way.

We wish to thank Ben Senkowich, J. Gliencke and C.B. Eom of Applied Superconductivity Center University of Wisconsin, USA for providing MgB_2 thin film sample. SDK acknowledges financial support by CSIR, New Delhi.

REFERENCES

[1] P. Grant, Nature 411, 532 (2001).
[2] V.G. Kogan and . L. Budko, Cond-mat 0212383 (2002).
[3] S.D. Kaushik, Shrikant Saini, R.J. Choudhary, Ravikumar, C.L. Prajapat, G. Yashwant, P.K. Mishra, S. Patnaik, presented at the 127th DAE solid state symposium (Amritsar), India.

5.2.26 Swift Heavy Ions induced paramagnetic centres in Ti^{4+} -substituted $Li_{0.5}Al_{0.1}Fe_{2.4}O_4$ spinel: Mössbauer study

M.C. Chhantbar[1], K.B. Modi[1], R.V. Upadhyay[2], RaviKumar[3], H.H. Joshi[1]

[1]Department of Physics, Saurashtra University, Rajkot-360 005
[2]Department of Physics, Bhavnagar University, Bhavnagar-364 002
[3]Nuclear Science Centre, New Delhi-110 067

In the present report we present the study of influence of Swift Heavy Ion irradiation induced defects [1,2] on the structural and magnetic properties of the spinel ferrites through ^{57}Fe Mössbauer spectroscopy. We have selected the three compositions of the spinel solid system $Li_{0.5(1+x)}Ti_xAl_{0.1}Fe_{2.4-1.5x}O_4$ x = 0.0, 0.1 and 0.3 for the SHI irradiation study by using 50 MeV Li^{3+} ions. The pristine compound $Li_{0.5}$ $Fe_{2.5}$ O_4 is known to have very high Curie temperature (942K) and the magnetic properties of these compounds are sensitive to the distribution of Fe^{3+} ions in the A- and B-sites. Therefore, the magnetic properties of the pre- and post SHI-irradiated specimens can be explained in the light of defect states and rearrangement of cations in the lattice sites.

The ferrite pellets were cut and polished to the required size as determined by using the SRIM-98 software for the SHI irradiation experiments. The porosity of the samples was maintained around 10%. XRD and EDAX well-characterized specimens were irradiated in vacuum with 50 MeV Li^{3+} ions with fluence of 5 x 10^{13} ions/cm^2 using 15 UD Pelletron accelerator at Nuclear Science Centre, New Delhi. The electronic energy loss (S_e) of 50 MeV Li^{3+} ions in these compounds calculated using the SRIM-98 code is around 12 eV/Å which is less than the S_{eth} = 1.2 KeV/ Å for columnar amorphization. This suggests that the SHI-irradiation has generated points/cluster of defects.

The representative Mössbauer spectra recorded at 300K for the unirradiated and irradiated samples of the composition x = 0.3 is displayed in Fig. 1. The Mössbauer spectra exhibit two superimposed asymmetric Zeemann sextets one due to the Fe^{3+} ions at tetrahedral (A) sites and other due to Fe^{3+} ions at octahedral (B) sites and the spectra for irradiated samples exhibit central enhancement or paramagnetic doublet superimposed on the magnetic sextet.

It is seen that all the post-irradiated specimens exhibit central paramagnetic doublet superimposed on the magnetic sextets showing quadrupole splitting of the order of 0.25 ± 0.02 mm/sec and the isomer shift 0.35± 0.03 mm/sec. It is known that the electronic energy loss threshold (S_{eth}) required to surmount for producing amorphization is generally of the order of 10^3 eV/Å, therefore it is difficult to comprehend the creation of columnar amorphization at the value of electronic energy loss (S_e) ~ 12 eV/Å. The amorphization is not reflected in the X-ray diffraction patterns of the irradiated samples. The generation of point/clusters of defects in theseTi^{4+} – Al^{3+} containing compounds inhibits the long-range ferrimagnetic order through redistribution of cation in the localized

defected region leadings to the formation of paramagnetic centres. These paramagnetic centres resulted from breaking of magnetic linkages coexist with long range magnetic ordering. The central paramagnetic enhancement in Mössbauer spectra can be explained on the basis of "paramagnetic centres". There are reports [3] on the elucidation of paramagnetic centres through the Mössbauer spectroscopy in Li-Al ferrites in the higher non-magnetic concentration. In the present samples, the paramagnetic centres may be thought of created by redistribution of cations induced by SHI-irradiation. Reduction in the saturation magnetic moment in the irradiated sample can be understood quantitatively, by considering the rearrangement of the cations and fractional formation of paramagnetic centres by SHI Irradiation. Thus, the central doublet in the Mössbauer spectra of the irradiated samples originates from the SHI-induced paramagnetic centres and not due to amorphous phase.

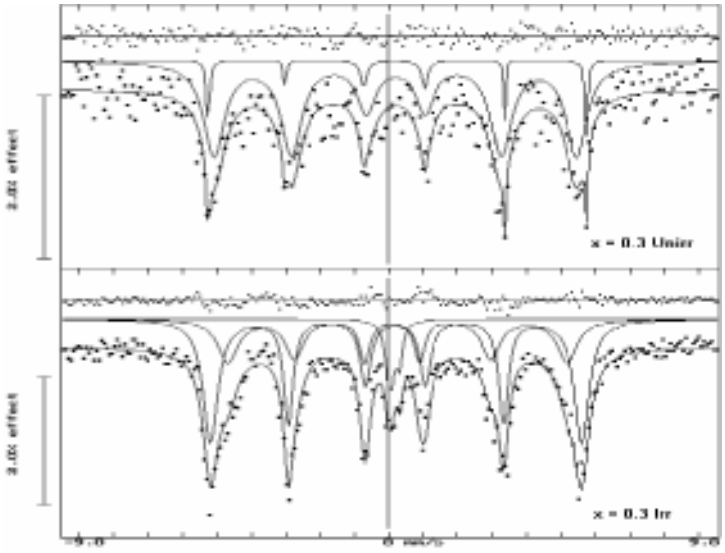

Fig. 1 : Mössbauer spectra at 300K

REFERENCES

[1] F. Thibaudau et al; Phys. Rev. Lett. 67 (12), 1582 (1991)
[2] G. Szenes, Phys. Rev. B5 1(13) 8026 (1995)
[3] S. K. Kulshreshtha, J. Mater. Sci. 5 638 (1986)

5.2.27 Effect of 50 MeV Li^{3+} Ion Irradiation on the Crystal Anisotropy of M – type Sr – Hexaferrite Crystals.

K.K. Bamzai[4], Balwinder Kaur[4], Monita Bhat[4], P.N. Kotru[4], F. Licci[1], Ravi Kumar[2], S.D. Kulkarni[3], P.A. Joy[3]

[1]Instituto MASPEC – CNR, Via Chiavari 18/A, 43100 Parma, Italy.
[2]Nuclear Science Centre, New Delhi.

[3]Physical Chemistry Division, National Chemical Laboratory, Pune.
[4]Crystal Growth and Materials Research Group, Department of Physics and Electronics, University of Jammu, Jammu.

In magnetic materials like $Y_3Fe_5O_{12}$, $BaFe_{12}O_{19}$ and $NiFe_2O_4$, magnetic properties are very sensitive to irradiation – induced defects that may result into decrease in the value of saturation magnetization [1–3]. Superexchange interactions in magnetic insulators like $Y_3Fe_5O_{12}$, $BaFe_{12}O_{19}$ or $SrFe_{12}O_{19}$ are sensitive to any changes in crystallographic positions, which may change the magnetic properties. It is confirmed by means of Mossbauer spectroscopy [4] that a paramagnetic phase is induced as a result of irradiation. In the present work, we have studied the effect of 50 MeV Li^{3+} ion irradiation effect on the magnetic anisotropy of $SrFe_{12}O_{19}$.

Single crystals of $SrFe_{12}O_{19}$ were grown by high temperature solution growth i.e., flux method [5]. The grown crystals were irradiated with 50 MeV Li^{3+} ion beams at a fluence of 1 x 10^{14} ions/cm^2 using 15 UD Pelletron accelerator at NSC, New Delhi. The magnetic measurements were carried out by using a fully computerized Vibrating Sample Magnetometer Model 4500. M – T measurements were also conducted on the single crystals of $SrFe_{12}O_{19}$.

Fig. 1 shows the variation of magnetization with the applied field for pristine as well as irradiated crystals. It is very clear from the figure that the value of saturation magnetization decreases after irradiation. The value of saturation magnetization (M_s)

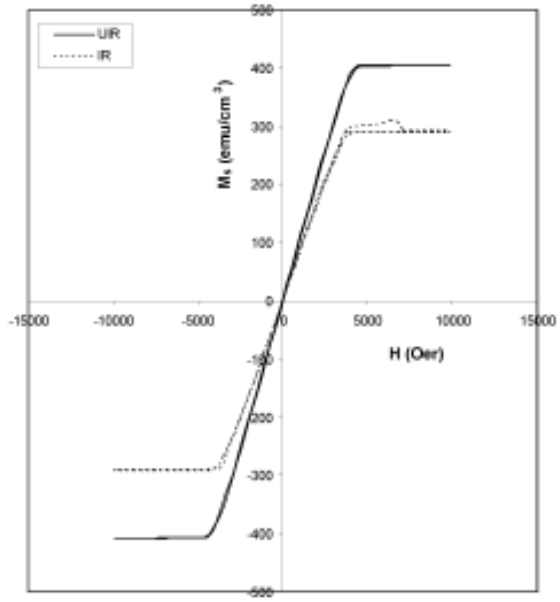

Fig. 1 : Plot shown the M-H curve for Pristine and irradiated $SrFe_{12}O_{19}$ along the c-axis.

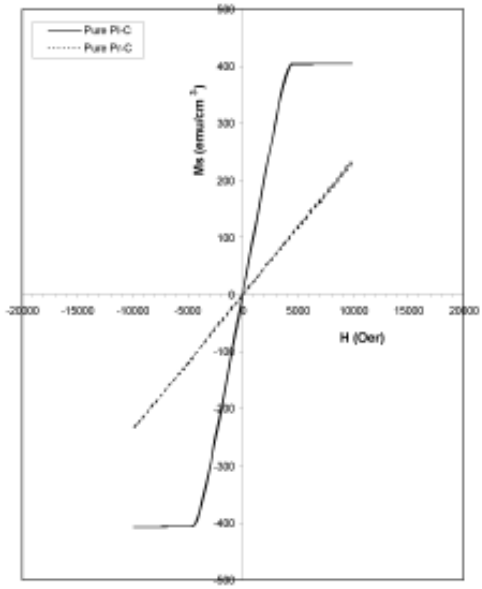

Fig. 2 : Shows the magnetization curves with applied field along the c-axis and perpendicular to c-axis in Pristine $SrFe_{12}O_{19}$.

before irradiation for $SrFe_{12}O_{19}$ was 404.76 (emu/cm^3) which reduces to 292.23 (emu/cm^3) after irradiation. This decrease in M_s may be due to defects/ disorders as already reported in other magnetic insulators [2 – 3]. This decrease is also attributed to the appearance of paramagnetic doublet instead of magnetic sextuplet [4]. Information on crystal anisotropy was obtained by magnetization measurements along basal plane or hard direction. It is well known [6] that for M – type hexaferrites, $K_2 << K_1$ and so relation $K_1 = (M_sH_a)/2$ holds, where H_a is the anisotropy field which can be calculated by the intersection of easy and hard direction magnetization curves at room temperatures. So, in the present case, the available applied field was insufficient to saturate the sample's magnetization in the hard direction and is a straight line. So, a straight-line extrapolation at higher fields was used to determine the intersection point [7] by extending both the curves. Fig. 2 shows the magnetization curves of pristine $SrFe_{12}O_{19}$ along and perpendicular to the c – axis. The values of H_a calculated in pristine $SrFe_{12}O_{19}$ was 17500 Oer, which becomes 18000 Oer after irradiation. The corresponding value of anisotropy constant (K_1) was 3.54 x 10^6 erg/cm^3 and 2.63 x 10^6 erg/cm^3 for pristine and irradiated $SrFe_{12}O_{19}$ respectively. From the M – T measurements, the value of Curie temperature was calculated and it comes out to be equal to 476 ^{0}C. The irradiation has no effect on the value of Curie temperature. Fig. 3 shows the M – T curves for pristine as well as irradiated $SrFe_{12}O_{19}$. The values of H_a, K_1 and T_c calculated in case of pristine $SrFe_{12}O_{19}$ are in agreement with the data reported by Shirk et al [7].

REFERENCES

[1] Z.W. Li, C.K. Ong, Z. Yang, F.L. Wei, X.Z. Zhou, J.H. Zhao, A.H. Morrish, Phys. Rev. B62 (10) (2000) 6530.

[2] G. Fuchs, F. Studer, E. Balanzat, D. Groult, M. Toulemonde, J.C. Jousset, Europhys. Lett. 3 (1987) 3.

[3] D. Groult, M. Hervieu, N. Nguyen, F. Studer, B. Raveau, G. Fuchs, E. Balanzat, Radiat. Eff. 90 (1982) 19.

[4] M. Toulemonde, G. Fuchs, N. Nguyen, F. Studer, D. Groult, Phys. Rev. B35 (13) (1987) 6560.

[5] S. Rinaldi, F. Licci, IEEE Trans. Magn. MAG – 20(5) (1984) 1267.

[6] J. Smit, H.P.J. Wijn, "Ferrites", (John Wiley & Sons, Inc., New York) (1959).

[7] B.T. Shirk, W.R. Buessem, J. Appl. Phys. 40(3) (1969) 1294.

5.2.28 Study of SHI induced modifications in elastic behaviour of spinel Ferrites

K. B. Modi[1], M. C. Chhantbar[1], Ravi Kumar[2] and H. H. Joshi[1]

[1]Department of Physics, Saurashtra University, Rajkot – 360 005
[2]Nuclear Science Centre, New Delhi 110 067.

The analysis of X-ray powder diffraction patterns recorded at 300K before and after irradiation by 50 MeV, Li^{3+} ions (5 x 10^{13} ions/cm^2) for typical composition of spinel ferrite $Li_{0.55}Al_{0.1}Ti_{0.1}Fe_{2.25}O_4$ through "powder X" software confirm the formation of single phase fcc spinel structure, with no extra lines corresponding any other crystallographic phase or unreacted ingredient for both the samples. The distribution of

cations among the available tetrahedral (A-) and octahedral (B-) sites of spinel lattice, is determined through X-ray intensity calculations by comparing intensity of theoretical and experimental ratio of Bragg's plane and it is given by:

Before irradiation - $(Fe_{0.95}\ Al_{0.05}\ )^{A}\ [Fe_{1.3}Al_{0.05}Ti_{0.1}Li_{0.55})^{B}\ O_4^{-2}$
After irradiation- $(Fe_{0.97}\ Ti_{0.03}\ )^{A}\ [Fe_{1.28}Al_{0.1}Ti_{0.07}Li_{0.55})^{B}\ O_4^{-2}$ ..... (1)

The lattice constant, X-ray density, bulk density and pore fraction values for both the samples are given in Table 1. The lattice constant is found to increase after irradiation. It may be due to occupancy of larger Ti^{4+} ions on A-site by replacing smaller Al^{3+} (0.51Å) ions, resulting in expansion of lattice and lattice constant.

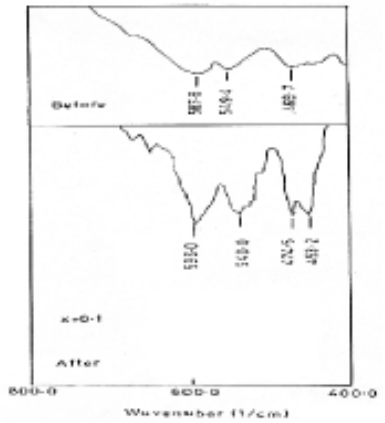

Fig. 1 : Infra-red spectra of Li-Ti-Al-Fe-O compositions at 300K

The room temperature (300K) infrared spectra for typical $Li_{0.5+0.5x}Ti_xAl_{0.1}Fe_{2.4-1.5x}O_4$ spinel ferrite composition before and after SHI irradiation are shown in Fig. 1. It can be seen from the Figure 1 that the IR spectra exhibit two bands in the range 400-700 cm^{-1}. No absorption bands were observed above 700 cm^{-1}. The high frequency bands υ_1 is caused by the stretching vibration of the tetrahedral metal-oxygen bond and the absorption band υ_2 are caused by the metal –oxygen vibrations in octahedral sites. The change in the band positions is expected because of the difference in the Fe^{3+}-O^{2-} distances for the octahedral (1.99 Å) and tetrahedral (1.89 Å) complexes.

The close examination of IR spectra revealed the well resolved splitting of the principal bands, after SHI irradiation as compared to unirradiated composition. This may be attributed to the Fe^{2+}ion induced Jahn-Teller distortion in the lattice due to a non-cubic component of the crystal field potential. This also suggest that irradiation induced defects hindered the distribution of vibrations.

The values of various elastic parameters like force constant, elastic wave velocities, bulk modulus, rigidity modulus, Young's modulus, Poisson's ratio, Debye temperature of porous compositions and corrected zero porosity are summarized in Tables 2 and 3. The

parameters are calculated using structural parameters; lattice constant, X-ray density, pore fraction, molecular weight obtained from X-ray diffraction and band positions from infrared spectroscopic measurements (Table 1) with the help of standard formulae available in the literature [1-3].

Table 1: Lattice constant (a), X-ray density (ρ), bulk density (d), pore fraction (f), molecular weight (M)and band position (ν) for Li-Al-Ti-Fe-O composition.

	a(Å) ±0.002Å	ρ d $(kg/m^3) \times 10^3$		f	M_1 M_2 $(kg) \times 10^{-3}$		ν_1 ν_2 $(m^{-1}) \times 10^2$	
Before	8.2814	4.59	4.28	0.0675	54.404	41.278	587.8 549.4	468.7
After	8.3368	4.50	4.28	0.0489	55.609	40.676	596 540	474.5 453.2

Table 2: Force constant (k), Elastic wave velocity (V), bulk modulus (B), Young's modulus (E), rigidity modulus (G).

	k_t k_o k (N/m) × 10^2			V_l V_s V_m (m/s)			B E G (Gpa)		
Before	1.3403	0.9630	1.1517	5504.21	3177.86	3528.06	139.06	125.15	46.35
After	1.3671	0.9294	1.1483	5532.09	3194.09	3546.08	137.73	123.96	45.91

Table 3: Poisson's ratio (σ), Debye temperature (θ), bulk modulus (B_o), Young's modulus (E_o) and rigidity modulus (G_o) (Corrected to zero porosity).

	σ	θ (K)	B_o(Gpa)	E_o	G_o	σ_o
Before	0.35	485.47	177.95	144.64	53.00	0.365
After	0.35	484.74	160.11	137.37	50.49	0.360

It is seen that after irradiation, force constant and elastic moduli corrected to zero porosity decrease, suggesting, weakening of interatomic bonding. Furthermore, percentage reduction in bulk modulus value is around 10.03% while it is 5.03% and 4.73% for Young's modulus and rigidity modulus respectively, which suggests volumetric deformation dominates all other deformation.

REFERENCES

[1] Ultrasonic Science and Technology, Baldev Raj Narosa Publication

[2] D. P. H. HASSELMAN and R. M. FULRATH, J. Amer. Ceram. Soc. 47 (1964)52.

[3] O. L. ANDERSON, in "Physical Acoustics" edited by W. P. Mason, Vol. 3B (Academic Press, New York, 1965) p. 45.

5.2.29 Radiation damage effect on mixed valence manganites

S. Chattopadhyay[1], A. Sarkar[2], R.J. Chaudhuri[3], Anjana Dogra[3], Ravi Kumar[3], B.K. Chaudhuri[4] and P.K. Bhattacharyya[1]

[1]Department of Physics, University of Calcutta, 92 A.P.C. Road, Kolkata- 700009
[2]Department of Physics, Bangabasi Morning College, 19 Rajkumar Chakraborty Sarani, Kolkata- 700 009
[3]Nuclear Science Center, New Delhi-110067
[4]Department of Solid State Physics, Indian Association for the Cultivation of Science, Jadavpur, Kolkata 700 032

In the present report, main thrust has been given on the systematic plan of our experiments to study the role of irradiation-induced defects and disorder on physical properties of the system. Polycrystalline La0.3Ca0.3MnO3 samples prepared by ceramic method are ball-milled to form nano-sized particles. The nano-sized samples are annealed at different temperatures to control the grain-growth and the particle size. We had certain motivations prior to this beam time experiment. Firstly, we intended to study the resistivity of this sample before irradiation as a function of temperature while cooling the sample down to liquid nitrogen temperature to have the feature in the unirradiated specimen. Secondly, we had an idea to study the online resistivity of the sample at the LN_2 temperature as a function of time while the beam is on. It was so planned to investigate the role of irradiation-induced defects and disorder in changing physical properties of the system. Finally, we planned to study the resistivity of the irradiated sample again while heating the sample up to room temperature.

We all faced some unusual problems in the whole experiments. While cooling the sample, one lead of the four-probe set up gets detached from the sample at the last stage of the low temperature resistivity measurement. That is why we were bound to perform the rest of the measurements with two-probe set up. The resistance of the sample as a function of the temperature is shown in the figure 1(a). Then we have performed the online resistivity measurement as a function of time with a final fluence of 3.5×10^{14} ions/ cm^2. The beam is intentionally set off time to time to investigate the role of annealing of defects. The moment when the beam is off is clearly identified by a substantial drop of resistivity time to time. The result so obtained has been depicted in figure 2. Finally the samples are heated to room temperature and the resistivity is measured once again as a function of temperature to identify the defects getting annealed with temperature. Here we lost some data (unfortunately in the vicinity of the transition region) due to power cut off very unusual in NSC. The data still collected is shown in the figure 1(b). These are the main results we have found from the last year's beam time experiment. This study is of great importance from the point of view that an idea of optimization of fluence, while ion-beam irradiation is used for material modification, may be obtained this way. Other supporting studies and analyses on this system are going on and will be reported later.

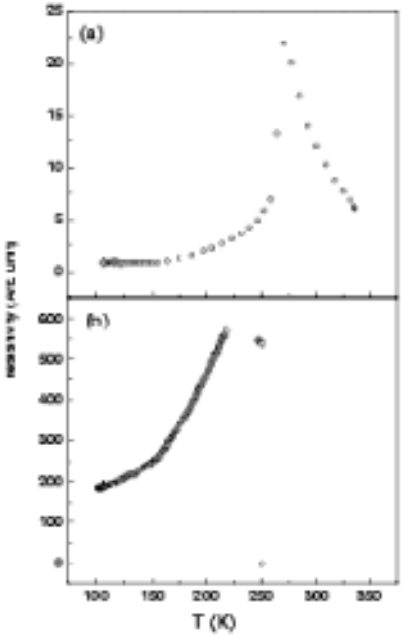

Fig. 1 : Variation of resistivity of $La_{a7}Ca_{a3}MnO_2$ with temperature (a) unirradiated and (b) irradiated with 50 MeVLi^{++} beam with a fluence of 3.5625 X 10^{14} ions/cm^2

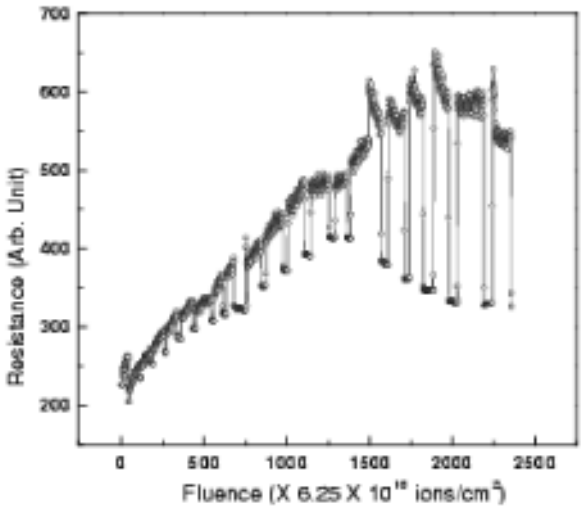

Fig. 2 : Online resistivity of the sample $La_{a7}Ca_{a3}MnO_2$ while irradiated by 50 MeV Li^{24} beam at fluence of 3.5625x10^{14} ions/cm^2 at the liquid nitrogen temperature

We gratefully acknowledge the helpful coopertaion from Mr R.N. Dutta during the low temperature resistivity measurement.

REFERENCES

[1] C.N.R. Rao, A.K. Raychoudhuri, in: C.N.R. Rao, B. Raveau (Eds.), Colossal Magnetoresistance, Charge Ordering and Related Properties of Manganese Oxides, World Scientific, Singapore,1998.

[2] C.H. Chen, V. Talyansky, C. Kwon, M. Rajeswari, R.P. Sharma, R. Ramesh, T. Venkatesan, John Melngailis, Z. Zhang, and W.K. Chu, Appl. Phys. Lett. 69 (1996) 3089.

[3] S. B. Ogale et al., J. Appl. Phys. 84 (1998) 6255.

[4] S. Chattopadhyay, A. Banerjee, A. Sarkar, Ravi Kumar, B.K. Chaudhuri, D. Banerjee, Radiat. Meas. 36 (2003) 689.

[5] S. Chattopadhyay, A. Sarkar, Aritra Banerjee, S. Karmakar, D. Banerjee, Ravi Kumar and B.K. Chaudhuri, Nucl. Instr. Meth. B. 226 (2004) 274

5.2.30 SHI Irradiation as a Tool for Controlled Creation of Optically Active F_2/F_3^+ Color Centers in LiF Thin Films

M. Kumar[1], F. Singh[2], S.A. Khan[2], A. Tripathi[2], D.K. Avasthi[2] and A.C. Pandey[1]

[1]Department of Physics, University of Allahabad, Allahabad 211 002, India
[2]Nuclear Science Centre, New Delhi 110 067, India

We have studied optically active F_2 and F_3^+ color centers, defect aggregates of F centers, which can emit intense and tunable light in the visible region and can be operated simultaneously under a single wavelength pumping. Generation of these defects can be controlled by proper choice of irradiation conditions. The LiF thin films were irradiated uniformly by 80 MeV Ni ions under high vacuum with different ion fluences. The fluence was varied from $1x10^{11}$ to $1x10^{14}$ ions/cm^2 for room temperature (RT) irradiation and $7x10^{11}$, $1x10^{12}$, $3x10^{12}$ ions/cm^2 for low temperature (LT) (218 K) irradiation. Photoluminescence (PL) spectroscopy has been performed in order to optimize experimental parameters for the controlled creation of F_2 and/or F_3^+ color centers and

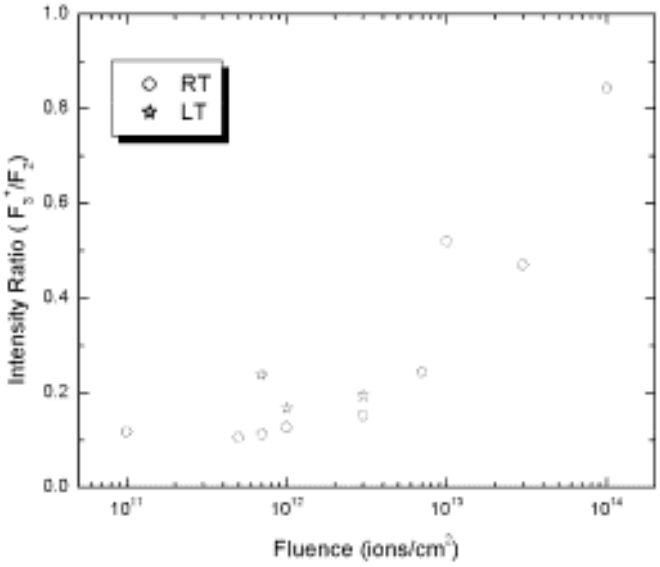

Fig. 1 : significant increase of their luminescence intensities.

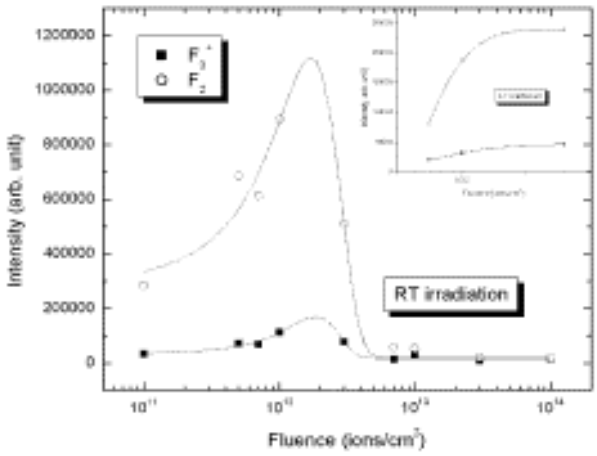

Fig. 2

The RT photoluminescence spectra of SHI irradiated samples at RT as well as LT show two broad bands peaking at about 534 and 665 nm corresponding to F_3^+ and F_2 color centers respectively [1]. Fig.1 shows the variation of the intensities of these two bands with ion fluence, the inset in the fig.1 is the change in emission intensity from the samples irradiated at LT. The intensities of both bands increase up to the fluence of $1x10^{12}$ ions/cm^2 followed by an exponential decrease. The LT irradiated samples also show the increase in the PL intensity with fluence.

The ratio of the intensities of F_3^+ and F_2 color centers increases with fluence as shown in fig.2. At higher fluence the intensities of both the color centers are comparable, although their intensities decrease. The ratio of the intensities of these bands is higher for the LT irradiated samples at the same fluence. Thus the irradiation at LT can improve this ratio at lower fluence than RT irradiation.

REFERENCES

[1] M. Kumar, F. Singh, S. A. Khan, V. Baranwal, S. Kumar, D. C. Agarwal, A. M. Siddiqui, A. Tripathi, A. Gupta, D. K. Avasthi and A. C. Pandey, J. Phys. D: Appl. Phys. 38 (2005) 637.

5.2.31 Heavy Ion Induced Modifications In Some Polymeric Track Recorders

Surinder Singh[1], Sangeeta Prasher[1]

[1]Department of Physics, Guru Nanak Dev University, Amritsar, 143005

Swift heavy ion (SHI) induced modifications in polymers have many promising applications in the field of applied sciences. SHI can induce significant modifications in polymeric systems that vary from polymer to polymer depending on the conformation of the molecular unit. In the present investigations the influence of heavy ions on the structural, optical and electrical properties of some polymers viz. CR-39, LR-115, PET, Lexan, Makrofol-KG and Kapton-H has been studied.

The polymers have been irradiated with the Li^{3+} and O^{6+} ion beams having energies of 40 and 80 MeV respectively using 15UD pelletron at Nuclear Science Centre, New Delhi. The beam current was maintained at 1pnA. Irradiation has been made at five fluences ranging from $3x10^{11}$-$3x10^{13}$ions/cm^{2}in case of lithium and 10^{11}-10^{13}ions/cm^2 for oxygen. The rate of energy loss and the range of the ions in the polymers have been calculated using SRIM-2003. The structural properties have been characterized by FTIR and UV-VIS spectroscopy. The changes in the band gap and Urbech's energy have been calculated from the UV-VIS spectra of the pristine and heavy ion treated polymers. The decrease in the band gap energy of all the polymers has been observed. The decrease in band gap energy is maximum for CR-39 and minimum for PET exposed to Li- ion beam. The decrease in the Urbech's energy of CR-39 and PET has also been observed. This may be due to the loss of crystallinity of these polymers with irradiation. However an increase in the Urbech's energy in case of Makrofol-KG and lexan with ion fluence has been

observed. The value of the Urbech's energy remains constant for Kapton-H. This shows the resistant behavior of the monomeric unit of this polymer towards irradiation.

Since all the polymers used for ion irradiation contain C=O linkage a band near 1730cm^{-1} has been observed and decrease in its intensity with ion fluence has also been noticed that may be attributed to the cleavage of the polymeric chain at this linkage. Except this band the increase in the intensity of the band near 2370 and 3600cm^{-1} has been observed indicating the evolution of CO_2 and generation of –OH group due to irradiations. The changes in the dielectric constant and dielectric loss tangents have also been calculated using Hewlett Packard LCR meter 4284A. The values of dielectric constant are found sensitive to ion fluence as well as frequency. It is found that the dielectric constant decreases rapidly with increasing frequency and reaches a constant value at 100 kHz.

5.2.32 Effect of Ion Beam Irradiation on Filled Natural Rubber, Carboxylated Styrene Butadiene Rubber Latices and their Blend

Ranimol Stephen[1], A.M. Siddique[2], Fouran Singh[2], Lekshmi Kailas[3], Kuruvilla Joseph[4] & Sabu Thomas[1*]

[1]School of Chemical Sciences, MGU, Kottayam, Kerala- 686 560
[2]Nuclear Science Centre, New Delhi
[3]
[4]Department of Chemistry, St. Berchuman's College, Mahatma Gandhi University, Kerala, India

Many researchers have shown interest on the studies of the chemical and physical structural modifications in the polymeric material induced by ion- bombardment. Lots of investigations have been performed to characterize the induced changes in polymers originated from ion- matter interactions, including changes in the resistance to solvents, in the optical and in electrical properties [1-4].

The present work deals with the effect of ion- beam irradiation on natural rubber, carboxylated styrene butadiene rubber latexes and their blends. The surface changes occurred in silica filled films were studied using X- ray photoelectron spectroscopy.

Natural rubber (NR) latex containing 60% dry rubber content was procured from Gaico rubbers Pvt. Ltd., Kottayam, Kerala, India. The synthetic latex Carboxylated styrene butadiene rubber (XSBR) latex with 48% dry rubber content was collected from Apar Industries Ltd., Mumbai.

The latex films were irradiated with $^{28}Si^{8+}$ ion beam of 100MeV in the General Purpose Sealtering Chamber (GPSC) at Nuclear Science Centre (NSC), New Delhi. The films were irradiated at varying fluences. The current was maintained at 2pnA.

The change in surface compositions on irradiation was determined quantitatively by X-ray photoelectron spectroscopy using SSX 100/206 Photoelectron Spectrometer from Surface Science Instruments (USA) equipped with a monochromatized microfocus Al X-ray source powered at 20mA and 10kV.

X-ray photoelectron spectroscopy

The binding energies of C_{1s}, O_{1s} and Si_{2p} of silica filled unirradiated and irradiated NR, XSBR and 70/30 NR/XSBR are determined. The binding energies of unirradiated systems for C_{1s}, O_{1s} and Si_{2p} are 285.8, 533.1 and 102.9 respectively for NR. The binding energies of C_{1s}, O_{1s} and Si_{2p} show almost same values for all system before and after irradiation. The unchanged binding energy values indicate the redistribution of elements within the system upon ion-beam irradiation.

For NR at lower fluence the peak area of C_{1s} increased and then decreased at higher fluence, indicating chain depletion. The peak area of O_{1s} decreases with increase in fluence. The area of Si_{2p} increases with ion fluence. In the case of XSBR the area of the peak C_{1s} and O_{1s} shows steep rise with ion fluence. The Si_{2p} peak area of XSBR increases constantly with fluence similar to that of NR.

The 70/30 NR/XSBR shows decrease in peak area of C_{1s} and O_{1s} compared to unirradiated. The minimum peak area can be observed at lower fluence. The change in peak area of Si_{2p} is quite different from the virgin polymers. The unirradiated system itself shows lower Si_{2p} peak area when compared to unirradiated NR and XSBR. This is due to the uneven distribution of silica filler in the two phases. In this case XSBR is dispersed in the continuous NR matrix. At lower fluence, the Si_{2p} peak area increases while at higher fluence it decreases. For 70/30 blend system, the C_{1s} percentage initially decreases, and then increases at higher fluences. The change in the atomic percentage of oxygen shows a trend similar to C_{1s} in 70/30 systems. The Si atomic percentage increases at lower fluence but drastically decreases at higher fluence.

REFERENCES

[1] E.H. Lee, Nucl. Instr. & Meth., B151 (1999) 29
[2] D.M. Ruck, J. Schulz, N. Deusch, Nucl. Instr. & Meth., B131 (1997)149
[3] L. Singh, R. Singh, Nucl. Instr. & Meth. B225, 4 (2004)478
[4] S. Takahashi, M. Yoshida, M. Asano, M. Notomi, T. Nakagawa, Nucl. Instr. & Meth. B217, 3 (2004) 435

5.2.33 C^{5+} Ion Irradiation Effects on Ionic Conduction in Lithium based Gel Polymer Electrolytes

D. Saikia[1], A.M.P. Hussain[1], A.Kumar[1], F. Singh[2], N.C.Mishra[3] and D.K.Avasthi[2]

[1]Department of Physics, Tezpur University, Napaam, Tezpur-784028, Assam

[2]Nuclear Science Centre, Aruna Asaf Ali Marg, New Delhi-110067
[3]P.G. Department of Physics, Utkal University, Bhubaneswar-751004

High energy ion irradiation of polymers leads to remarkable changes in their physical and chemical properties [1]. Permanent modifications in the molecular weight distribution and solubility [2], electrical [3], optical [4] and mechanical properties [5] of polymers and other materials have been detected after ion irradiation. P(VDF-HFP)-(PC+DEC)-$LiClO_4$ and P(VDF-HFP)-(PC+DEC)-$LiCF_3SO_3$ gel polymer electrolyte systems were irradiated with 70 MeV C^{5+} ion beam with different fluences 5×10^9, 7×10^9, 10^{10}, 2×10^{10}, 6×10^{10}, 10^{11}, 3×10^{11}, 7×10^{11} and 10^{12} ions/cm^2 using GPSC high vacuum chamber. Polymer gel electrolyte samples have been prepared by solution casting technique with film thicknesses < 30 μm. The ionic conductivity for all the irradiated samples with different fluences and temperatures was obtained from the complex impedance analysis. SEM and XRD analysis have been carried out for microstructural characterization and crystallinity study respectively. FTIR study has been conducted to investigate the molecular level polymer-ion interactions in irradiated gel polymer electrolytes.

Figs. 1 and 2 show the conductivity versus temperature inverse plots for C^{5+} ion irradiated P(VDF-HFP)-(PC+DEC)-$LiClO_4$ and P(VDF-HFP)-(PC+DEC)-$LiCF_3SO_3$ gel polymer electrolytes respectively. From the figures it is observed that the ionic conduction in both the ion irradiated gel polymer electrolyte systems obey the VTF (Vogel-Tamman-Fulcher) relation [6-8], which describes the transport properties in a viscous matrix [9]. If the conductivity versus temperature dependence curve is linear in larger temperature region then it is said to be Arrhenius. VTF (curved) behavior can be modeled as Arrhenius (linear) behavior by dividing the entire temperature regime into smaller temperature regions. The interconnection between Arrhenius and VTF behavior of σ (T) are widely reported and discussed in literature [10]. This behavior is rationalized by arguing that since VTF dependence is governed by the energy interval $k(T-T_0)$ and the Arrhenius dependence by the energy kT (where k Boltzmann constant), for $T \gg T_0$ [11] i.e. when T_0 is quite smaller than T, the curvature of conductivity versus temperature plot becomes small and VTF equation approaches Arrhenius equation.

X-ray diffractograms of pristine, and C^{5+} ion irradiated P(VDF-HFP)-(PC+DEC)-$LiClO_4$ and P(VDF-HFP)-(PC+DEC)-$LiCF_3SO_3$ gel polymer electrolyte systems are shown in Figs. 3 and 4 respectively. X-ray diffraction from crystalline regions of P(VDF-HFP) gives sharp and well-defined peaks located at 2θ angular positions at 18°, 18.5° and 20°. From the Bragg's law, interplanar spacing of 0.492, 0.479 and 0.443 nm are obtained, corresponding respectively to the (100), (020) and (110) atomic planes of PVDF [12]. From Fig. 3 it is observed that crystallinity decreases in C^{5+} ion irradiated P(VDF-HFP)-(PC+DEC)-$LiClO_4$ system after low fluence ion irradiation (= 10^{11} ions/cm^2) and increases at higher fluence (> 10^{11} ions/cm^2) ion irradiation.

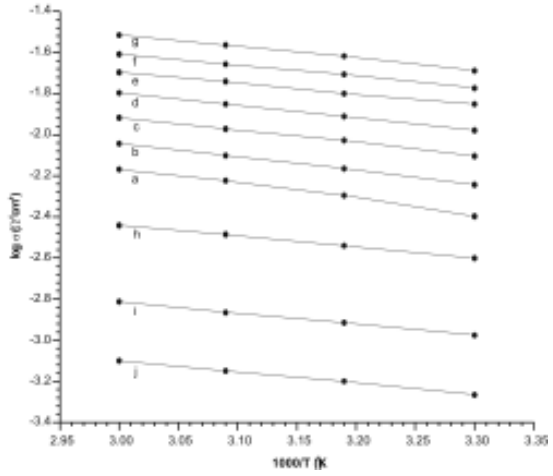

Fig. 1 : Temperature dependence of ionic conductivity of C^{5+} ion irradiated P(VDF-HFP)-(PC+DEC)-$LiClO_4$ (20:70:10 wt%) gel polymer

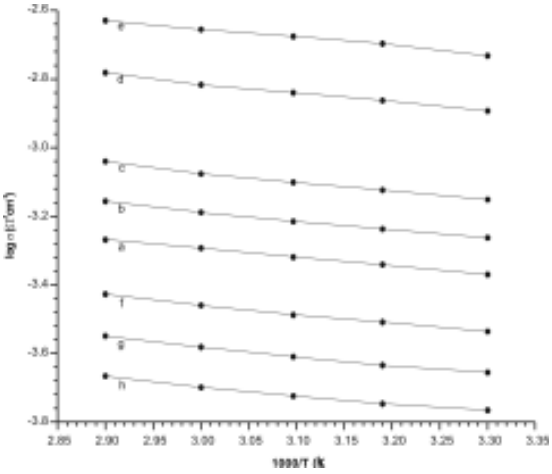

Fig. 2 : Temperature dependence of ionic conductivity of C^{5+} ion irradiated P(VDF-HFP)-(PC+DEC)-$LiCF_3SO_3$ (20:70:10 wt%) gel polymer electrolyte (a) unirradiated, (b) 10^{10}, (c) 2×10^{10}, (d) 6×10^{10}, (e) 10^{11}, (f) 3×10^{11}, (g) 7×10^{11} and (h) 10^{12} ions/cm^2.

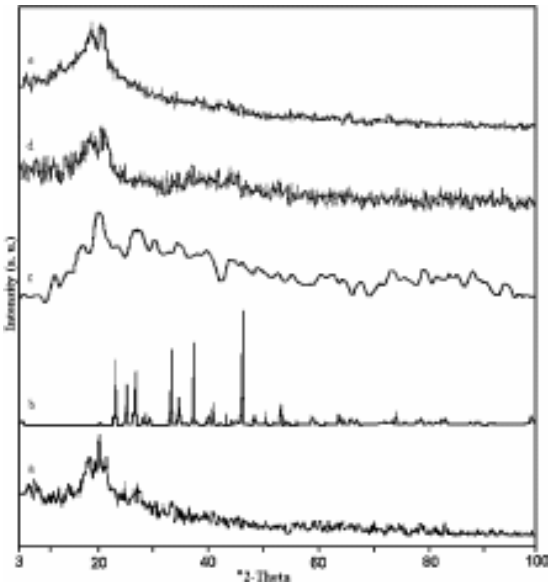

Fig. 3 : XRD patterns of (a) P(VDF-HFP), (b) $LiClO_4$, (c) unirradiated P(VDF-HFP)-(PC+DEC)-$LiClO_4$, (d) C^{5+} ion irradiated P(VDF-HFP)-(PC+DEC)-$LiClO_4$ (5×10^9 ions/cm^2) and (e) C^{5+} ion irradiated P(VDF-HFP)-(PC+DEC)-$LiClO_4$ (10^{12} ions/cm^2) gel polymer electrolyte.

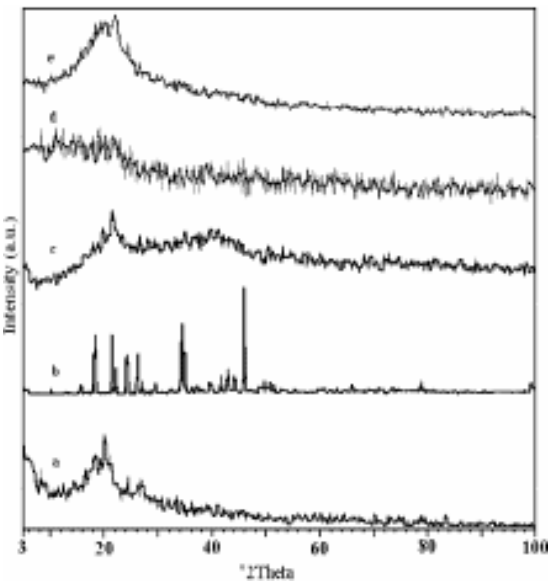

Fig. 4: XRD patterns of (a) P(VDF-HFP), (b) $LiCF_3SO_3$, (c) unirradiated P(VDF-HFP)-(PC+DEC)-$LiCF_3SO_3$, (d) C^{5+} ion irradiated P(VDF-HFP)-(PC+DEC)-$LiCF_3SO_3$ (10^{10} ions/cm^2) and (e) C^{5+} ion irradiated P(VDF-HFP)-(PC+DEC)-$LiCF_3SO_3$ (10^{12} ions/cm^2) gel polymer electrolytes.

After low fluence ion irradiation (= 10^{11} ions/cm^2) crystallinity decreases due to breaking of bonds which amorphizes the sample. But at fluence 10^{12} ions/cm^2, reordering and crosslinking of bonds take place which form the new crystalline region in the polymer electrolyte

The values of percentage of degree of crystallinity for pure P(VDF-HFP), unirradiated P(VDF-HFP)-(PC+DEC)-$LiClO_4$ (20:70:10 wt%) and C^{5+} ion irradiated P(VDF-HFP)-(PC+DEC)-$LiClO_4$ (20:70:10 wt%) gel polymer electrolyte with fluence of 5×10^9 and 10^{12} ions/cm^2 are found to be 30%, 13.64%,11.5% and 18.75% respectively. For unirradiated P(VDF-HFP)-(PC+DEC)-$LiCF_3SO_3$ (20:70:10 wt%) and C^{5+} ion irradiated P(VDF-HFP)-(PC+DEC)-$LiCF_3SO_3$ (20:70:10 wt%) system with fluence of 10^{10} and 10^{12} ions/cm^2, the percentage of degree of crystallinity are found to be 21.8%,10.2% and 29.2% respectively. It is observed that after low fluence (10^{10} ions/cm^2) ion irradiation crystallinity decreases as compared to that of unirradiated gel polymer electrolyte and increases at higher fluence (10^{12} ions/cm^2) ion irradiation. This suggests that threshold fluence is required for recrystallization to takes place.

REFERENCES

[1] L. Calcagno and G. Foti, Nucl. Instr. and Meth. B 19/20 (1987) 895.
[2] G. M. Mladenov and B. Emmoth, Appl. Phys. Lett. 38 (1981) 1000.
[3] S. Schiestel, W. Ensinger and G. K. Wolf, Nucl. Instr. and Meth. B 91 (1994) 473.
[4] D. Fink, M. Müller, L. T. Chadderton, P. H. Cannington, R. G. Elliman and D. C. McDonald, Nucl. Instr. and Meth. B 32 (1988) 125.
[5] E. H. Lee, Y. Lee, W. C. Oliver and L. K. Mansur, J. Mater. Res. 8 (1993) 377.
[6] H. Vogel, Z. Phys. 22 (1922) 645.
[7] V. G. Tammann and H. G. Hesse, Anorg. Allg. Chem. 19 (1926) 245.
[8] G. S. Fulcher, J. Am. Ceram. Soc. 8 (1925) 339.
[9] H. Wang, H. Huang and S. L. Wunder, J. Electrochem. Soc. 147(8) (2000) 2853.
[10] J. R. MacCallum and C. A. Vincent in: Polymer Electrolyte Review 1 (1987) 185.
[11] Th. Joykumar Singh, T. Mimani, K.C.Patil and S.V.Bhat, Solid State Ionics 154/155 (2002) 21.
[12] R. Percolla, L. Calcagno, G. Foti and G. Ciavola, Appl. Phys. Lett. 65(23) (1994) 2966.

5.2.34 Optoelectronic Processes In 75 MeV Oxygen Ion Irradiated Polyimide Film

J K Quamara[1], Maneesha Garg[1], T. prabha[1], Anu sharma[1], Geetika[1]

[1]Dept. of Applied Phys., National Institute of Technology, Kurukshetra-136119

Kapton-H polyimide a highly thermally stable insulating polymer is known to exhibit interesting optoelectronic properties including photo-conduction, photoelectret and autophotoelectret state [1-3]. In the present report the results of autophotoelectret state i.e. persistent internal polarization by illumination alone (without applying any electric field) have been discussed for 75 MeV oxygen ion irradiated kapton-H film at fluences 3.1 X 10^{12} and 1.8 X10^{13} ions/cm^2. The kapton-H samples (thickness: 25 μm, area:1 cm^2) which were vacuum metallized on one side by aluminum, were sandwiched between

this aluminum electrode and conducting NESA glass. The autophotoelectret effect was studied, using specially prepared electrode assembly with visible light (100 watt tungsten filament lamp) at different temperatures ranging from 32° to 250°C.

There is variation of photo-current in irradiated as well as pristine kapton-H samples by illuminating the sample surface at 80 ^{0}C. As soon the sample is illuminated, an exponential rise in the photo-current is observed which reaches maximum in ~ 50 sec. Thereafter, it starts decaying slowly and attains a saturation with in 10 to 15 minutes. There was dependence of this maximum photo-current (I_{PC}) on temperature for $3.1x10^{12}$ ions/cm^2 irradiated kapton-H samples. The autophotoelectret phenomena can be explained as follows: in metal-polymer–metal system a contact potential difference always appears at high temperature and this difference is more pronounced if the electrodes are of different materials as in the present case, where one electrode is of aluminum and other of NESA glass (tin oxide). As soon as the sample is illuminated, the photo generated charge carriers are expected to move under the influence of this internal field. Now if the sample were short-circuited through the electrometer a current would be registered in it. A decrease in this current after some time followed by saturation may be due to the establishment of a dynamic equilibrium between the generation and thermal recombination of these photo-charges. The effect of ion irradiation appears to decrease the autophotoelectret state character in kapton-H. This may be attributed to the reduced lifetime and mobility of the charge carrier [4]. The increase in photo-current as a result of increase in the temperature of the metal-polymer-metal system is quite obvious, as the contact potential difference would increase with increase in temperature of the electrodes.

REFERENCES

[1] JK Quamara, R P Bhardwaj, P K C Pillai and B L Sharma, Acta Polymerica, 34 (1983) 355.
[2] JK Quamara, R P Bhardwaj and B L Sharma, Applied Physics A 35 (1984) 267.
[3] T Matsuura, Y. Hasuda, S Nishi and N Yamada, macromolecules (1992).
[4] Yoshiaki Takai, Mitsunari Inagaki, Masumi Inoue, Teruyoshi Mizutani and Masayuki Ieda, J. Phys. D: Appl. Phys. 20 (1987) 93.

5.2.35 Investigation of effects of 160 MeV Ni^{12+} Ion Irradiation on Polypyrrole Conducting Polymer Electrode Materials Supercapacitor

A.M. Pharhad Hussain[1], D. Saikia[1], A. Kumar[1], F. Singh[2], D.K. Avasthi[2]

[1]Department of Physics, Tezpur University, Napaam, Tezpur, Assam-784 028
[2]Nuclear Science Centre, Aruna Asaf Ali Marg, New Delhi-110 067

Conducting polymer polypyrrole thin films doped with $LiClO_4$, $LiCF_3SO_3$, $[CH_3(CH_2)_3]_4NBF_4$ and $[CH_3(CH_2)_3]_4NPF_6$ synthesized electrochemically on ITO coated glass have been irradiated by 160 MeV Ni^{12+} with different fluence $5X10^{10}$, $5X10^{11}$ and $3X10^{12}$ ions cm^{-2}. Irradiated and unirradiated polymer films have been used as electrode materials for all polymer supercapacitor devices.

The conductivity of the polymer films before and after irradiation are measured by using standard four probe setup and are presented in Table 1. The increase in conductivity of the polymer films after SHI irradiation could be attributed to cross-linking due to deposition of huge amount of electronic energy, leading to increase in crystallinity which facilitates inter chain electron hopping required for conduction between the chains. Defect sites in the molecular structure of the polymer chain created by SHI irradiation also contribute to higher dc conductivity as charge accumulation takes place which produces charge carriers.

Dopant	**Unirradiated (S/cm)**	**$5x10^{10}$ions/cm^2 (S/cm)**	**$5x10^{11}$ions/cm^2 (S/cm)**	**$3x10^{12}$ions/cm^2 (S/cm)**
$LiClO_4$	105-110	145-155	155-165	170-175
$LiCF_3SO_3$	102-109	150-160	158-167	165-174
$[CH_3(CH_2)_3]_4NBF_4$	110-115	155-165	158-167	174-180
$[CH_3(CH_2)_3]_4NPF_6$	110-117	155-165	160-170	172-180

Table 1: Conductivity measurements of polypyrrole conducting polymer films before and after irradiation

The UV-Vis spectra of the conducting polymer films recorded using Beckman DU® 530 Life Science UV-VIS spectrophotometer before and after SHI irradiation are presented in figure 1. The unirradiated polypyrrole films show its characteristic absorption peak at around 320 nm which is a $\pi - \pi^*$ transition of the heteroaromatic pyrrole ring [1]. The absorption peak at about 440 nm is the polaron absorption peak of polypyrrole conducting polymer [1]. The intensity of absorption is directly proportional to the quantity of carrier present in the polymer film. After SHI irradiation, the intensity of this peak goes on increasing with increase in fluence which is consistent with the conductivity measurement results. The broadening of the carrier absorption peak may occur due to increase in defect sites of the polymer chain in SHI irradiation. The increase in absorption towards higher wave number is an indication of high dc conductivity of conducting polymer.

The XRD spectra of the polymer films before and after SHI irradiation are presented in figure 2. Upon SHI irradiation the degree of crystallinity of the polymer films shows significant increase. The crystallinity of polymer films arises due to systematic alignment of polymer chains by chain folding or by the formation of single or multiple helices, for at least part of their length [2]. The degree of crystallinity is observed to increase with the increase in ion fluence (Fig.2). The increased crystallinity gives rise to increased hopping of charge carriers resulting in increased dc conductivity.

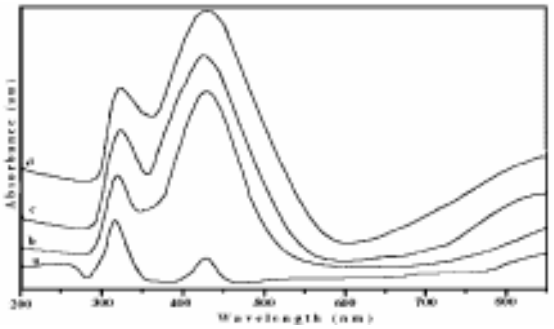

Figure 1 : UV-Vis absorption spectra of polypyrrole before irradiation (a), after irradiation with fluence $5x10^{10}$ (b), $5x10^{11}$ (c) and $3x10^{12}$ ions/cm^2 (d).

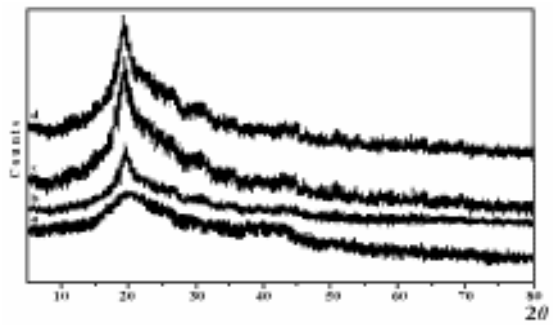

Figure 2 : X-Ray diffractogram of polypyrrole before irradiation (a), after irradiation with fluence $5x10^{10}$ (b), $5x10^{11}$ (c) and $3x10^{12}$ ions/cm^2 (d).

REFERENCES

[1] J. Chen, C. O. Too, G.G. Wallace and G.F. Swiegers, *Electrochimica Acta,* **49** (2004) 691.

[2] *Applications of Electroactive Polymers* ed. by Bruno Scrosati, Chapman & Hall, London (1993).

5.2.36 Electrical Studies of Polyethelene Terephthlate (PET) Modified By Swift Heavy Ions of Silicon

Virendra Singh[1], Tejvir Singh[1], Amita Chandra[2], U.W. Scherer[3] and Alok Srivastava[1]

[1]Department of Chemistry, Panjab University, Chandigarh-160014, India
[2]Department of Physics, Panjab University, Chandigarh-160014, India
[3]Aachen University of Applied Sciences, Ginsterweg-1, D-52428 Juelich, Germany

Thin films of polyethylene terephtalate (PET) were exposed to beam of 120 MeV of Silicon ions with an ion fluence ranging from 1.3 x 10^{11} to 2.5 x 10^{13}. The electrical properties were investigated in terms of change in capacitance as a function of ion fluence, temperature and frequency.

In the present work the modification brought about in PET by swift heavy nickel ions at two different energies is reported in terms of optical changes with a view to study the role of bombarding energy on the overall modification process.

A stack comprising of 8 foils of 12 μm thickness was exposed to different fluence 120 MeV Silicon ions at the Material Science Irradiation Facility of the Nuclear Science Facility in New Delhi which has a 15 UD Pelletron. The irradiations were carried out at room temperature and under vacuum (10^{-6} torr) for time periods ranging from 10

to 1200 sec. The ion beam was scanned using a magnetic scanning system, so that an area of one square centimeter was uniformly irradiated. The beam current was kept low to suppress thermal decomposition and was monitored intermittently with a Faraday cup. The films exposed to different fluence of silicon ions were characterized for their electrical properties by carrying out measurements using two probe method and a HIOKI LCR Bridge. The measurements were carried out nearly three months after the irradiation of the foils hence the reported results represent the stationary state of the irradiated foils where the metasatable defects if any are expected to have got annealed and the radiation enhanced oxidation if any would have got completed.

Figures 1 and 2 shows the capacitance of pristine and irradiated the PET films as a function of frequency and temperature respectively for different ion fluences. It is observed from Figure 1 that the capacitances of the pristine as well as the irradiated films remain nearly constant at frequencies higher than 10 kHz. However at lower frequencies a strong dependence of capacitance on frequency was observed and this dependence seemed to become stronger with increase in fluence. It was further observed that the capacitance at a given frequency was higher for films exposed to higher fluence. It is observed from Figure 2 that the capacitance for both pristine as well as irradiated films show a strong dependence with the ion fluence at any given temperature. It can be stated that under the present experimental conditions of exposure, swift heavy ion bombardment could be used to increase the capacitive nature of the polymeric material of interest in controlled way. It was further observed that a distinct shift in the relaxation peak occurred when the ion fluence was increased from 10^{11} to 10^{13}.

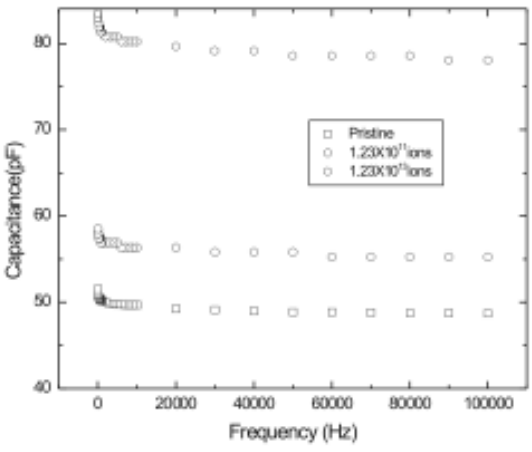

Figure 1. The frequency dependence of capacitance capacitance of pristine and irradiated PET

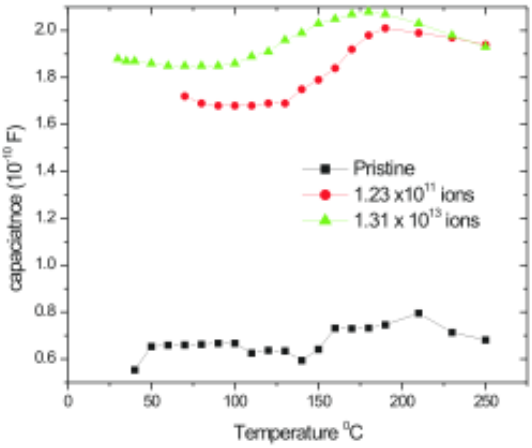

Figure 2. The temperature dependence of pristine and irradiated PET

REFERENCES

[1] A. Srivastava, T.V. Singh, S. Mule, C.R. Rajan and S. Ponrathnam Nucl. Instr. Meth. B 192,402 (2002).

[2] J.P. Biersack, A. Schmoldt. D. Fink and G. Schiwietz, Rad. Eff. Def. in Solids 140, 63 (1996).

[3] L. Calcagno, G. Compagnini and G. Foti, Nucl. Instr. Meth. B65, 413 (1992).

[4] Zhiyong Zhu, Youmei Sun, Changlong Liu,Jie Liu and Yunfan Jin, Nucl. Instr. Meth B 193, 271 (2002).

[5] Nandlal Singh, Anita Sharma and D.K. Avasthi, Nucl. Instr. Meth B 206, 1120 (2003).

5.2.37 Study of $^{35}Cl^{9+}$ ion irradiated nanocomposite membrane

Y.K. Vijay[1], N.K. Acharya[1], Vaibhav Kulshrestha[1], K.Awasthi[1], Balram Tripathi[1], M. Singh[1], S.A.Khan[2], and D.K. Avasthi[2]

[1]Department of Physics, University of Rajasthan, Jaipur-302 004, INDIA
[2]Nuclear Science Centre, Aruna Asaf Ali Marg, New Delhi- 110 067, INDIA

In past few decades the membrane based gas separation technology is of great interest for scientific community. The gas permeability of a dense polymer membrane is high and show relatively less selectivity due to inherent free volume distribution. In present study, the efforts are made to improve the selectivity of the membrane. In this regard the doping of nanoparticles powder of size ~10 nm in polymer matrix is used for preparation of samples. The composite membrane has good permeability and selectivity for gases depending upon the operating conditions. The solubility and diffusivity of the penetrant in the polymer matrix control the transport through non-porous dense membrane. In present work, the nano size (~10 nm) particles of $Co_{0.6}Zn_{0.4}Fe_2O_4$, prepared by the co-precipitation method. The Nano-composite polycarbonate membranes were irradiated by $^{35}Cl^{9+}$ swift heavy ion (SHI) of 120 MeV at Nuclear Science Centre, New Delhi. The membranes were irradiated at different fluence using rotating flywheel attachment. The pre and post irradiation study of nanocomposite membrane has been done using various standard techniques: gas permeation, optical microscopy. It was found that membrane containing nanoparticles shows low permeability with high permselectivity. The post irradiated membranes show high permeability as well as better permselectivity for hydrogen over other gases. The permeability of hydrogen and carbon dioxide decreases by increasing the doping concentration of nanocomposite material. The gas permeation data is shown in Table 1 and Table2. The optical micrographs of different concentration of nonocomposite material in polycarbonate at 40 magnification is shown in Figure 1 (a), 1 (b) and 1 (c), where the doped nanoparticles are found to be clustered. The effect of SHI is to homogenize the doping which is partially observable as shown in Figure 1(c). The gas permeability data also supports these observations.

Table 1: Permeability data for nanocomposite doped PC membrane

S.No.	Sample (PC + $Co_{0.6}Zn_{0.4}Fe_2O_4$) nanoparticles	Permeability (in barrer)		$P(H_2)/P(CO_2)$
		H_2	CO_2	
1.	PC (pure)	13.6	11.1	1.22
2.	PC+ 0.3%	5.56	4.1	1.35
3.	PC+ 1%	5.3	3.78	1.40
4.	PC+ 2%	4.6	2.7	1.70
5.	PC+ 5%	4.28	1.83	2.33

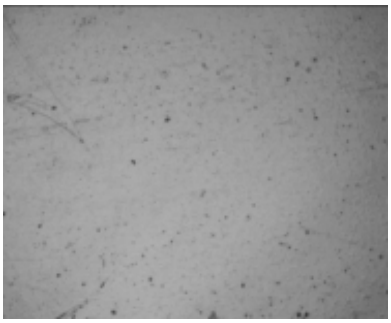

(a)

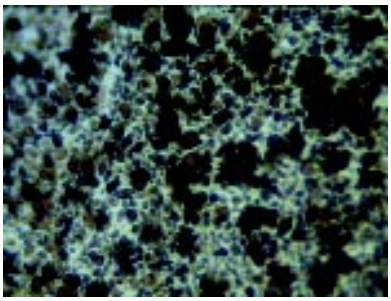

(b)

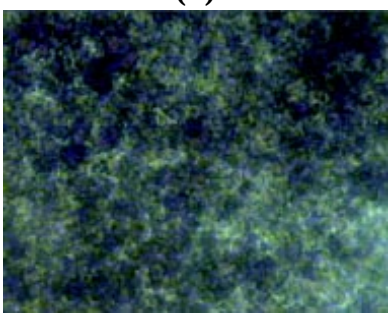

(c)

Fig. 1 : Photographs of PC membrane (a) without doping (b) Nanoparticle doped (c) Irradiated samples

Table 2: Permeability of ion irradiated membrane

S.No.	Sample (PC+5%[$Co_{0.6}Zn_{0.4}Fe_2O_4$]) nanoparticles	Permeability (in barrer)		$P(H_2)/P(CO_2)$
		H_2	CO_2	
1.	Unirradiated	4.28	1.83	2.33
2.	Irradiated at flunce 10^6	12.1	4.3	2.81
3.	Irradiated at flunce 10^7	14.9	4.5	3.31
4.	Irradiated at flunce 10^8	16.3	4.8	3.39

REFERENCES

[1] E. Coronado, J. R. Galan-Mascaros, C. J. Gomez-Garcia, V. Laukhin, Nature 408 (2000) 447
[2] T. J. Pinnavaia, Science 220 (1983) 365
[3] B. D. Freeman, Macromolecules 32 (1999) 375
[4] Y.K. Vijay, S. Wate, N. K. Acharya, J. C. Garg, Int. J. of Hydrogen Energy, 27 (2002) 905-908

5.2.38 Study of Ion Beam Modification of CR-39 (DOP) Polycarbonate

Rajesh Kumar[1], Rajendra Prasad[1], Y. K. Vijay[2], N. K. Acharya[2], K. C. Verma[3], and U. De[3]

[1]Department of Applied Physics, Z. H. College of Engineering & Technology, Aligarh Muslim University, Aligarh-20 2002.
[2]Department of Physics, University of rajasthan, Jaipur-302004.
[3]Variable Energy Cyclotron Centre, 1/AF, Bidhan Nagar, Kolkata-700064.

CR-39, a homopolymer and high grade optical plastic has been widely used as ion track detector due to its intrinsic property of ion track detection [1]. The optical and etching properties of CR-39 can be improved by incorporating additives such as dioctyl phthalate (DOP) in the polymer [2]. The irradiation by energetic ions affects the physico-chemical properties of the polymeric materials. The primary phenomena associated with the interaction of irradiation with the polymers are chain scission, chain aggregation, molecular emission and formation of double bonds [3]. 250 ìm thick sheets of CR-39 (DOP), specially prepared by adding 0.2 % dioctyl phthalate (DOP) to the CR-39 monomer ($C_{12}H_{18}O_7$ and sp.gr. 1.32 gml^{-1}) were obtained from Pershore Moulding Ltd. (UK). Samples (1.5 x 1.5 cm^2) were exposed to 70 MeV C^{5+} ion beam from 15 UD Pelletron accelerator at NSC, New Delhi. The fluence was varied from 10^{11} to 10^{13} ions/cm^2. The modifications have been characterized by XRD analysis and FTIR Spectroscopy. XRD with Cu K_α radiation was done in a Philips Analytical X-ray B.V. diffractometer. FTIR Spectroscopy was performed in transmission mode in a NICOLET-550 FTIR spectrometer in the range of 4000-400 cm^{-1}.

Fig. 1 shows the XRD patterns for CR-39 (DOP) in virgin and irradiated conditions for 70 MeV C^{5+} irradiations up to the fluence of 10^{13} ions/cm^2. The virgin polymer shows only one prominent X-ray peak at $2\theta = 20.49^0$. The irradiadiated ones also show an identical diffraction pattern except that the effect of ion irradiation are (i) a shift of this peak towards lower angle, with most of the shift occurring at 10^{11} ions /cm^2, the lowest fluence used, and (ii) a broadening of the XRD peak. This shift of the XRD peak implies an increase of lattice spacing [4], while broadening can be attributed to a decrease of the size of the crystallites or crystals in the polycarbonate sample.

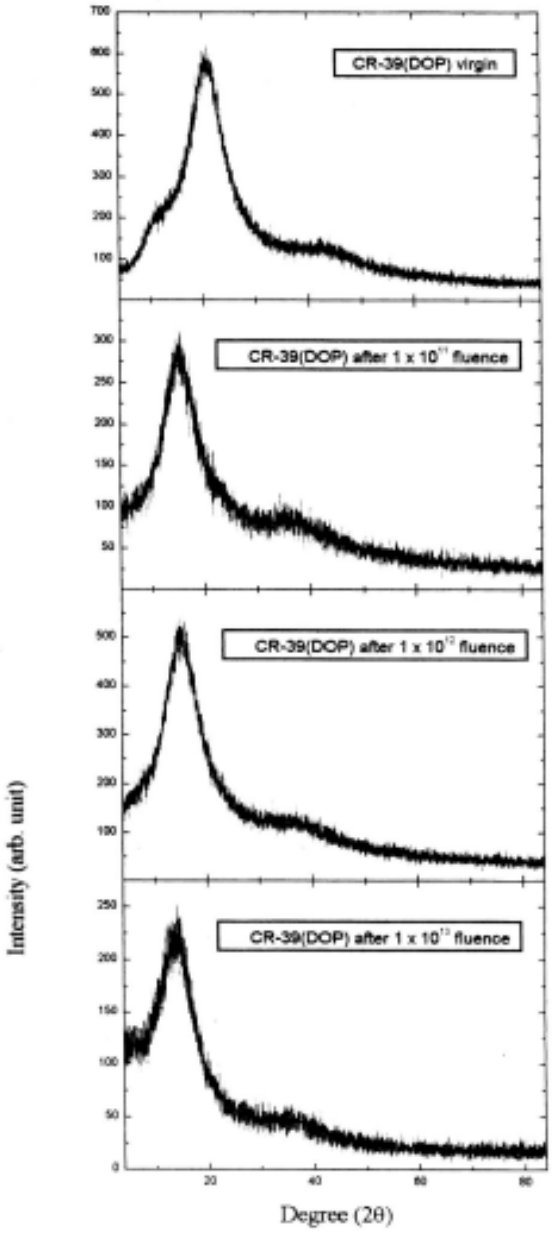

Fig. 1 : X-Ray Differaction pattern of CR-39 (DOP) Polycarbonate

It was observed that the average crystallite size reduced by about 21 % on irradiation to a fluence of 10^{13} ions/cm^2 with only marginal change at lower fluences. FTIR spectra indicate that the intensity of the absorption band appearing in the region 3400- 3600 cm^{-2} increased with the ion fluence, but there appears to be no appreciable change in 1800-1600 cm^{-1} region. This indicates that the scissoring is not taking place at carbonate site but it occurs at $–CH_2$-O-CH_2- site resulting in the formation of hydroxyl group. Another absorption band of weak intensity appears at 560 cm^{-1}indicating the C-C skeletal vibration. The FTIR spectra of irradiated samples show considerable changes at the fluences of 10^{12} and 10^{13} ions/cm^2, where following modifications are clearly evident: (i) the intensity of the absorption peaks at 2500 and 2200 cm^{-1} decreases on increasing the fluence and (ii) the marked change in the spectrum in the region 600-800 cm^{-1} which is due to ethylenic twisting (-CH=CH_2).

REFERENCES

[1] J. Davenas, X.L. Xu, G. Boiteux, D. Sage, Nucl.Instr. and Meth. B 39(1989) 754.
[2] E. Balanzat, S. Bouffard, A. Le Moel, N. Betz, Nucl. Instr. and Meth. B 91(1994)140.
[3] T. Steckenreiter, E. Balanzat, H. Ruse, C. Trautmann Nucl. Instr. and Meth. B 131 (1997) 159.
[4] H.S. Virk, Nucl. Instr. and Meth.B 191 (2002) 739.
[5] L.V. Azaroff, X-ray Crystallography, Mc Graw Hill Book co., USA, 1968, p. 551.

5.2.39 Positron Annihilation Lifetime Study Of Swift Heavy Ion Irradiated Polyamide Nylon-6 Polymer

Rajesh Kumar and Rajendra Prasad

Department of Applied Physics, Z. H. College of Engineering & Technology, Aligarh Muslim University, Aligarh-20 2002, India.

Swift heavy ions produce permanent damage in polymeric material as latent tracks along their path. Some of the modifications by incident ions have been attributed to the scissoring of the polymer chains, breaking of covalent bonds, promoting the cross-linkages, carbon cluster formation, liberation of volatile species and even the formation of new chemical bonds in some cases [1,2]. The effectiveness of these modifications produced in the polymer depends on the structure and the ion beam parameters (energy, fluence, mass, charge) and the nature of the target material itself. Three positron lifetimes (τ_1, τ_2, τ_3) are often found in polymers ranging from 100 ps to 5 ns due to (i) self annihilation of para positronium (p-Ps) (ii) annihilation of free positron and (iii) pickoff annihilation of orthopositronium (o-Ps). o-Ps lifetime is directly correlated to the free volume size and its intensity to the number concentration of free volume sites. The damage produced in the form of latent tracks by heavy ions results into the change of free volume properties of the material which have strong correlation with its macroscopic properties [3]. Positron Annihilation Spectroscopy (PAS) has emerged as a unique and potent probe for characterizing the free volume properties of polymers [4].

Self supporting Polyamide Nylon-6 (PN-6) film of thickness 250 μm were exposed to 70 MeV C^{5+} ion beam at 15 UD Pelletron accelerator of NSC, New Delhi. Three fluences used were 10^{11}, 10^{12} and 10^{13} ions/cm^2. Positron Annihilation Lifetime measurements were made at Inter University Consortium for DAE Facilities, Kolkata Centre. The thickness of the samples is adequate enough to absorb more than 99% of positrons emitted. Fast- fast coincidence spectrometer (FWHM = 280 ps) which entails monitoring the signal (1.28 MeV gamma ray from positron decay of the source as start time and 0.511 MeV gamma ray from the positron annihilation in the material sample under study as the end time), was used for recording the PAL spectra. BaF_2 scintillators coupled to Phillips XP2020 photomultipliers were used. ORTEC CFD selected the energy and provided time signals to TAC.

PAL spectra were analyzed by finite term lifetime analysis using PATFIT-88 program [5]. In polymers, 3 lifetimes give the best χ^2 (<1.1) and most reasonable standard deviations. o-Ps annihilation in the spherical free volume is described by simple quantum mechanical model of spherical potential well with an electron layer of thickness ΔR. The results of o-Ps lifetime (τ_3), the longest lifetime due to o-Ps annihilation were employed to obtain the mean free volume hole radius.

The lifetime and intensities after resolving the spectra into three components are tabulated in table 1. In PALS, it is the o-Ps lifetime which is directly correlated to the free volume hole size. The intensity of this component contains information about free volume hole concentration. The energy transfer by the ion leads to radical formation, bond scission and cross-linking of polymer chains. The dominance of scissioning or cross-linking depends essentially on the polymer and energy loss per unit path length or linear energy transfer (LET). For low LET, spurs develop far apart and independently; the deposited energy tends to be confined in one chain (not in neighbouring chain) leading to scission. In case of high electronic LET, the probability of two radical pairs to be in neighbouring chains is increased and cross-linking is facilitated. The scission causes increase in the free volume whereas the cross-linking causes decrease in the free volume [6, 7]. o-Ps lifetime and, therefore, the average free volume are found to be decreased due to irradiation at the fluences used in the present experiment. At high fluences the track area where cross-linking is predominant becomes comparable to the sample area. The average free volume of the micro-voids decreases by 4.3 %, 3 % and 9.3% at the fluences of 10^{11}, 10^{12} and 10^{13} ions/cm^2. Present results obtained for o-Ps lifetime (τ_3), free volume hole radius (R) and micro-void volume (V_f) for virgin and irradiated samples at different fluences. Ion irradiation reduces the available free volume. With the increase in the flux scissioned segments crosslink randomly, resulting into the decrease of average free volume due to overlapping of the tracks.

Table 1. Lifetime and intensities of unirradiated and irradiated Polyamide Nylon-6 polymer

Fluence (ions/cm^2)	τ_1 (ns)	I_1 (%)	τ_2 (ns)	I_2 (%)	τ_3 (ns)	I_3 (%)	**R (Å)**	**V_f (Å^3)**
Unirradiated	0.188 ± 0.007	37.766 ± 2.265	0.429 ± 0.010	43.732 ± 2.129	1.949 ± 0.012	18.502 ± 0.202	2.808	92.682
10^{11}ions/cm^2	0.160 ± 0.007	31.425 ± 1.927	0.391 ± 0.008	49.265 ± 1.809	1.905 ± 0.011	19.310 ± 0.181	2.767	88.680
10^{12} ions/cm^2	0.156 ± 0.007	31.904 ± 1.791	0.390 ± 0.007	49.150 ± 1.677	1.918 ± 0.011	18.946 ± 0.176	2.780	89.936
10^{13}ions/cm^2	0.164 ± 0.006	31.756 ± 2.012	0.384 ± 0.008	48.830 ± 1.896	1.854 ± 0.011	19.414 ± 0.183	2.718	84.051

REFERENCES

[1] E.H. Lee, Polyimides: fundamentals and applications (Marcel Dekker Inc., New York, 54 (1996).

[2] L.S. Wielunski, R. A. Clissold., E. Yap, D.G. McCulloch, D.R. McKenzie and M.V. Swain, Nucl. Instr. and Meth. B 127/128 (1997) 698.

[3] T. Venkatesan, Nucl. Instr. and Meth B 7 / 8 (1985) 461.

[4] C. Liu, Z. Zhu, Y.Jin, Y. Sun, M. Hou, Z. Wang, X. Chen, C. Zhang, J. Liu, B. Li, Y. Wang, *Nucl. Instr and Meth B* 166 & 167 (2000) 641.

[5] Virk. H.S., *Nucl. Instr. and Meth B* 191 (2002) 739.

[6] Jean,Y C, Dai,G H. Free volume hole distribution of polymers probed by positron annihilation spectroscopy. Nucl. Inst. Meth. B 79 (1993) 356.

[7] Rajesh Kumar, S. Rajguru, Das. D, Prasad R, *Radiation Measurements* 36 (2003). 151.

5.2.40 Effect of 50 MeV Lithium Ion Beam Irradiation on Magnetic Characteristics of $HoFeO_3$ Single Crystals

K.K.Bamzai[1], Monita Bhat[1], Balwinder Kaur[1], P.N.Kotru[1], B.M.Wanklyn[2], Ravi Kumar[3], P.A.Joy[4], S.D.Kulkarni[4]

[1]Crystal Growth and Materials Research Group, Dept. of Physics & Electronics, University of Jammu, Jammu 180006.
[2]Dept. of Physics, Clarendon Laboratory, University of Oxford, U.K.
[3]Nuclear Science Centre, New Delhi – 110067.
[4]Physical Chemistry Division, National Chemical Laboratory, Pune.

The orthoferrites of the chemical formula $RFeO_3$, crystallize with a distorted orthorhombic perovskite – like lattice symmetry, with four Fe ions and four rare-earth ions per unit cell and conform to the space group D_{2h}^{16} - Pbnm [1,2]. The rare earth orthoferrites possess extremely high velocities of the domain wall motion and it is expected that they find many applications in communications techniques, in optical internet, in sensors for magnetic fields and electric currents, mechanical quantities, etc.

The crystals of $HoFeO_3$ were irradiated with 50 MeV Lithium ion beam using 15 UD Pelletron accelerator facility at Nuclear Science Centre, New Delhi. In the present study, the modifications in the structural and magnetic properties of $HoFeO_3$ crystal were studied after irradiating at a fluence value of 1×10^{14} ions/cm^2.

The rare earth orthoferrites are highly anisotropic as the magnetization along three different planes is absolutely different. The maximum magnetization produced along (001) plane of unirradiated $HoFeO_3$ crystal is 0.065 emu/g whereas after irradiation, it is 0.0096 emu/g. Thus the magnetization decreases after irradiation due to amorphous region created by defects [5]. Moreover, a change in the coercivity and remanent magnetization of $HoFeO_3$ crystal after irradiation is also observed. The magnetic moment is produced along two planes only in case of rare earth orthoferrites i.e., (001) and (010) whereas no magnetic moment is produced along (110) [6]. Same is the case observed in case of $HoFeO_3$ crystal as it exhibits weak ferromagnetism along (001) and (010) planes only and is completely paramagnetic along (110). However, after irradiation it is paramagnetic along (010) and the other two planes exhibit weak ferromagnetism. This implies that the easy axis of magnetization changes on irradiation as observed earlier [7] with the increase in temperature for rare earth iron perovskites.

REFERENCES

[1] S. Geller, J. Chem. Phys. 24, 1236 (1956).
[2] S. Geller and E. A. Wood, Acta Crystallogr. 9, 563 (1956).
[3] R. M. Bozorth, V. Kramer and J. P. Remeika, Phys. Rev. Lett. 1, (1958) 3.
[4] D. Treves, J. Appl. Phys. 36 (1965) 1033.
[5] Yuri S. Didosyan, Hans Hauser and Georg A. Reider, Inter. J. Appl. Electr. Mech. 13 (2001/ 2002) 215-218.
[6] F. Studer and M. Toulemonde, Nucl. Inst. Meth. In Phys. B 65 (1992) 560.
[7] M. M. Scheiber, Experimental Magnetochemistry, Wiley & Sons, New York, 1967, p. 314.

5.2.41 Formation of aligned carbon nano clusters along the ion trajectories in Si-based polymer

Amit Kumar[1], F. Singh[1], S.A. Khan[1], D.C. Agarwal[2], J.C. Pivin[3], D.K. Avasthi[1]

[1]Nuclear Science Center, Post Box 10502, New Delhi 110067, India
[2]RBS College, Agra, India
[3]CSNSM, 91405 Orsay Campus, France

This work reports the formation of discontinuous carbon nanowires in Si-based polymers. Films of Si-based polymer (methy-triethosilane - MTES) were prepared on Si substrate by sol-gel technique [1] and irradiated by 120 MeV Au ions. The energy filtered TEM was performed to evaluate the size of nanowires. On line ERDA measurements to determine the track radius of H evolution under ion irradiation.

The loss of hydrogen as a function of ion fluence from the MTES polymers films for irradiation by 120 MeV Au ions are shown in figure 1a. From the figure, we see that H content from the sample decay exponentialy with the ion fluence. The kinetics of H evolution was fitted using following equation [2],

$$N = N_o \exp(\sigma\phi)$$

where ϕ is the ion fluence in ions/cm^2 and σ is hydrogen release cross section in cm^2. N_o is the initial hydrogen content at $\phi = 0$ fluence and N is the hydrogen concentration as a function of fluence. The fitting is shown in figure 1 by a solid line.

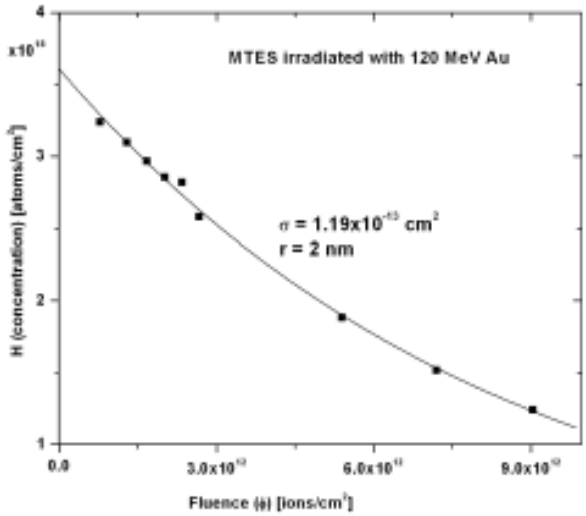

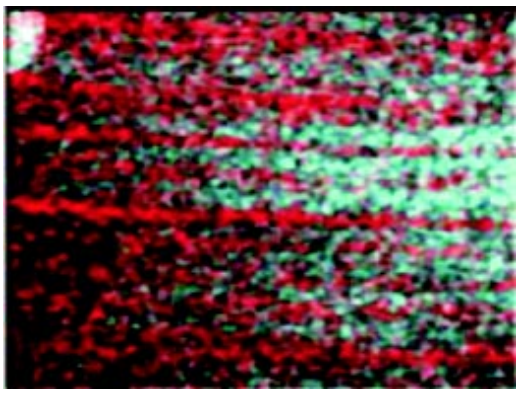

Fig 1: a) Kinetics of H release, measured by means of ERDA with 120 MeV Au ions irradiation of MTES. b) EFTEM image of MTES (red: carbon, touquise: Silicon) irradiated at fluence of 3 x 10^{11} ions/cm^2 with 120 MeV Au ions

From the measured H release cross section, we derived the effective ion track radius. The radius of the ion track is calculated from $r_{track} = (\square \quad)^{1/2}$. In the present case the hydrogen release cross-section $\square = 1.19 \times 10^{-13}$ cm^2, therefore the effective radius is around 2 nm.

The distributions of carbon and silicon are shown on the EFTEM images of Figs. 1b for MTES irradiated at fluences of 3×10^{11} ions/cm^2. The images clearly evidences that part of the C atoms has segregated into aligned clusters under ion irradiation. The carbon clusters are almost peculating into wires with diameters of ~ 4 nm.

Our main aim to form continuous carbon nanowires by ion beam. These carbon nanowires, like their extremely-studied cousins, carbon nanotubes, will and have useful electrical and optical properties.

REFERENCE

[1] J.C. Pivin, et al.,, Nucl. Instr. and Meth. in Phys. Res. B 215 (2004) 373.
[2] V. K. Mittal, et al., Rad. Eff. and Def. in solids, 147, 199 (1999).

5.2.42 Modification of magnetic anisotropy in metallic glasses using high-energy ion irradiation

Kavita Amrute[1], D.C Kothari[1], and D Kanjlilal[2]

[1]Department of Physics, University of Mumbai, Mumbai
[2]Nuclear Science Centre, New Delhi

Ion beam of 100 MeV energy has been utilized for irradiating the ferromagnetic metallic glasses of composition $Fe_{40}Ni_{38}Mo_4B_{18}$ and $Fe_{78}B_{13}Si_9$ at various fluences ranging from 5×10^{12} to 1×10^{14}. The effect of irradiation on magnetic anisotropy and hyperfine magnetic field was investigated by taking Mossbauer spectra of all the samples. The correlation has been found in the change in magnetic anisotropy and the irradiation fluence and the results have been published, (Surface Coating and Technology, 2004). The observed change in magnetic anisotropy is believed to be caused by residual stress induced by swift heavy ion irradiation. As annealing releases the stresses, the few irradiated samples have been annealed below glass transition temperature Tg (Tg~ 275 C), at 220 C only to release the stresses without causing re-crystallization. The Mossbauer spectra and XRD taken after annealing clearly show partial crystallization in both the metallic glasses, although the crystallization temperature is ~ 400 C. Few irradiated but un-annealed samples have been studied 1 year after irradiation. These samples show increase in magnetic anisotropy and reduction n hyperfine magnetic field. The magnetic moment again turns towards in-plane direction as in the virgin samples. The XRD shows a broad peak for these samples indicating glassy structure, but the peak is narrower than that for the virgin samples.

5.2.43 Heavy Ion Testing of Integrated Circuits

S.B.Umesh[1], A.R.Khan[1], *G.R.Joshi[1], M.Ravindra[1], S.R.Kulkarni[2] and R.Damle[2]

[1]Components Division, ICG, ISAC, Bangalore-17
[2]Department of Physics, Bangalore University, Bangalore-56

1. Introduction

The device types FPGA's RH1280A and RT54SX16S, 12 bit ADC AD1671 and MDI DC – DC Converter EU grade 5680 were taken for heavy ion testing at Nuclear Science Centre, New Delhi. The reason for testing is as mentioned below.

(i) FPGA RH1280A

The RH 1280A FPGAs are being used extensively in many on board subsystems such as AOCE, Star sensor, payload, TM/TC, IISU elements etc. of IRS missions. It is also being used for the first time in INSAT 4A, BMU of Cartosat – 2 & GSAT 4. There are no on board related problems such as Single Event Upsets until now reported for this device type. The FPGA has two types of modules Sequential (S - Module) with SEU LET_{th} between 3 – 8 MeV/mg/cm^{2}and Combinational (C- Module) with SEU LET_{th} greater than 17 MeV/mg/cm^2. The radiation sensitivity of the device depends on circuit design. Designs which predominantly using C- Modules and designs with redundancy incorporated, will have high SEU immunity as compared to the designs which use S- Modules and no mitigation techniques adapted.

The PRB which reviewed the critical parts for INSAT 4A, CARTO-2 & GSAT4 recommended for conducting the Heavy ion radiation testing on RH1280A FPGA to asses its sensitivity.

(ii) FPGA RT54SX16S

The FPGA 54SX16S is a radiation tolerant device with manufacturer specifying a SEU LET_{th} of greater than 17 MeV/mg/cm^2. This device is being used in BDH system of Cartosat – 2. The RT versions manufactured in Matsushita foundry Japan, generally have variation in SEU LET thresholds for different lots. Therefore it was decided to conduct heavy ion radiation testing on this FPGA.

(iii) A- D CONVERTER AD1671

The ADC AD1671 is a high speed 12-bit converter available in 883 up-screened version being used in IRS missions. There is also a requirement for the usage of 12 bit ADCs in INSAT systems. PRB recommended for a heavy ion testing of this ADC to characterize the device for SEU & SEL so that it can be considered for the usage in GEO

missions.

(iv) MDI DC – DC CONVERTER 5680 EU GRADE

The MDI make Space grade DC – DC converters are being proposed for usage in BDH, SSR, Sensors, IISU of IRS & INSAT missions. Due to non-availability of Space grade devices in IRS P5 time frame, up-screened EU grade devices are to be used in IRS P5 BDH. To evaluate the MDI make converter performance for SEE effects in general and for IRS P5 in particular, the device was taken up for heavy ion testing.

2. TEST SET UP AND DEVICE UNDER TEST DETAILS

The ion species requested by ISAC to NSC are with the following LETs

1. F^+ – 4 MeV/mg/cm^2
2. Si^+ - 10 MeV/mg/cm^2
3. Cl^+ - 15 MeV/mg/cm^2
4. Ag^+ - 42 MeV/mg/cm^2

Only two ion species Si^+(10 MeV/mg/cm^{2}and Ni^+ (33 MeV/mg/cm^2) were available and the devices were used only to these beams.

The table below describes the details of the devices tested for heavy ions.

Table – I DUT details

S. No.	**Device type**	**Manu-facturer**	**Function**	**Pro-cess**	**Quality level**	**Total Ionizing Dose (TID)**	**Mfr. Specified SEU LET_{th} MeV-cm^2/mg**	**SEL LET_{th}**
1.	RH1280A	ACTEL	FPGA	0.8µ CMOS	EX3 FLOW	100Krads	S: 3-8 C: > 17	100 MeV-cm^2/mg
2.	RT54SC16S	ACTEL	FPGA	0.6µ CMOS	EX3 FLOW	80Krads	S: > 17 C: > 43	100 MeV-cm^2/mg
3.	AD1671	ANALOG DEVICES	12-BIT A-D CONVERTER	Bi-CMOS	883 CLASS S UP-SCREENED	30Krads	Not specified	Not specified
4.	5680 EU	MDI	3.3V O/P DC – DC CONVERTER	Hybrid	EU Grade	30Krads	Not specified	Not specified

(i) RH1280A FPGA

The radiation test circuit for detecting SEUs is developed by configuring the Sequential modules and Combinational modules as storage elements. The modules are configured as 8 x 8 array memory using D flip-flops. RH1280A test circuit has eight blocks of 8 x 8 array using S- modules and two blocks using CC modules. A data pattern of checkerboard & its complement is stored in the arrays and the array outputs are monitored for detecting upset that occur in the block.

(ii) RT54SX16S FPGA

The circuit configured is same as that of RH1280 with 12 blocks of S-module arrays and 4 blocks of CC modules array. All the blocks are individually monitored for the upsets that occur during irradiation.

(iii) AD1671 A-D Converter

In the ADC test circuit, the input voltage is given such that the 12 digital outputs are driven to the pattern of alternate 0's and 1's. The outputs are continuously monitored during irradiation for detecting bit upsets. The ADC supply current is monitored for detecting any occurrence of SCR Latch – up event.

(iv) 5680 EU DC – DC converter

The DC – DC converter's output voltage and input current are continuously monitored during irradiation.

Table – II shows the test results of SEU and SEL of all the devices exposed to heavy ion irradiation.

The manufacturers test data for RH1280A shows the LET threshold of S – modules for between 3 to 8 MeV/mg/cm^2. The requested ion in this range was not available and the device was tested to an LET of 10 MeV/mg/cm^2 only and upsets were observed as expected. This confirms the device sensitivity of S- modules to upsets for lower LETs. But no upsets were observed in the C – modules. The device RT54SX16S did not show any upset for 10 MeV/mg/cm^2 ion. However upsets were observed for 33 MeV/mg/cm^2 ion in S- modules and no upsets were observed in C – modules. This also confirms with the manufacturers test data.The ADC AD1671 did not have any SEU or SEL failures up to an LET of 33 MeV/mg/cm^2. The device functionality was normal. The MDI DC – DC converter 5680 EU also did not show any malfunction and the device parameters are normal up to 33 MeV/mg/cm^2.

Table – II Test results

S. No.	Device type	ion	Energy MeV	LET MeV -cm^2/mg	Flux P/cm^2/s	Fluence P/cm^2	SEU	SEL
1.	RH1280A	$^{28}Si^{8+}$	100	11	500	2.7 x 10^5	S – module > 100 upsets C- modules No upsets	No Latch – up
		$^{107}Ni^{10+}$	100	33	—	—	Not tested due to Facility Breakdown	—
2.	RT54SX16S	$^{28}Si^{8+}$	100	11	500	2.7 x 10^5	No upsets	No Latch – up
			100	33	500	2.7 x 10^5	> 100 upsets C- modules No upsets	No Latch – up
3.	AD1671	$^{28}Si^{8+}$	100	11	500	2.7 x 10^5	No upsets	No Latch – up
		$^{107}Ni^{10+}$	100	33	500	2.7 x 10^5	No upsets	No Latch – up
4.	5680 EU DC – DC converter	$^{28}Si^{8+}$	100	11	500	2.7 x 10^5	No upsets	No Latch – up
		$^{107}Ni^{10+}$	100	33	500	2.7 x 10^5	No upsets	No Latch – up

3. Conclusion

The calculated upset rates with RH1280A in GEO and LEO orbits are 3.5 x 10^4 and 9.8 x 10^{-5} upsets/bit – day respectively. With all the S modules uses on the circuit the upsets rates per device are 2.2 upsets in 10 days and 6 upsets in 100days for GEO and LEO orbits. SEU mitigation techniques are required to be implemented if RH1280A is used in critical systems. CC modules are found to be more tolerant for SEUs than S modules. In critical functional blocks CC modules can be used as storage elements.